X-Ray synchrotron radiation in physicochemical studies

2001 Russ. Chem. Rev. 70 373

(http://iopscience.iop.org/0036-021X/70/5/R02)

Russian Chemical Reviews **70** (5) 373 – 403 (2001)

DOI 10.1070/RC2001v070n05ABEH000656

X-Ray synchrotron radiation in physicochemical studies

Ya V Zubavichus, Yu L Slovokhotov

Contents

Abstract. Modern modifications of the conventional X-ray methods of physicochemical analysis (X-ray and electron spectroscopy, diffraction methods, *etc*.) and new combined techniques using X-ray synchrotron radiation are considered. Unique characteristics of synchrotron radiation are noted, namely, continuous spectrum, exceptionally high intensity, polarisation, coherence, pulse nature, *etc*. The key trends in the use of combined methods in chemistry and materials science including studies of substances under extreme conditions, the study of rapid processes, studies with high spatial resolution are discussed. The achievements in the applications of synchrotron radiation are illustrated by examples from various fields of chemistry and related sciences. The bibliography includes 405 references..

I. Introduction

Development of modern science relies to a great extent upon the set of available investigation tools. Many methods of physicochemical analysis commonly applied in chemistry are based on interaction of a substance under study with electromagnetic radiation of various spectral ranges. Several independent groups of methods can be distinguished based on the spectral range used, *e.g*., infrared, visible, ultraviolet and X-ray radiation. Radiation in the required spectral range is usually generated using special sources (such as gas discharge tubes, lamps, lasers, X-ray tubes) characteristic of classical versions of each method. Each source type requires its own experimental methodology, which takes into account the specific features of the interaction of this radiation with matter.

Integration of natural sciences over the last decade of the XXth century affected the techniques of physicochemical analysis stimulating their convergence. A unified approach to the generation of electromagnetic radiation of different spectral ranges is based upon a fundamental principle of electrodynamics: the electromagnetic radiation is generated by a charged particle moving with an acceleration. In particular, electrons or positrons, which move along a curved trajectory in a magnetic field with a velocity close to the velocity of light, generate a flux of photons in a broad spectral range, *i.e*., synchrotron radiation (SR) (Fig. 1).

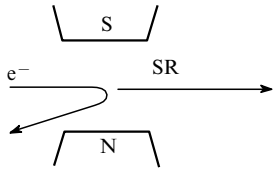

Figure 1. Generation of synchrotron radiation upon movement of an electron in a magnetic field.

Accelerators of charged elementary particles (typically, electrons or positrons) operating in a stationary regime of a storage ring can conveniently serve as powerful SR sources. In such large-scale facilities, ultrarelativistic electrons,† moving along a closed-loop orbit in an evacuated chamber of a storage ring with curvature radius of a few tens of meters, emit extremely intense electromagnetic radiation with a continuous spectrum ranging from far infrared to hard X-ray (Fig. 2). The energies of electrons in storage rings of different constructional designs can vary from hundreds of eV up to several GeV. Upon an incremental increase in the electron energy, the spectral maximum of the SR generated shifts from ultraviolet through hard ultraviolet (vacuum ultraviolet, VUV) and soft X-ray up to hard X-ray, respectively.[1–8]

Modern SR sources gradually become collective use research centres. Such centres accommodate up to a few tens of experimental stations, which function in the 24×7 mode shift by shift servicing specialists from various institutions and fields of science — from nuclear physics to molecular biology and materials science. Along with synchrotron modifications of established and widely accepted methods using traditional X-ray sources, unique purely synchrotron-based specialised techniques are rapidly developing. Applications of SR in industry are also expand-

Ya V Zubavichus, Yu L Slovokhotov A N Nesmeyanov Institute of Organoelement Compounds, Russian Academy of Sciences, ul. Vavilova 28, 117813 Moscow, Russian Federation. Fax (7-095) 135 50 85. Tel. (7-095) 135 93 04. E-mail: yan@xafs.ineos.ac.ru (Ya V Zubavichus) E-mail: slov@xafs.ineos.ac.ru (Yu L Slovokhotov)

Received 1 February 2001
Uspekhi Khimii **70** (5) 429 – 463 (2001); translated by Ya V Zubavichus

† The term ultrarelativistic particles is commonly referred to those, the kinetic energy of which $E \gg m_0c^2$, where m_0 is the rest mass of the particle and c is the velocity of light. Velocities of such species are virtually constant and very close to the velocity of light; thus any increase in their kinetic energies leads to the increase in their relativistic masses.

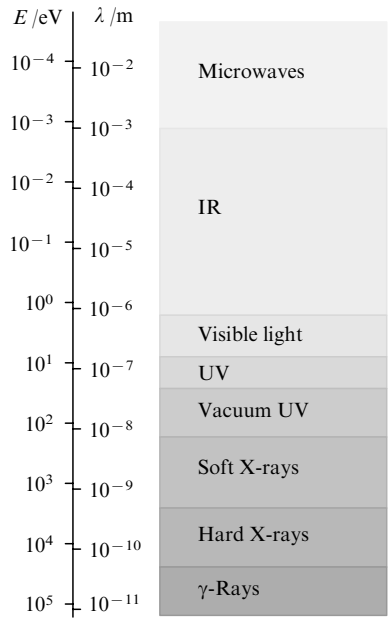

Figure 2. Spectral ranges of electromagnetic radiation, which can be generated by modern synchrotron radiation sources.

ing, in particular, in the manufacture of microelectronics (microchips, printed circuit boards, *etc*.) and micromechanics (micromotors, micropumps) devices. In this connection, applied industrial methods, such as deep X-ray lithography and LIGA technology (German acronym for a 3-stage technological process of microfabrication including lithography, electrodeposition and moulding), have made tremendous progress.[9] Medical applications utilising SR are evolving as well, especially ones aimed at early diagnostics and radiotherapy of various diseases, including cancer and at imaging of human internal organs and tissues with high contrast and spatial resolution (mammography, angiography, radiography).[10] Synchrotron techniques are successfully used in environmental studies, *e.g*., for detection of trace amounts of heavy metal pollutants in industrial wastes, aerosols, soils and in biological objects — plants, living tissues, *etc*.[11]

Currently, there are about 40 operating SR sources worldwide and more than 10 new sources are under construction. In Russia, starting from the late 70's, the Siberian Synchrotron Radiation Centre (SSRC) continuously functions on the basis of the VEPP-3 ‡ storage ring (2 GeV) at the G I Budker Institute of Nuclear Physics of the Siberian Branch of the Russian Academy of Sciences in Novosibirsk.[12] Recently, a new upgraded VEPP-4 storage ring (6 GeV) has been put into operation in the SSRC. Construction of a dedicated storage ring 'Sibir'-2' (2.5 GeV) has been finished at the Kurchatov Synchrotron Radiation Source (KSRS) in the Russian Research Centre 'Kurchatov Institute' in Moscow;[13] two new synchrotron centres in Dubna and Zelenograd are in the construction phase.

An important benefit of storage rings is their environmental safety,§ which distinguishes such facilities advantageously from, for example, neutron sources, *viz*., nuclear reactors. Even a major accident on an electron storage ring cannot result in any radiation pollution of the environment. Work at a synchrotron radiation centre does also not imply any health risk for researchers provided that they obey elementary safety rules and regulations.

All of the main methods utilising electromagnetic radiation are represented at the modern synchrotron radiation centres. A substantial organisational advantage of the SR sources is that all the state-of-the-art techniques and advanced instrumentation are concentrated in one centre and even in one building. This makes it possible to conduct comprehensive studies with the use of a broad range of complementary experimental techniques as well as stimulates mutual influence and integration of different experimental approaches and ideas.

This review is devoted to applications of SR in chemistry and related disciplines, *viz*., chemical materials science, biochemistry and molecular biology. Since it is virtually impossible to cover all modern trends in the SR applications, we have confined ourselves to discussion of only instrumental techniques based on X-ray part of the synchrotron radiation spectrum. For the same reason, we did not consider such technological applications of SR as X-ray lithography and the methods in which synchrotron radiation is used for triggering physicochemical processes, *e.g*., photochemical reactions and radiation-induced degradation (to get familiar with this field one may see, for example, Ref. 14, where synthesis of amino acids from a gaseous mixture of nitrogen, water and carbon dioxide at atmospheric pressure under irradiation by intense photon beams is described). For a detailed review of modern technological applications of SR see Ref. 15. Among non-X-ray synchrotron methods we should mention various types of UV spectroscopy [5] and synchrotron IR spectroscopy, which have been actively developed over the last years, especially its varieties with high spatial (microspectroscopy) [16] and time resolution.[17]

X-Ray-based instrumental techniques, which are most important for chemistry, include X-ray diffraction methods (in particular, single-crystal X-ray crystallography), X-ray and electron spectroscopy. In 'classical' laboratory versions of these methods, allowing detailed exploration of atomic and electronic structures of substances, traditional X-ray sources, *viz*., X-ray tubes, are used. However, synchrotron radiation sources have several significant advantages. Synchrotron X-ray beams are more intense than radiation of the high-energy X-ray tubes with rotating anodes by several orders of magnitude. Such a gain in intensity allows one to shorten the data acquisition time and investigate fine effects which would require very lengthy experiments with traditional sources. A considerable portion of energy emitted by an X-ray tube lies in a narrow spectral range (anode characteristic radiation), whereas the high intensity of synchrotron radiation is uniformly distributed over the entire X-ray spectral range. With 'white' synchrotron radiation, it is possible to select the wavelength most appropriate in each particular case or scan over a certain wavelength range during the experiment, which extends significantly the potential of traditional X-ray techniques. Yet another advantage of SR is relatively small cross-section and low divergence of X-ray beams, which can further be focused and collimated using X-ray optics. This approach is successfully applied in X-ray microprobe methods and in studies of substances under extreme ¶ conditions (it has to be mentioned, however, that focusing X-ray optics is now frequently used in laboratory devices as well). Pulse structure, polarisation and coherence of synchrotron radiation are other factors, which are of great interest and potential for applications.

II. Design of a storage ring and parameters of synchrotron radiation

1. Building blocks of a storage ring

A storage ring is an accelerator of charged light particles (electron or positrons) in which ultrarelativistic particles move along a closed-loop trajectory with velocity close to the velocity of light emitting an intense photon flux. The energy lost by electrons during each revolution as emitted radiation is compensated in a special electromagnetic acceleration system, *viz*., radiofrequency

‡ Russian acronym for electron-positron colliding beams.

§ In this respect, it is indicative that several storage rings are constructed in residential areas of large cities, *e.g*., BESSY (Berlin) and KSRS (Moscow).

¶ The term extreme condition refers here to the limiting achievable (high and low) temperatures and superhigh pressures, which are created using specialised instruments to apply to substances under study.

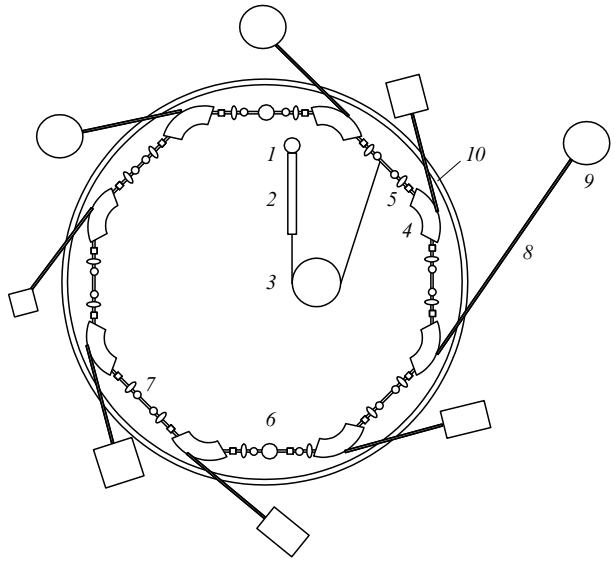

Figure 3. Design of a storage ring, the SR source: (*1*) is an electron gun, (*2*) is a linear preaccelerator (linac), (*3*) is a ring preaccelerator (booster), (*4*) is a bending magnet, (*5*) is a system of 'magnetic lenses', (*6*) is a radiofrequency resonator, (*7*) is a straight section suitable for accommodation of specialised insertion devices, (*8*) is a channel, (*9*) is an experimental station, (*10*) is a biological protection concrete wall.

resonator. The storage ring is designed to maintain a stationary regime of particles' movement rather than to generate a single pulse of particles with the maximum energy (as in the case of elementary particle accelerators in nuclear physics).

A storage ring includes the following indispensable components (Fig. 3):

— an electron source (*1*), which is, as a rule, a standard high-power electron gun based on the thermoelectric emission;

— a system for preacceleration and injection of electrons: linear (linac) (*2*) or ring (booster) (*3*) preaccelerators;

— a hollow torroidal chamber of the accelerator where the beam of ultrarelativistic electrons moves. High vacuum has to be maintained in this chamber (10^{-9}–10^{-10} Torr) in order to reduce energy losses of the electrons due to collisions with background molecules;

— a system of bending magnets (magnetic dipoles) (*4*), which define closed-loop trajectory of the electrons' movement. Between the bending magnets the particles move linearly. It is in the bending magnets that the synchrotron radiation directed tangentially to the beam trajectory is generated (see Fig. 1);

— a system of magnetic lenses (*5*), *viz*., magnetic quadrupoles and higher-order magnets, which is used for the electron beam focusing;

— an electromagnetic system (*6*) is used for the acceleration of electrons up to ultrarelativistic velocities as well as for compensation of energy losses due to emitted radiation (radiofrequency resonator);

— specialised magnetic devices (insertion devices) (*7*), *viz*., undulators and wigglers, are inserted in straight sections between the bending magnets. These devices are used for the generation of SR with enhanced characteristics compared to the bending magnet radiation. Though these are optional components of a storage ring, they are installed in the majority of modern storage rings;

— a biological protection concrete wall (*10*) adsorbs background radiation of the storage ring. Photon beams are guided by evacuated channels (*8*) through the biological protection wall to the experimental station (*9*), where experimental stations and all devices for investigations and other works based on SR utilisation are situated.

2. Design parameters of a storage ring and characteristics of synchrotron radiation

The main parameters of a storage ring as an SR source are as follows: the orbit radius R, along which the electrons move (in modern facilities, it is typically 10–30 m), electron energy E (1–6 GeV), magnetic field (B) in bending magnets (1–2 T) and their number and electron current I, which is an integral measure of the total number of electrons in the storage ring chamber (50–500 mA). These parameters are interlinked by the following relations:[4–7]

$$R = \frac{E}{eB}\,, \tag{1}$$

where e is the electron charge;

$$I = \frac{2\pi e N_e R}{c}\,, \tag{2}$$

where c is the velocity of light and N_e is the total number of electrons in the chamber.

The stability of an electron (or positron)† beam is characterised by a beam lifetime, which is the time required for the electron current to decrease by a factor of $\sim$2.7 (it corresponds to a decrease in $\ln I$ by unity). Beam lifetime depends primarily upon the vacuum quality in the chamber and can range from a few to a few tens hours. This governs the frequency of electron re-injections to the storage ring chamber required in order to maintain the intensity of SR at the appropriate level.

Design parameters of a storage ring determine the characteristics of SR it generates. Spectral distribution of the SR is commonly characterised by a critical wavelength λ_c or critical energy

$$E_c = \frac{hc}{\lambda_c}\,,$$

(h is the Plank constant); λ_c is chosen so that the total energy emitted by the source at the wavelengths longer than λ_c was equal to the total energy emitted at shorter wavelengths.

Size of a synchrotron radiation source is defined by the emittance ε; this quantity is the product of a linear size of the emitting area of the electron beam by the divergence angle of the photon beam. Typical values of the vertical and horizontal emittances of modern SR sources lie in the range of 10^{-10}–10^{-8} and 10^{-8}–10^{-6} m rad, respectively.

The intensity of SR is characterised by its brilliance, which is determined as number of photons emitted in 1 s from the emitting surface unity into the solid angle unity within the certain photon energy bandwidth (BW). Usually, the bandwidth is chosen to be equal to 0.1% of E_p (E_p is the photon energy), the so-called 0.1% BW. Thus, the unit of measure of the brilliance is photon s^{-1} mm^{-2} rad^{-2} (0.1% BW)$^{-1}$. Other intensity characteristics include spectral flux, which is obtained by multiplication of the brilliance by horizontal and vertical emittances, and total flux, which is obtained by integration of the spectral flux over the entire range of the wavelengths emitted.

Total power W emitted by the electron beam per revolution and the critical wavelength depend on the electron energy in the beam, electron current and the orbit radius:

$$W \sim \frac{I\gamma^4}{R}\,, \tag{3}$$

where $\gamma = E/m_0c_2$ is the relativistic (Lorentz) factor of an electron (m_0 is the rest mass of the electron) and

† Positron beams are used, for example, in the DCI storage ring (Orsay, France). The design of all storage rings in the SSRC (VEPP series) allows physical experiments using colliding electron–positron beams (which are accelerated in opposite directions within the same chamber). Similar principles are implied in the German PETRA accelerator (Hamburg, Germany): its name stands for Positron-Electron Tandem Ring Accelerator.

$$\lambda_c = \frac{4\pi eR}{3\gamma^3}. \quad (4)$$

Most widespread types of insertion devices are undulators and wigglers. These are multipole magnetic systems with an intense magnetic field B (0.1 – 10 T depending on the device type) and alternating polarity. The trajectory of electrons becomes strongly curved in the magnetic field of insertion devices, thus the synchrotron radiation with specially selected characteristics can be generated (Fig. 4). Spectral distribution of synchrotron radiation emitted by a bending magnet, wiggler and undulator is shown in Fig. 5; the spectrum from a 'classical' X-ray tube is also given for comparison. Yet another type of specialised magnetic insertion devices is long undulators or free-electron lasers (FEL), which act as sources of coherent monochromatic SR. Currently, more than 100 insertion devices are in operation in the synchrotron radiation centres world-wide.

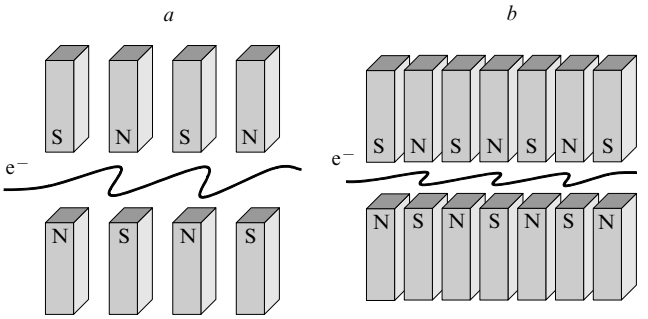

Figure 4. Specialised insertion devices: wiggler (*a*) and undulator (*b*)

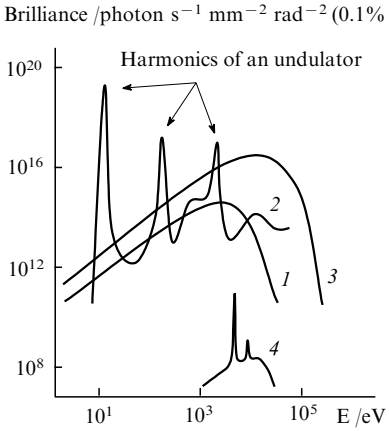

Figure 5. Spectral distribution of SR generated by bending magnet (*1*), undulator (*2*) and wiggler (*3*). For comparison, emission spectrum of an X-ray tube is also shown (*4*).

Adjacent curved sections of the electrons' trajectory within an N-pole wiggler emit independently, which leads to an increase in the intensity of SR by a factor of N compared to radiation of a bending magnet. Yet another advantage of wigglers is that they allow for creation of magnetic fields much stronger (5 – 10 T) than in a bending magnet since in the latter the value of B is linked to the orbit radius [see Eqn (1)], which results in a shift of the critical wavelength to higher energy. This is achieved by using superconducting magnets, which induce transverse 'beats' of the electrons' trajectory with amplitude of a few tenths mm. One wiggler may contain from several up to several tens of magnetic poles.

Compared to wiggler, an undulator is characterised by a larger number of magnetic poles, smaller separation between them and a weaker magnetic field ($\sim$1 T). The operation parameters of an undulator are chosen so as to achieve interference of the emission by adjacent curved trajectory sections. As a result of this interference, spectral distribution of the SR generated exhibits intensity maxima, *i.e.*, the so-called undulator harmonics. The intensity of the harmonics, which is proportional to N^2 is much higher than that generated by both bending magnets and wigglers. Furthermore, the radiation emitted by an undulator is more directed, *i.e.*, its emittance is diminished.[18] Due to differences in physical background and underlying mathematical formalism, synchrotron and undulator radiation are considered separately in the high-energy physics.

An important parameter of the SR is its polarisation, *i.e.*, the existence of preferred directions of the electric field vector. There are two types of the 'pure' polarisation, *viz.*, linear polarisation (the electric field vector oscillates in a certain plane) and circular one (the electric field vector precesses clockwise or counter-clockwise in the plane perpendicular to the direction of the wave propagation). In contrast to X-rays generated by X-ray tubes, synchrotron radiation is always completely polarised. The bending magnet radiation is linearly polarised in the plane of electrons' movement. Upon deviations from this plane up or down, the radiation becomes partially circularly polarised (elliptic polarisation). The synchrotron radiation generated in insertion devices (wigglers or undulators) also exhibits linear or circular polarisation depending on the design of the corresponding device (for example, for generation of circularly polarised SR, helical undulators or elliptic multipole wigglers can be used).

Yet another important characteristic of SR is its coherence, *i.e.*, correlation in oscillations of the electromagnetic field at different space points and at different time moments. The coherence determines the ability of radiation to produce an interference pattern; the planned fourth-generation SR sources approach lasers in this respect. There are two types of coherence, *viz.*, temporal (longitudinal) coherence, which depends mostly on monochromaticity of the SR beam and is characterised by the longitudinal coherence length, and spatial (transverse) coherence, which is, first of all, determined by the emittance of the source.

Synchrotron radiation has a pulse structure. Due to relativistic effects, the electron beam in the storage ring is split into separate moving clusters (bunches), each bunch is of a few cm in length. Therefore, electron current through a bending magnet is not continuous and the SR generated contains periodic pulses with duration of a few tens ps with nanosecond intervals between them. Under certain injection conditions, it is possible to achieve the state where only one bunch of electrons moves in the storage ring (single-bunch mode). In this case, both pulse durations and intervals between them are highly regular, which can be of great importance for time-resolved studies of fast processes.

The key parameter of a SR source is its emittance. It is the emittance, which depends upon perfection of the magnetic system of the source, that reflects most clearly the level of industrial technology involved in the construction of the storage ring. As a rule, the emittance is correlated with the brilliance: the smaller the emittance the higher the brilliance. In addition brilliance depends on the electron current. According to the value of emittance, all the operating synchrotron centres (Table 1) can be conventionally subdivided into generations. First-generation storage rings built in the 60's have the emittance of 100 – 500 nm rad. They were designed and constructed within the scopes of nuclear physics research programmes and thus were not optimised for applications based on utilisation of the synchrotron radiation and such applications took only small portion of the all available beamtime. SR studies on the first-generation storage rings were often conducted in parallel to the main studies on high-energy physics of the electron, positron, or electron – positron colliding beams (in the so-called 'parasitic' mode). In the 80's, the second-generation storage rings with emittance of the order of 50 – 150 nm rad appeared. These accelerators were specialised for SR applications, so they are often referred to as dedicated sources. Most of storage rings which are in operation nowadays belong to the second

Table 1. Characteristics of several storage rings.

Storage ring name (city, country)	Circumference /m	Energy /GeV	Maximum current /mA	Emittance /nm rad	Number of stations	Startup year [a]
DORIS III (Hamburg, Germany)	289.2	4.5	120 (e^+)	404	42	1974 (1995)
VEPP-3 (Novosibirsk, Russia)	74.4	2.0	250 (e^-)	270	9	1975
SRS (Daresbury, UK)	96	2.0	250 (e^-)	104	39	1980
DCI (Orsay, France)	94.6	1.85	300 (e^+)	1600	21	1980
Photon Factory (Tsukuba, Japan)	187	2.5	770 (e^-)	36	21	1982 (1997)
NSLS (Stoney Brook, USA)	170.1	2.6	300 (e^-)	100	70	1982
VEPP-4 (Novosibirsk, Russia)	366	6.0	80 (e^+, e^-)	1200	7	1979 (1992)
BEPC (Bejing, PRC)	65	2.2	100 (e^+, e^-)	76	7	1988
ALS (Berkeley, USA)	196.8	1.9	400 (e^-)	6	19	1993
PLS (Pohang, South Korea)	280.6	2.0	100 (e^-)	12	7	1994
MAX II (Lund, Sweden)	90	1.5	200 (e^-)	8.8	7	1994
SRRC (Hsinchu, Taiwan)	120	1.5	240 (e^-)	19	8	1994
ESRF (Grenoble, France)	844	6.0	200 (e^-)	4	50	1994
ELETTRA (Trieste, Italy)	259.2	2.0	300 (e^-)	7	9	1995
APS (Chicago, USA)	1104	7.0	300 (e^-)	8.2	68	1996
LNLS (Campinas, Brazil)	93.2	1.37	160 (e^-)	100	9	1996
SPRing-8 (Harima, Japan)	1436	8.0	100 (e^-)	5.6	61	1997
Sibir'-2 (Moscow, Russia)	124.1	2.5	300 (e^-)	76	4	1999

[a] In parentheses, the year of last large update of the storage ring is specified.

generation. Several most modern storage rings built in the 90's are classified as third-generation storage rings. They are characterised by emittance of the order of 1 – 10 nm rad and, as a constructive design feature, contain many straight sections in their vacuum chamber between bending magnets for installation of insertion devices. Brilliance of SR sources increases by 2 – 3 orders of magnitude with each new generation.[19] For example, brilliance [photon s^{-1} mm^{-2} rad^{-2} $(0.1\%\ BW)^{-1}$] of first-generation SR sources is $10^9 - 10^{12}$, of second-generation SR sources, it is $10^{12} - 10^{15}$, of third-generation SR sources, it is $10^{18} - 10^{23}$ and $> 10^{24}$ as expected for X-ray free-electron lasers. For comparison, brilliance of standard X-ray tubes and X-ray tubes with rotating anode is only $10^6 - 10^7$.

The modern SR sources generate radiation, which is more intense than that of X-ray tubes by a factor of $10^8 - 10^{14}$. Further modernisation of third-generation storage rings will soon lead to a 'diffraction limit' of a single electron emittance (ε_0)

$$\varepsilon_0 = \frac{\lambda}{2\pi}$$

(where λ is the wavelength of emitted photons), which is equal to 16 pm at $\lambda = 1$ Å ($E = 12$ keV). Thus the currently exploited SR sources are close to the physical limit of brilliance 10^{24} photon s^{-1} mm^{-2} rad^{-2} $(0.1\%\ BW)^{-1}$. The advent of fourth-generation sources with emittance of the order of 0.01 nm rad is related to new technological schemes, such as utilisation of linear accelerators or multi-ring recuperator accelerators and FELs.[12]

3. Components of experimental stations

Special channels guide synchrotron radiation generated in bending magnets, wigglers or undulators to experimental stations (see. Fig. 3). High vacuum should be maintained in these channels, as in the main chamber, in order to minimise losses and radiation background due to absorption of photons by molecules of gases within the channel. Though exact instrumentation of each station largely depends on the specificity of the method used, several main components are common for most stations. These are X-ray optics elements, X-ray monochromators and X-ray detectors.[20]

Virtually in all the cases, optical transformation of the primary SR beam is necessary for experiments, *viz*., collimation (transformation of a divergent beam into a parallel one) and focusing (transformation of a divergent or parallel beam into a convergent one). X-Ray beams with small linear sizes are widely used in X-ray microprobe techniques, X-ray microscopy and microspectroscopy. X-Ray monochromators, which allow one to extract a narrow spectral band with certain (and variable in most cases) wavelength from 'white' synchrotron radiation, are also often considered as X-ray optical elements.

The main tasks of the X-ray optics development include the increase in the energy and spatial resolution and the decrease in the intensity losses associated with the interaction of the respective elements with SR beams. Optical schemes for focusing and monochromatisation of visible light beams (and also, to a great extent, in IR and soft UV spectral ranges), *viz*., lenses, prisms, *etc*., are based on the dispersion phenomenon, *i.e*., the dependence of the refraction coefficient on the wavelength. However, the refraction coefficient for X-rays in most of materials is very close to unity and virtually independent of the wavelength (see below). Besides, soft X-rays are strongly absorbed by virtually all materials (including air). Thus alternative basic principles are used in X-ray optics, such as total external reflection at incidence angles less than 0.1° (grazing incidence), Fresnel scattering and Bragg diffraction.

Most typical optical elements aimed at collimating and focusing the synchrotron X-ray beams include: grazing incidence concave mirrors (toroidal, spherical, cylindrical, *etc*.), curved single crystals, Fresnel zone plates (FZP), Bragg Fresnel lenses (Bragg Fresnel optics, BFO) and tapered capillaries (Fig. 6). Minimal linear size of an X-ray beam achieved in modern SR centres using microcapillary techniques is 20 – 50 nm. The disadvantage of tapered capillaries is strong divergence of the focused beam after the focal point, so they should be mounted very closely to the sample under investigation. FZP and BFO allow one to produce virtually parallel X-ray beams with linear sizes of the order of 1 μm. In applications which do not require very high spatial resolution, concave X-ray mirrors are most commonly used. Generally, an X-ray mirror represents a glass or silicon support coated with a fine and extremely smooth layer of non-oxidisable noble metals (Rh, Pt or Au). A focusing mirror allows amplification of SR beam intensity by 1 – 2 orders of magnitude at the costs of decrease in its linear size.

Some of the aforementioned optical elements (curved crystals, FZP, BFO) can also play a role of a monochromator. In addition, multilayer periodical structures and coatings as well as gratings are often used as monochromators for soft X-rays. Multilayer X-ray mirrors produce sufficiently high intensity of the reflected

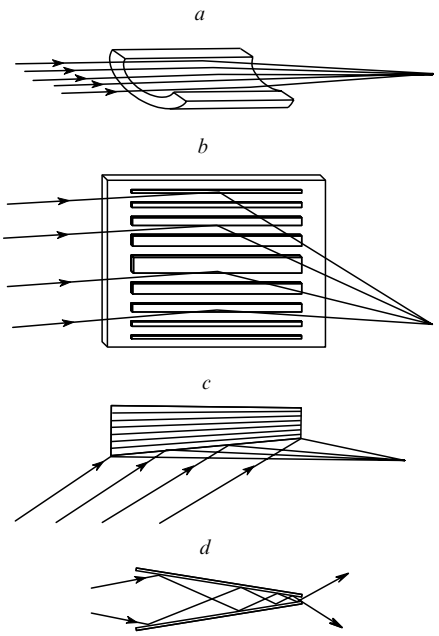

Figure 6. Main types of optical elements for collimating and focusing X-ray SR:
(*a*) X-ray mirror, (*b*) Bragg trensel lens, (*c*) focusing multilayer mirror, (*d*) tappered capillary.

beam even at usual incidence angles (up to a few degrees) and simultaneously focus and monochromatise the primary beam.

In the hard X-ray range, single crystals oriented in a diffracting position by one of its crystallographic planes are most typical monochromators. Among such monocromators, flat single-crystal plates, channel-cut monochromators and more advanced double crystal monochromators with two independent drives are well known. Upon variation of an incident radiation wavelength, the exit-axis of a channel-cut monochromator can drift by a few millimeters, whilst the independent drives of two single crystals make it possible to fix the spatial direction of the monochromatised beam.

The most important characteristic of a monochromator is its energy (or wavelength) resolution $\Delta E/E$ (or $\Delta\lambda/\lambda$). For example, energy resolution of a monochromator based on a flat mosaic graphite crystal with the diffracting plane [002] is $\sim 10^{-2}$; for double crystal monochromator with Si [111] crystals, this value is $\sim 10^{-4}$. Higher resolution can be achieved by utilising low-intensity reflections from higher-order crystallographic planes along directions almost perpendicular to the crystal surface (back reflections). For instance, monochromators with Si [13 13 13] crystals in the back reflection geometry allow one to reach a $\Delta\lambda/\lambda$ resolution of $\approx 10^{-8}$. For experiments requiring very high energy resolution, systems of nested double crystal monochromators are often applied (Fig. 7). A very promising direction in the field of X-ray monochromatisation is the utilisation of the resonance nuclear diffraction phenomenon, which allows one to reach resolutions down to 10^{-10}. It has to be noted that monochromatisation of a 'white' SR beam (extraction of a narrow spectral band) is always accompanied by great losses in intensity.

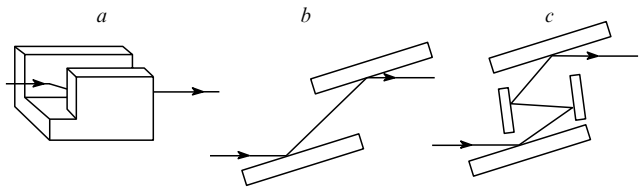

Figure 7. Examples of X-ray monochromators: (*a*) channel-cut monochromator, (*b*) double-crystal monochromator with independent drives for both crystals, (*c*) a system of two nested double-crystal monochromators.

An X-ray beam monochromatised using Bragg diffraction from a single crystal is always contaminated with higher harmonics, *i.e.*, radiation components with an energy multiple of the main component. In order to reject these harmonics, grazing incidence mirrors are often used with parameters adjusted so that the total reflection condition holds for the main component only; higher harmonics in this case pass without changing direction. In double-crystal monochromators, the harmonic rejection can be achieved by slight detuning of the two diffracting crystalline planes (this is however accompanied by noticeable losses in the main component intensity).

In some methods, (*e.g.*, in the energy-dispersive modification of XAFS spectroscopy, see below), similar X-ray optical elements based on Bragg diffraction (in particular, curved single crystals) are used not for monochromatisation but for decomposition of the 'white' beam into spectral components and defining certain spatial directions for photons with different energies (crystal-polychromators).

For control and modification of SR polarisation properties, a specialised polarised optics is used: crystal-polarisers, X-ray quarter-wave plates, phase retarders, *etc*. The state-of-the-art of modern X-ray optics is discussed in detail in a number of reviews (see, for example, Refs 1–4, 20–22).

Virtually any experiment utilising X-ray radiation requires measurement of beam intensities (primary, transmitted through a sample, fluorescent, *etc*.). For this purpose, X-ray detectors are used. Basic characteristics of an X-ray detector are sensitivity, linearity range, maximum load, counting rate, energy and spatial resolution. The following types of detectors are most often used in modern synchrotron radiation centres: photographic films and plates, ionisation chambers, proportional counters, scintillation detectors, solid state semiconducting detectors and charge-coupled devices (CCD).

Depending on spatial resolution, all detectors can be subdivided into point and position-sensitive detectors (PSD). In turn, the latter can be linear (1*D*) or two-dimensional (2*D*). PSDs allow registration of X-ray intensity distribution over a certain spatial area. Of them, multichannel (multiwire) proportional counters, detectors of the type Image Plates (which transform X-rays into visible light in recurring cycles 'energy storage as crystalline lattice defects – stimulated emission in the visible spectral range upon laser irradiation') and CCDs are most popular.

Scintillation counters and ionisation chambers are 'classical' X-ray detectors. They possess extremely high sensitivity (down to registration of single photons). Ionisation chambers are often used as primary beam monitors due to their wide linearity range and ability to operate under conditions of very intense X-ray beams. For some specific tasks (such as imaging, small angle scattering, sample adjustment in a beam), photofilm and photosensitive paper are still in use.

Solid-state semiconducting detectors exhibit high energy resolution. They are applied in cases where a spectral distribution analysis of the detected X-ray radiation is required. Avalanche photodiodes (APD), where each photon coming into the semiconducting diode generates an 'avalanche' of electron – hole pairs are the fastest of the modern X-ray detectors. Such detectors allow intensity measurements for very short pulses of SR (~ 0.1 ns), so they are widely adopted in time-resolved studies of fast processes.

III. Interaction of X-rays with matter

Upon interaction with the matter, X-ray radiation can be scattered or absorbed. These processes as well as combined phenomena of inelastic and anomalous scattering form the basis of X-ray methods of physicochemical analysis.

When a photon is scattered on a particle of a medium and changes its directions, its energy can either be conserved (elastic scattering) or partially transferred to the matter (inelastic scattering). Inelastic scattering can be due to various channels of energy transfer including excitation of collective vibrations of atomic nuclei in a crystalline lattice (phonons) or charge carriers, *viz*., electrons and holes in a conduction zone (plasmons); excitation of electrons from valence zone to vacant energy levels with creation of electron – hole pairs; ionisation of core level electrons of light elements (the so-called X-ray Raman scattering).

For standard energy of a primary beam of ~ 10 keV, inelastic losses due to phonon excitations have the order of a few meV, plasmon losses and losses due to electron – hole pairs creation lie in the range of 0.5 – 10 eV, ionisation of core electron levels may lead to losses of several tens or hundred eV (depending on the binding energy of the excited level). In the case of very hard X-ray radiation, the energy of which is much larger than the binding energies of electrons in atoms, the dominant channel of inelastic scattering is the Compton scattering of X-ray photons on quasi-free electrons (without quantum restrictions on the momentum and energy transfer). Harder γ-radiation with energy starting from several MeV (which usually is not produced by standard SR sources and thus is not considered in detail in this review ‡) interacts with the matter through the mechanisms of elementary particles' transformation, for example, by generation of electron – positron pairs.

Elastic (coherent) scattering of X-ray photons depends primarily on their interaction with electron shells of atoms (Thomson scattering). Since the energies (*i.e*., the wavelengths) of all the scattered photons are the same, elastic scattering can lead to diffraction, *i.e*., a spatial redistribution of the scattered beam intensity as a result of interference of waves coming from different atoms. When atomic arrangement has a translational symmetry (as in crystals), diffraction reflections, *i.e*., narrow maxima of the scattered wave intensity arise at certain directions. Furthermore, a persistence of a mean local atomic order even in amorphous substances gives rise to sinusoidal oscillations of the smooth (without sharp maxima) elastically scattered background as a function of the scattering angle. Diffraction phenomena form the basis of a number of experimental techniques which allow studies of fine details in the structure of the matter, including local atomic environment, supramolecular arrangement and periodicity elements (types of partial ordering).[23, 24]

Absorption of X-ray photons leading to attenuation of the photon beam as it propagates in a medium is primarily related to the photoelectric effect, *i.e*., photoionisation of inner electronic shells of atoms. In this case, a vacancy (hole) in the respective core electron level and a free electron are generated. All the methods of X-ray absorption spectroscopy are based on the analysis of X-ray absorption coefficient as a function of the energy of incident photons. Energy and spatial distribution of the photoelectrons generated in this process are the main subject of X-ray photoelectron spectroscopy techniques.[25]

The excited state with a vacancy in the core level (X-ray term), to which an atom transfers upon absorption of an X-ray photon, is metastable with a lifetime not longer than 10^{-15} – 10^{-16} s. The photoionised atom tends to diminish its energy by filling the core level hole with an electron from higher-lying levels. This can be achieved either through emission of an X-ray photon of lower energy (X-ray fluorescence) or through a radiationless two-electron process involving a transition of one electron from a higher electronic level to the core level vacancy with simultaneous detachment of a second electron (the Auger process). X-Ray fluorescence is the dominant direction of decay of an X-ray term with a *K*-shell hole (*K*-term) for atoms with atomic numbers $Z > 20$ and with $Z > 90$ for an *L*-term (Fig. 8).

‡ Recently, generation of hard γ-rays using Compton back scattering of a laser light on ultrarelativistic electrons has been developed in several synchrotron radiation centres (see, for example, Ref. 12).

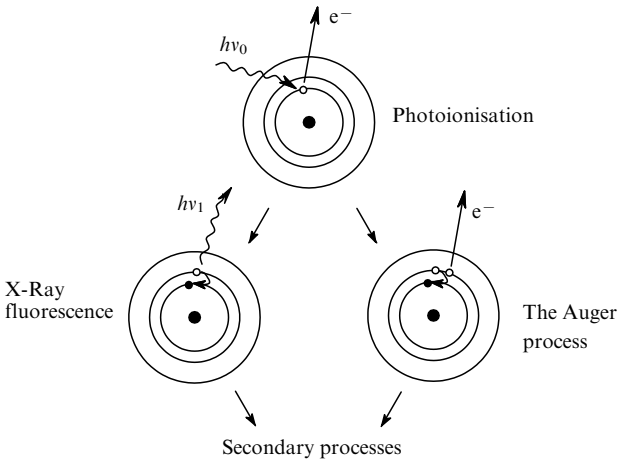

Figure 8. The main processes occurring in matter upon absorption of an X-ray photon.

X-Ray fluorescence and the Auger process result in new holes and thus evoke a cascade of secondary processes, such as emission of secondary electrons, fluorescence in the longer wavelength region, *etc*. In particular, secondary processes can lead to the appearance of luminescence in the visible light range. This phenomenon forms the physical background of the XEOL (X-ray excited optical luminescence) method. Energy transferred to the system from the absorbed X-ray photon can result in cleavage of chemical bonds and detachment of molecular fragments (photostimulated ion desorption, PSID). X-Ray absorption by semiconducting materials is accompanied by an increase in concentration of charge carriers in the conduction zone and thus by an increase in their conductivities. Secondary processes initiated by absorption of X-ray photons are widely utilised in various techniques like X-ray fluorescence spectroscopy, Auger electron spectroscopy, secondary electron spectroscopy, *etc*.

Absorption of X-ray photons in matter can also occur due to nuclear excitations. In particular, the Mössbauer spectroscopy is based on this phenomenon. Generally, this technique is not considered as a sort of X-ray spectroscopy but rather referred to as a distinct field, *viz*., γ-spectroscopy. However such a discrimination is arbitrary: the energy of the nuclear transition in the ^{57}Fe isotope, most often exploited in the Mössbauer spectroscopy (14.4 keV) is close and even slightly less than the energy of characteristic radiation produced by an Mo K_α X-ray tube, which is most popular in X-ray diffraction experiments (17.4 keV). The energy of nuclear excitations for many other isotopes commonly studied by Mössbauer spectroscopy lies also in the range of 10 – 100 keV attainable with modern SR sources. As in the case of electron excitations, excited nuclear states are metastable (however their lifetimes are substantially longer than that of electronic states, *viz*., $\sim 10^{-7}$ s) and the excited nucleus reverts back to its ground state with emission of an X-ray photon of the corresponding energy. The energy of emitted photon may be equal to (elastic or coherent nuclear scattering), or slightly less (inelastic scattering) than, that of the initial radiation. Due to longer lifetime of excited nuclear states, absorption and emission bands associated with nuclear transitions are exceptionally narrow.[26]

When X-ray beam strikes an interface, X-ray reflection occurs with the reflection angle equal to the incidence angle. However, in contrast to, for example, visible light, the probability of the X-ray reflection decreases rapidly with an increase in the incidence angle and for large incidence angle common for visible light optics, the X-ray beam simply crosses the interface not changing its direction. Noticeable X-ray reflection can be observed only at very small grazing incidence angles ($\sim 0.1\,^\circ$) under conditions of the so-called total external reflection. Under this condition, the penetration

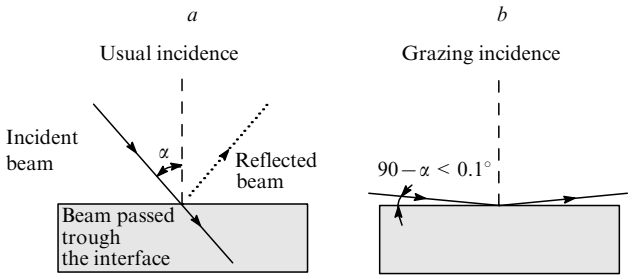

Figure 9. Reflection of an X-ray beam from a surface under conditions of usual (*a*) and grazing (*b*) incidence.

depth of X-ray radiation into the matter is only of a few atomic layers (Fig. 9). This phenomenon has to be taken into consideration in design of X-ray mirrors and focusing microcapillaries; moreover, it is the basis of a number of surface investigation techniques.

IV. X-Ray methods of physicochemical analysis

All X-ray-based research methods can be classified based on the processes which accompany interaction of X-rays with the matter. According to this principle, the following groups of methods can be formulated: X-ray spectroscopy, X-ray electron spectroscopy, X-ray diffraction and X-ray inelastic scattering. Additional independent groups include methods utilising effect of the resonance nuclear scattering (Mössbauer spectroscopy) and imaging techniques.

1. X-Ray spectroscopy

a. X-Ray absorption spectroscopy

The subject of X-ray absorption spectroscopy is the analysis of the X-ray absorption coefficient (μ) as a function of the incident photons energy $\mu = \mu(E)$. In the most common transmission mode, the linear absorption coefficient is determined by the formula

$$\mu = \ln\frac{I_0}{I_t}, \qquad (5)$$

where I_0 and I_t are intensities of the incident X-ray beam and the beam transmitted through the sample. This formula coincides with the respective relations for linear absorption coefficients in other spectral ranges (UV, visible, IR), since X-ray absorption also obeys the Bouguer – Lambert – Beer law, which links attenuation and optical path of radiation propagating in a medium. The major part of modern X-ray absorption spectroscopy studies is performed using SR, since they require scanning the incident beam energy over a broad spectral range.

The X-ray absorption coefficient increases sharply for certain values of incident radiation energy superimposed on a smooth $\mu(E)$ curve monotonically decreasing with an increase in the energy. This resonance absorption induced by photoionisation of atoms of a certain element (see above) define 'triangular' shape of X-ray absorption bands (Fig. 10 *a*). Near the absorption edge, the $\mu(E)$ manifests a fine structure. The fine structure is subdivided into two types, *viz*., X-ray absorption near-edge structure XANES (Fig. 10,*b*) and extended X-ray absorption fine structure expressed as $\psi(k)$ EXAFS (Fig. 10 *c*). XANES covers the energy range from ~50 eV before the absorption edge up to 100 – 150 eV after it. This fine structure is composed of relatively narrow resonance bands generated by electron transitions from the core level to vacant energy levels up to complete ionisation (*i.e*., photoionisation) along with broader bands associated with electron transitions to quasi-bound states (multiple scattering). The oscillatory structure EXAFS, which appears as a result of a free photoelectron scattering on the local atomic environment, is observed in the energy range of 100 – 1000 eV above the absorption edge.

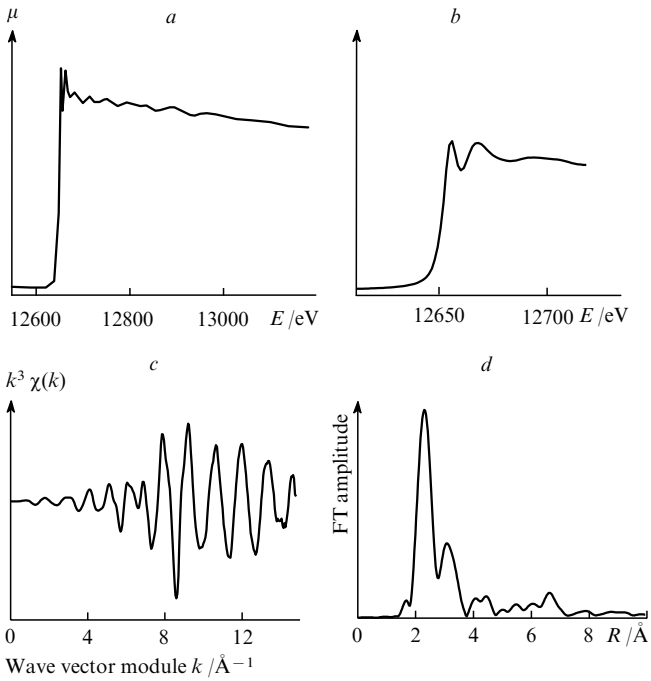

Figure 10. Steps of an EXAFS data processing:
(*a*) an experimental X-ray absorption spectrum; (*b*) the amplified XANES region; (*c*) the normalised EXAFS curve, *i.e*., the oscillating part of the X-ray absorption coefficient; (*d*) the Fourier transform (FT) of the normalised EXAFS curve, the maxima of the Fourier transform correspond to the coordination spheres around the central atom.

XANES spectroscopy is used in studies of electronic structure of substances, including determination of the energy and symmetry of vacant orbitals in molecules or unoccupied zones above the Fermi level in solids. In particular, using this method, information on the oxidation state and coordination symmetry of the central atom can be obtained.[27,28] Analysis of EXAFS gives additional structural information on the local order around the absorbing atom, including the type and the number of closest neighbours as well as interatomic distances within a sphere with the radius of 5 – 6 Å (see Fig. 10 *d*).[29,30] In addition to the interatomic distances, bond angles can be found using such modern approaches as the assessment of multiple photoelectron scattering or simultaneous fitting of spectra measured at the absorption edges of several elements in the sample. In modern X-ray absorption spectroscopy, a common term XAFS (or XAS), which covers both EXAFS and XANES, is often used.

Since the intensities of all the secondary processes are determined by the number of X-ray photons absorbed (*i.e*., by the number of holes generated in the core level), the quantum yields of these processes are proportional to the X-ray absorption coefficient and their energy dependencies exhibit XAFS-like fine structures. For example, such a fine structure is manifested in the dependence of the X-ray fluorescence intensity I_f on the energy of incident photons. Due to substantially higher signal-to-background ratio, the fluorescence yield defined as the ratio of I_f to the intensity of the excitation radiation I_0

$$\mu(E) = \frac{I_f}{I_0},$$

is 10 to 100-fold more sensitive to the oxidation state and local atomic environment of the photoionised atom than the X-ray absorption coefficient measured in the transmission mode.

XAFS in the fluorescence yield mode can be used for the analysis of the oxidation state and coordination of admixture atoms (in concentrations down to 0.1% – 0.2%).[31] Registration of the total or the Auger electron yield

$$\mu(E) = \frac{i_e}{I_0},$$

(where i_e is the electron current) as a function of incident photon energy leads to enhancement of EXAFS sensitivity to surface layers of the sample since the escape depth of electrons does not exceed 50–100 Å.[32] The optical luminescence yield in XEOL [33] or the ion yield in PSID [34] can be used in a similar way.

XAFS allows investigations of substances in any aggregate state. Therefore, it is applicable to the solution of a broad range of structural chemical problems related to the electronic state and local atomic surroundings of a certain element. Methods of X-ray absorption spectroscopy proved to be efficient in structural investigations of semiconductors,[35] superconductors,[36] amorphous glasses and alloys,[37] polymeric electrolytes,[38] ceramics,[39] metallocentres in biomolecules,[40–42] supported catalysts,[43–45] metallic nanoclusters,[46–48] *etc*. XAFS studies of solutions reveal information on structural rearrangements of molecules,[49] solvation mechanisms and structures of solvate shells of ions.[50,51] This method can be used for structural monitoring of reactions in solutions (*e.g*., electrochemical processes).[52] Structural studies of melts give important information on the nature of the interatomic interactions.[53]

In the soft X-ray range at the absorption edges of light elements, such as B, C, N, O and F (the excitation energies from 100 to 1000 eV), the X-ray absorption fine structure is usually referred to as NEXAFS (near-edge X-ray absorption fine structure).[54] Soft X-rays are strongly absorbed in matter (photon free path is only a few tens of nm), therefore NEXAFS is a surface-sensitive technique. The corresponding spectra are generally recorded in vacuum or in a helium atmosphere in the total electron yield mode. The NEXAFS spectroscopy is widely applied for characterisation of polymers,[55] chemisorbed molecules,[56] adsorbed monolayers,[57] Langmuir–Blodgett films, *etc*. For example, thin films of higher fullerenes, which are available only in minute quantities, have been characterised using this method.[58] Though extended oscillating structure is not very prominent in NEXAFS spectra, they are sensitive to the long-range atomic ordering,[57,58] which allows identification of, for example, conformations of long-chain hydrocarbon fragments or individual atomic clusters C_n with $n \leqslant 96$ (Fig. 11).[58]

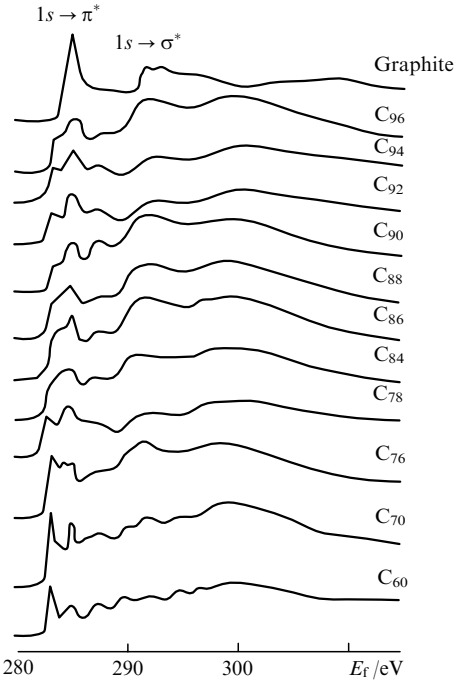

Figure 11. Carbon *K*-edge NEXAFS spectra for a series of fullerenes C_n ($n = 60–96$). Electronic transitions making principal contributions into the respective absorption bands are shown.[58]

Recently, significant attention has been drawn to XAFS spectroscopy in the energy range of 1.5–3 keV, which is intermediate between hard (> 5 keV) and soft (< 1 keV) X-rays.[59] Such techniques require expensive ultrahigh vacuum equipment, which is generally utilised in the soft X-ray region, but methodological approaches developed for hard X-ray studies can be applied to them. As an example, SOEXAFS (soft EXAFS) may be mentioned. The aforementioned energy range covers *K* absorption edges of such key elements as magnesium (~1.30 keV), aluminium (~1.56 keV) and silicon (~1.84 keV), which form the base for many building materials and composites, natural minerals, supports for catalysts, organometallic reagents, *etc*.[60–62] Furthermore, *K*-edges of phosphorus (2.14 keV) and sulfur (2.47 keV), which are constituent of many organic molecules, also belong to this region.[63]

b. X-Ray fluorescence spectroscopy

Methods of X-ray fluorescence (emission) spectroscopy (XRF) are based on detection and spectral analysis of the secondary radiation emitted by a substance following absorption of monochromatic or 'white' synchrotron radiation. They are in active use for elemental analysis of specimens of various origin.[64] An X-ray emission spectrum in XRF analysis measured usually in a broad energy range (typically up to a few tens keV) presents a set of characteristic emission lines corresponding to electron transitions from occupied levels to core holes. Modern synchrotron radiation-based X-ray fluorescence analysis is one of the most sensitive and accurate non-destructive methods for the determination of trace element concentration. In routine multi-element analysis, the lowest detection limit for a broad range of elements from calcium to actinides reaches the level of 0.1 ppm (*i.e*., 10^{-7} g g^{-1});[65] ~0.1 mg of a sample is required to carry out the measurement and the measurement itself takes a few minutes. This enables compositional analysis of samples available only in very small amounts, such as in the case of microelement distribution in lunar rock probes (Fig. 12).[66] In dedicated studies optimised for quantitative analysis of a single element or a limited range of elements, the sensitivity as high as ~1 ppb (*i.e*., 10^{-9} g g^{-1}) and even several ppt (*i.e*., 10^{-12} g g^{-1}) in the analysis of aerosols pumped through a filter, can be achieved.[67]

High-resolution X-ray fluorescence spectroscopy is an established technique for characterisation of the electronic structure of matter, *viz*., for the determination of energy distribution of occupied electronic states below the Fermi level. Information on the electronic structure collected by this method is complementary

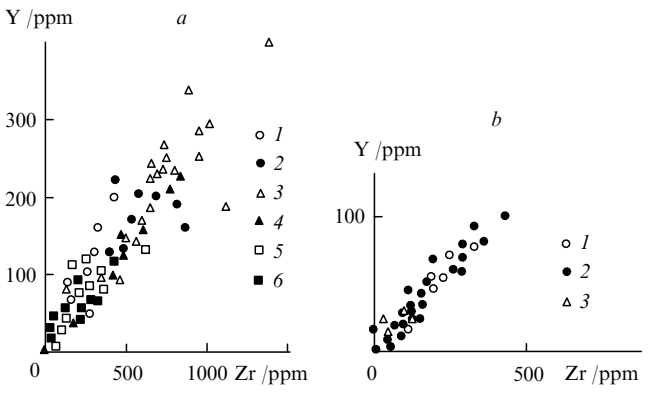

Figure 12. Zirconium *vs*. yttrium concentration correlations in samples of lunar rocks collected in 'Apollo' (*a*) and 'Luna' (*b*) space missions as determined using synchrotron X-ray fluorescence analysis.[66]
(*a*): (*1*) Apollo-11, (*2*) Apollo-12, (*3*) Apollo-14, (*4*) Apollo-15, (*5*) Apollo-16, (*6*) Apollo-17; (*b*): (*1*) Luna-16, (*2*) Luna-20, (*3*) Luna-24.

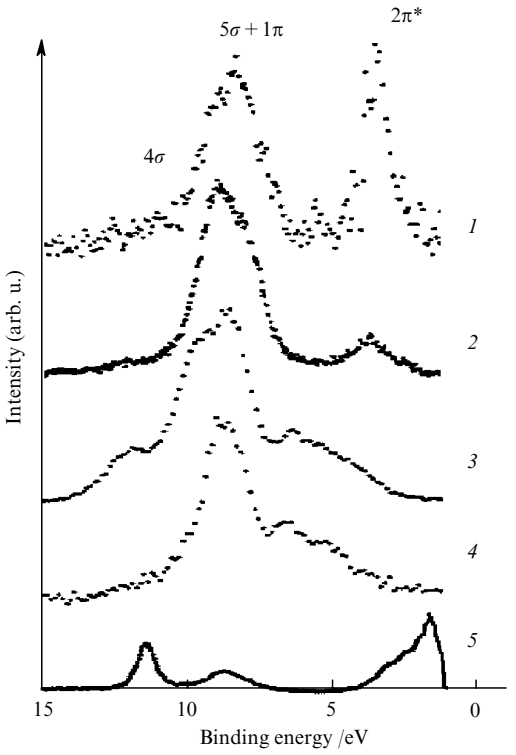

Figure 13. High-resolution soft X-ray fluorescence (C K_α and O K_α) of CO adsorbed on the (100) face of Ni single crystal.[70]
X-ray C K_α fluorescence: (*1*) perpendicular to the surface of Ni(100) face (π-components make major contribution); (*2*) parallel to the adsorbed layer. X-ray O K_α fluorescence: (*3*) parallel to the adsorbed layer; (*4*) perpendicular to the adsorbed layer; (*5*) usual XPS spectrum.

to that obtained using X-ray absorption spectroscopy. Exact positions of X-ray fluorescence lines recorded with high precision depend upon the oxidation state and coordination environment of the element under study.[68] High-resolution XRF spectroscopy can thus be considered as an analogue of the X-ray photoelectron spectroscopy (see next section), which does not require recourse to ultrahigh vacuum equipment. X-Ray fluorescence spectroscopy in the soft X-ray region is particularly informative in studies of organic molecules.[69–71] Resonant photoionisation of atoms of a certain element achieved using monochromatic radiation with the specially adjusted energy (resonant X-ray emission) enhances selectively the intensities of transitions to the vacant level generated in this process and of all the transitions in the cascade of associated secondary processes. This leads to a substantial increase in the sensitivity.[72] For instance, in a study of CO chemisorbed on metallic Ni, this approach allowed one to demonstrate experimentally donation of electrons from the Ni atoms to the $2\pi^*$ molecular orbital of CO (Fig. 13 and Scheme 1).

Scheme 1

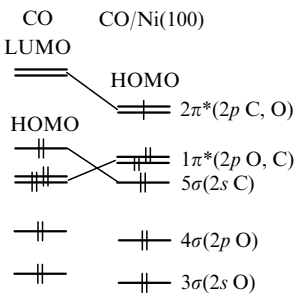

(LUMO is the lowest unoccupied molecular orbital; HOMO is the highest occupied molecular orbital).

Recent achievements in the field of applications and instrumentation of synchrotron X-ray fluorescence spectroscopy are discussed in reviews.[64, 73, 74]

c. X-Ray electron spectroscopy

In traditional methods of X-ray electron spectroscopy, the energy distribution of electrons knocked out of the sample by an X-ray beam is analysed. There are several types of X-ray electron spectroscopy, such as X-ray photoelectron spectroscopy (XPS, sometimes also referred to as ESCA, *i.e.*, electron spectroscopy for chemical analysis), Auger electron spectroscopy (AES), secondary electron spectroscopy (SES), *etc.* All the electron spectroscopy techniques are used for surface studies since the electron escape depth in the energy range typical of these methods does not exceed 50 – 100 Å.

XPS and AES are common methods for quantitative analysis of the surface chemical composition. Positions of lines in the XPS spectra correspond to binding energies of the corresponding electron levels, *i.e.*, they give information on the electronic state of atoms at the surface (chemical shift of core levels) and energy structure of the valence zone. Several other effects are manifested in XPS and give additional information, *viz.*, spin-orbit splitting of lines into multiplets, two-electron excitation processes (low energy shake-up and shake-off satellites), inelastic energy losses of photoelectrons (characteristic bulk and surface plasmons). The use of SR increases the sensitivity and energy resolution of the method noticeably due to high intensity of SR and availability of strictly monochromatic X-ray beams, respectively.[75] Variation of the excitation energy, for example, allows one to distinguish photoelectron and the Auger lines in complex spectra (the positions of the Auger lines, in contrast to photoelectron ones, do not depend on the excitation energy).[25, 76]

As in the case of XRF, additional information can be obtained from XPS spectra provided that the excitation energy is chosen close to one of the edges of resonance absorption (resonant photoemission). This method, in particular, can be used for the determination of contributions of certain atomic orbitals to molecular orbitals, which is important for chemical bonding description, for example, in transition metal complexes with π-ligands (Fig. 14).[77, 78] By varying energy of the incident beam, incidence angle or electron escape angle, one may reconstruct concentration *vs.* depth profiles of the elements under study.

A new promising branch of photoelectron spectroscopy, *viz.*, angular-resolved X-ray photoelectron spectroscopy (ARXPS),[79]

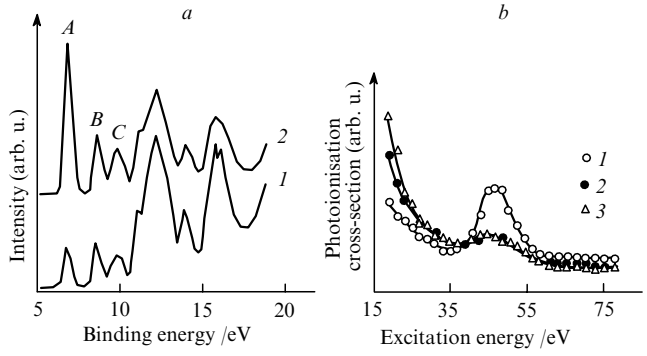

Figure 14. Valence zone photoelectron spectra of the π-complex $Ti(\eta^7\text{-}C_7H_7)(\eta^5\text{-}C_5H_5)$ for two different excitation energies (*a*) and dependence of relative photoionisation cross-sections for bands *A*, *B* and *C* upon the excitation energy (*b*).
(*a*) Excitation energy /eV: (*1*) 33, (*2*) 48; (*b*) band: (*1*) *A*, (*2*) *B*, (*3*) *C*. Sharp increase in the band *A* intensity for the excitation energy of ~48 eV due to approach of the excitation energy to the $M_{II,III}$ absorption edge of Ti ($3p \rightarrow 3d$ resonance) indicates that this band is mostly composed of Ti $3d$ atomic orbital; bands *B* and *C* correspond to molecular orbitals with significant contribution of the ligand orbitals.[77]

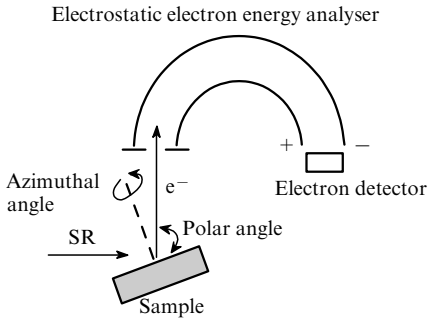

Figure 15. A scheme of a photoelectron spectrometer for recording angular-resolved spectra.

is actively developing in modern SR centres over the last years. This method is based on registration of a spatial distribution of photoelectrons with certain kinetic energies (Fig. 15). Analysis of this distribution allows one to extract the contribution of photoelectron scattering on local atoms surrounding the photoionised atom, *i.e.*, the effect of the photoelectron diffraction. In contrast to other techniques utilising electron diffraction, such as low-energy electron diffraction (LEED) or reflected high-energy electron diffraction (RHEED), the photoelectron diffraction is observed in systems both with and without long-range atomic ordering of a surface. ARXPS, like XAFS, allows studies of local atomic environment of photoionised atoms in samples with disordered or partially ordered surface structure. In particular, this method proved its effectiveness in studies of sorption–desorption processes. This allows one to reveal positions and orientations of diatomic or more complex molecules adsorbed on crystallographic faces of metal single crystals and to estimate adlayer–support distances as a function of adsorbate concentration. Photoelectron diffraction can be applied to structural characterisation of various surface systems, *viz.*, thin films, epitaxial deposits, surface alloys, metal–semiconductor interfaces, oxide layers, supported metal nanoclusters, products of ion-implantation, as well as processes like growth of interfaces and surface phase transitions including melting.[80–82]

Further development of the theory and instrumentation of ARXPS has lead to appearance of a new method for surface structural studies, *viz.*, photoelectron holography. Photoelectron holography is based on mathematical processing of large body of data on the intensities of photoelectron lines obtained by varying the sample orientation relative to the incident beam and detector (both azimuthal and polar scans) and excitation X-ray radiation energy. Holographic processing of ARXPS data allows complete reconstruction of spatial arrangement of atoms within the sphere with a radius of 5–20 Å around the photoionised atom with an accuracy in atomic positions of 0.02–0.05 Å.[83] Similar approaches are being developed in Auger electron spectroscopy and X-ray fluorescence spectroscopy.[84]

2. X-Ray diffraction methods

a. Single crystal X-ray diffraction

X-Ray diffractometry is a most important experimental method of modern structural chemistry. This allows one to determine the atomic structure of a single crystal (including unit cell parameters, space group, coordinates and types of atoms within the unit cell and parameters of their thermal vibrations). Based on atomic coordinates, any structural characteristics like interatomic distances, bond and torsion angles, *etc.*, can easily be calculated. In contrast to the majority of structural methods, X-ray diffractometry allows complete objective determination of a crystal structure without prior knowledge of any of its structural characteristics and even chemical composition.

The set of experimental data measured by X-ray diffractometry includes angle coordinates and intensities of reflections generated by diffraction of X-rays on a single crystal. The scattering of X-rays occurs primarily on electron shells; thus, mathematical processing of the experimental data (Eulerian angles and intensities of reflections) allows reconstruction of the electron density distribution $\rho(r)$ in the unit cell. In routine diffraction experiments, distinct maxima of the $\rho(r)$ function corresponding to the centres of atoms, are revealed with the accuracy of 0.01–0.02 Å. Based on high-precision data, fine features of the electron density distribution functions, such as valence electrons redistribution due to formation of chemical bonds, as well as other physicochemical characteristics of a crystal related to $\rho(r)$ can be analysed. Qualitatively, the redistribution of electron density can be visualised in deformational electron density maps $\Delta\rho(r)$ obtained by subtraction of the promolecule's electron density [composed of spherically symmetric non-interacting atoms whose positions are determined from the 'high-angle' refinement of the structure versus reflections with high $(\sin\theta)/\lambda$ ratio, where θ is the diffraction angle and λ is the wavelength] from the total experimental $\rho(r)$ function.

Currently, the most popular technique in chemical X-ray crystallography is the conventional single crystal diffractometry based on diffraction of monochromatic X-ray beam on a single crystal. X-Ray tubes are most often used as an X-ray source. A serious disadvantage of this method is very strict requirements to the quality of a sample under study. It has to be a well-formed single crystal with linear dimensions of approximately 0.1–1 mm and a sufficient diffraction power at a fixed wavelength (typically, characteristic Mo K_α $\lambda = 0.71$ Å or Cu K_α $\lambda = 1.54$ Å radiation). If a crystal is smaller than the dimensions mentioned or it is of poor quality (due to domain misorientation, static or dynamic disorder of molecules or molecular fragments in the unit cell, *etc.*), the routine structure solution becomes very complicated or even impossible. Such accompanying phenomena as X-ray absorption, anomalous dispersion, multiple diffraction and extinction (deviations of X-ray reflection intensities from the values predicted by the kinematic X-ray scattering theory) further decrease accuracy of the X-ray diffraction results.[23,24]

The use of SR in X-ray crystallography eliminates many restrictions of this method. Due to high intensity of SR beams with a capability of their further focusing and collimation by X-ray optics, it is possible to collect reflection sets of satisfactory quality for weakly diffracting and very small crystals. Low divergence of SR beams leads to improvement of angle resolution in high-precision diffraction experiments.[85–88]

Routine synchrotron X-ray crystallographic studies of low-molecular-weight compounds are now developing in two principal directions, *viz.*, investigations of samples not applicable to laboratory diffractometry (*e.g.*, due to a weak diffraction power)[89,90] and experimental investigations of electron density distribution in crystals.[91] Nowadays, crystals with linear dimensions down to several micrometers can be characterised by X-ray diffraction in synchrotron centres.[92,93] Such crystals are commonly formed in a chemical synthesis[94] and they are particularly typical in geology and mineralogy.[95,96] For mounting of such small crystals onto a diffractometer, special methods and devices (for example, on the stage of an electron microscope) are required.[97,98]

In the 90's, systematic studies of electron density distribution in crystals based on high-precision diffraction experiments were started in synchrotron radiation centres. Data acquisition time required for these studies shortened down to 15–20 hours from 10–15 days needed with laboratory equipment. Furthermore, requirements for the quality of single crystals for the studies also became not so strict as, for example, in high-precision studies (Fig. 16).[99–102] Application of hard X-ray radiation reduces absorption and extinction and increases the resulting accuracy due to larger number of observed reflections with high $(\sin\theta)/\lambda$ ratio. In high-precision laboratory experiments, Ag K_α line of X-ray tubes ($\lambda = 0.56$ Å) is used whereas several studies with synchrotron radiation wavelengths as short as 0.3–0.1 Å have been reported.[103–105]

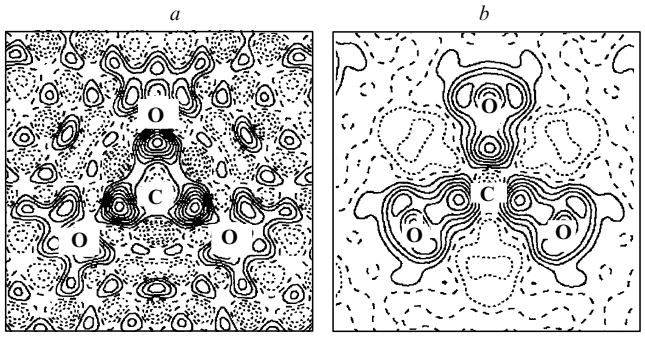

Figure 16. Static deformational electron density maps $\Delta\rho(r)$ reconstructed in high-precision X-ray diffraction studies of $MnCO_3$ single crystal (section in the plane of the carbonate group, solid lines correspond to positive and dashed lines to negative deformational electron density; contours are drawn with a step of 0.1 e $Å^{-3}$): (*a*) data collected on a laboratory diffractometer, (*b*) SR data (Photon Factory, Tsukuba, Japan).[100]

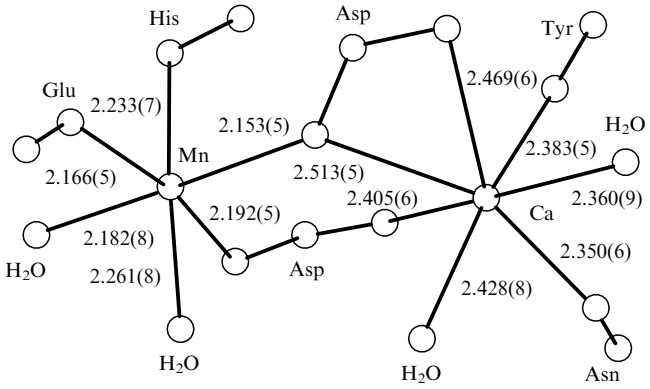

Figure 17. Geometry of the metallocentre in the protein concanavalin A determined using synchrotron X-ray single-crystal diffraction with accuracy typical of low molecular-weight compounds (the synchrotron centre CHESS, Ithaca, USA, $\lambda = 0.92$ Å). Only the atoms of amino acid fragments coordinated to the metal atoms are shown. The crystallographic parameters are as follows: orthorhombic, $a = 89.55(2)$ Å, $b = 86.46(2)$ Å, $c = 62.11(1)$ Å, space group $I222$, 116923 observed reflections, 19158 least-squares parameters refined for 2134 independent non-hydrogen atoms, $R_F = 12.2\%$.

In processing of high-precision synchrotron X-ray diffraction data, the most advanced computational techniques are applied, *viz*., multipole refinement and topological analysis of the $\rho(r)$ function.[99,106] Comparison of SR-based and laboratory approaches shows that the accuracy of synchrotron diffraction experiments is at least not lower than that obtained using laboratory diffractometers and is noticeably higher in many cases (see Fig. 14).[100,107,108] For example, one of the most accurate structures ever solved from single crystal X-ray diffraction data is racemic DL-serine: data collected at HASYLAB (Hamburg, Germany) at the wavelength of 0.45 Å.[99]

Currently, X-ray crystallography is widely applied in studies of biological macromolecules (proteins, nucleic acids, polysaccharides, viruses, *etc*.).[109] Single crystals of biopolymers possess large unit cells with parameters of 50 – 500 Å containing up to several hundred thousand independent atoms. For this reason, measurement and structure solution techniques applied in this field have to be noticeably altered. The 'classical' X-ray diffraction study allows one to reconstruct the electron density map of the crystal of a biopolymer with a relatively low resolution (3 – 5 Å), in which typical functional groups or fragments rather than single atoms can be seen on a partially resolved background of hydration water molecules (which can occupy 15% – 20% of the crystal volume). Furthermore, large and well formed single crystals of biopolymers are extremely difficult to grow and they easily decompose under X-ray irradiation, since the standard data acquisition can take several weeks on a laboratory diffractometer.

Distinct advantages of synchrotron radiation-based techniques caused a very fast growth of their application to crystallographic studies of proteins and other biopolymers.[100–113] According to Biosync (an international organisation of SR users in the field of structural biology), the fraction of SR in all diffraction studies of new crystal structures of biological macromolecules has grown from 18% in 1990 to 44% in 1996.[114] Presently, almost a half of all studies in protein crystallography is performed using SR sources. In a number of cases, the use of SR allowed one to achieve the resolution comparable to the standard resolution in small-molecule X-ray crystallography. Thus in an X-ray diffraction study of the protein concanavalin A (molecular weight 25 000), the resolution of 0.93 Å has been reached, which made it possible to reveal and refine the positions of all 2134 non-hydrogen atoms within the unit cell in the anisotropic approximation.[115] Since the ratio of the number of independent reflections *vs*. refined parameters was relatively high, accuracy comparable to that of small-molecule crystallography has been obtained (Fig. 17). Even higher resolution of 0.54 Å has been achieved in the diffraction study of the oligopeptide cramine and the deformation electron density map has been analysed for the first time for a protein molecule (data collected at HASYLAB).[116]

As a recognition of great importance of structural biology for the modern science, the 1997 Nobel prize in chemistry was awarded to the international team including J E Walker (UK), P D Boyer (USA) and J C Skou (Dennmark) for the determination of the enzymatic mechanism of the intercellular synthesis of adenosine triphosphate (ATP). The key stage of the investigation was the single crystal structure study of the enzyme complex F1-ATPase using SR diffraction data collected in Daresbury Laboratory (UK).

This enzyme is a constituent of the ATP-synthase complex, which catalyses the last stage of the intercellular ATP synthesis by oxidative phosporylation of adenosine diphosphate. The solution of the structure of F1-ATPase (molecular weight 371 000, orthorhombic, unit cell parameters $285 \times 108 \times 140$ Å, space group $P2_12_12_1$) took 12 years. To date, it is the largest non-centrosymmetric crystal structure solved from X-ray diffraction data.[117]

In addition to conventional diffractometry, the Laue diffraction method is widely applied in synchrotron crystallographic studies of proteins. In this method, the diffraction pattern is obtained by 'white' X-ray beam scattering on a rotationally fixed single crystal. Combined utilisation of intense synchrotron radiation and area detectors allows investigations of extremely small single crystals (with a volume of ~ 0.1 μm^3) with a very short data acquisition time (several ns). The unprecedented volume for a single crystal of gold studied by this method[118] is $\sim 10^{-3}$ μm^3. During recent years, special techniques for data recording and processing have been developed in this field, which allow at present the *ab initio* (*i.e*., without any *a priori* structural models) solution of relatively simple structures solely from Laue diffraction data[119,120] and refinement of structures of any complexities.[121]

Yet another direction in the development of synchrotron X-ray crystallography is magnetic scattering. The incorporation of relativistic effects gives corrections of the X-ray scattering amplitude due to interaction of X-ray photons with magnetic moments of electrons. In a classical X-ray diffraction studies, scattering of photons on magnetic moments is several orders of magnitude weaker than that on charge density. However, the magnetic component increases in the case of very hard X-rays (80 – 100 keV). Furthermore, the magnetic scattering intensity can be substantially enhanced (by 3 – 4 orders of magnitude) when the scattered wavelength approaches an absorption edge of an element with unpaired electrons in the sample (the so-called X-ray

resonance exchange scattering). In this case, the intensity of magnetic scattering of photons achieves the intensity of scattering on electron charge density.[122]

Magnetic X-ray scattering leads to the appearance of forbidden diffraction maxima (extinction condition violations) and superstructure reflections corresponding to the sublattice of magnetic atoms. With synchrotron X-ray sources of high intensities it is possible to record magnetic reflections both in the resonance region and far from the absorption edges.[123,124] It allows investigations of magnetic structures of paramagnetic crystals. In this respect, magnetic scattering of SR turns into an important alternative for the traditional technique in this field, *viz*., magnetic scattering of polarised neutrons. Magnetic X-ray scattering is widely used for studies of magnetic ordering in compounds of *f*-elements (lanthanides and actinides).[125] One of the first demonstrations of research capabilities of the technique has been the confirmation of helical magnetic structure (*i.e*., heliomagnetism, a particular case of antiferromagnetic ordering) in a number of rare-earth metals, in particular, in holmium.[126]

Yet another emerging trend of synchrotron X-ray crystallography is the so-called perturbation crystallography, covering structural investigations of crystals in an external perturbing field, such as mechanical deformation, electrostatic or magnetic field and crystals of substances in excited states.[127] For instance, an X-ray diffraction study has been performed for a single crystal of 2-methyl-4-nitroaniline (exhibiting non-linear optical and piezoelectric properties) in an external electric field (NSLS, Stony Brook, USA). Changes in unit cell parameters and intensities of selected reflections for the crystal placed into the electrostatic field of 3.9×10^6 V m^{-1} have been explained by rotation of the molecules tending to align their dipole moments with the direction of the external field.[128] Changes in unit cell parameters and electron charge density redistribution have been observed in a crystal of deuterated potassium dihydrophosphate KD_2PO_4 (manifesting segnetoelectric and piezoelectric properties) in the electrostatic field of 1.3×10^6 V m^{-1}. Upon application of the external field, a phase transition with alteration of space group and syngony ($I42d \rightarrow Fdd2$) has been detected.[129]

A combined study using IR and X-ray diffraction data for a single crystal of the $Na_2[Ru(NO_2)_4(NO)OH] \cdot 2H_2O$ photochromic complex with excitation by a laser pulse has been carried out in ESRF (Grenoble, France).[130] An excited state of the molecule (with relative population of 0.2–0.3) has been detected and structurally characterised. The excitation is accompanied by elongation of the N–O bond by 0.19(5) Å and decrease in the Ru–N–O bond angle by 6(2)°. Earlier, a non-zero population of an excited state with changed geometry of the MNO fragment has been observed for (η^5-C_5H_5)NiNO by XAFS spectroscopy.[131]

b. X-Ray powder diffraction

Techniques of X-ray powder diffraction (XRD) or X-ray phase analysis are the main fast methods for structural characterisation of polycrystalline samples. In XRD, the dependence of scattering intensity as a function of a single scattering angle 2θ, is measured. Compared to single crystal X-ray diffractometry, X-ray powder diffraction methods are much more versatile allowing studies of a broader range of samples including compact workpieces, partially ordered multiphase systems, polymers, thin films, layered nanocomposites, minerals and so on. XRD is applicable to solution of such problems as qualitative identification and semi-quantitative analysis of crystalline phases in mixtures, estimation of degree of crystallinity and sizes of crystallites in polymers, analysis of preferred orientation and textures in materials, investigations of phase transitions and equilibria in solids, determination of unit cell parameters as a function of the phase chemical composition or external conditions (pressure, temperature), structural monitoring of solid-phase reactions, *etc*.

XRD is routinely used in laboratories with X-ray tubes as the X-ray source. However, during the last decade measurement of XRD patterns in synchrotron centres (especially for samples with low diffracting power and substances available in small amounts) become more and more common (Fig. 18). Most important areas of the SR X-ray powder diffraction are high-precision and high-resolution diffractometry, which allows *ab initio* structure solution in combination with the structure refinement using the full-profile analysis (Rietveld method) solely from powder diffraction data; diffraction investigations of partially ordered and amorphous samples; time-resolved studies of processes in solids.[12,20,132] As in synchrotron X-ray crystallography, position-sensitive detectors are widely utilised in SR-based XRD (typically, curved linear 1*D* PSDs capable of simultaneous full pattern registration in the 2θ range from 0° up to 165–170°).

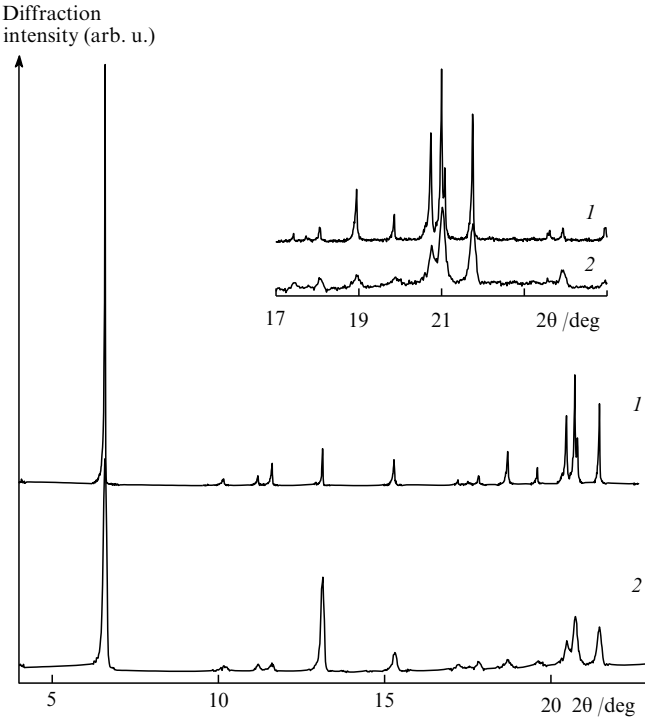

Figure 18. X-Ray powder diffraction patterns for radical-ion salt $BEDTTTF^+ \cdot C_{60} \cdot I_3^-$ (BEDTTTF stands for bis-ethylenedithiotetrathiafulvalene).
(*1*) – SR pattern (VEPP-3 storage ring, Novosibirsk, $\lambda = 1.5402$ Å, angle step 0.01°, exposure time 1 h); (*2*) – laboratory pattern (DRON-3 diffractometer, X-ray tube Cu K_α, $\lambda \approx 1.5418$ Å, 45 kV × 20 mA, angle step 0.02°, exposure time 20 h).

Depending on the instrumental setup, two methods of XRD can be distinguished: conventional angle-dispersive diffraction (when a fixed-wavelength monochromatic X-ray beam is used) and energy-dispersive diffraction (when the scattering intensity is measured at the constant scattering angle and the wavelength of the incident beam is varied).[133] Energy-dispersive X-ray powder diffraction can be accomplished only on SR sources; this modification of XRD is very useful in structural investigations of matter under extreme conditions. In the case of angle-resolved diffractometry, due to high collimation and degree of monochromaticity of X-ray beams, resolution of weak reflections is substantially better than that obtained using laboratory diffractometers; the profiles of reflections are narrower and more regular. Using SR, it becomes possible to achieve good signal-to-noise statistics for very short time intervals (down to ms); thus it allows registration of minor crystalline phases present in the sample in very low concentration (~0.1%).[134] All these factors substantially facilitate data processing including full-profile analysis of powder patterns by the Rietveld method. The latter is used to refine positions of atoms within the unit cells by fitting the calculated intensity profile $I(2\theta)$ to the experimental curve; the

accuracy of this procedure may approach that of single crystal X-ray crystallography.[135]

The main unsolved problem in the powder crystallography is the selection of the initial approximation, *i.e.*, structure solution. In synchrotron XRD patterns, up to a few hundred individual reflections can be revealed. Thus it turns possible to solve *ab initio*, in a routine mode, relatively complex structures with up to several tens of independent atoms in the unit cell. For structure solution, both algorithms widely adopted in crystallography of small-molecular-weight compounds (direct methods, the Patterson method) and *ad hoc* techniques (maximum entropy, maximum likelihood and Monte Carlo methods, trial-and-error search among sterically allowed orientations of a fragment with known geometry in the unit cell with variation of selected structural parameters such as torsion angles, *etc.*) are used. The reliability of the Rietveld refinement results can be enhanced by fitting the structural model *versus* several independent experimental data sets (for example, *vs.* synchrotron diffraction patterns measured at different wavelengths). Recently, the Rietveld refinement combined with trial-and-error search for most probable atomic configurations proved to be very efficient in structure solution from powder diffraction data.[136–139]

The number of various structures of organic,[140–142] inorganic,[143–146] and organometallic[147,148] compounds solved *ab initio* based on synchrotron XRD data has now reached several hundreds. Synchrotron XRD is actively employed in structural studies of fullerene derivatives,[149] such as endohedral metallofullerenes $Sc@C_{82}$,[150] $Y@C_{82}$, $Sc_2@C_{84}$ (which are available only in a few mg),[151] dimeric azafullerene $(C_{59}N)_2$,[152] low-temperature modification of fullerene bromide $C_{60}Br_{24}\cdot 2Br_2$ (see Ref. 153), *etc*. In certain cases, this method allows one to solve independently several components of a multiphase system without their separation. For example, it was possible to determine crystal structures of two polymorph modification of cyclopentadienyl rubidium from synchrotron powder diffraction pattern of their mixture (Fig. 19).[154] The electron density distribution revealing features at the subatomic level for a series of simple inorganic solids, *viz.*, BN, Mg, Be, was successfully reconstructed based on synchrotron X-ray powder diffraction and using the maximum entropy method (MEM).[155–157]

Structural investigations of textured samples, which can be considered as an intermediate step between a single crystal and a polycrystalline powder with random orientation of crystallites, can also be facilitated if SR is used up to the possibility of routine structure solutions by direct methods.[158] In this case, a typical routine includes measurement of an XRD pattern at different orientations of the sample in the X-ray beam. In contrast to synchrotron experiments, such a procedure with the laboratory diffractometers usually leads to a substantial line broadening due to high divergence of the incident beam produced by an X-ray tube.

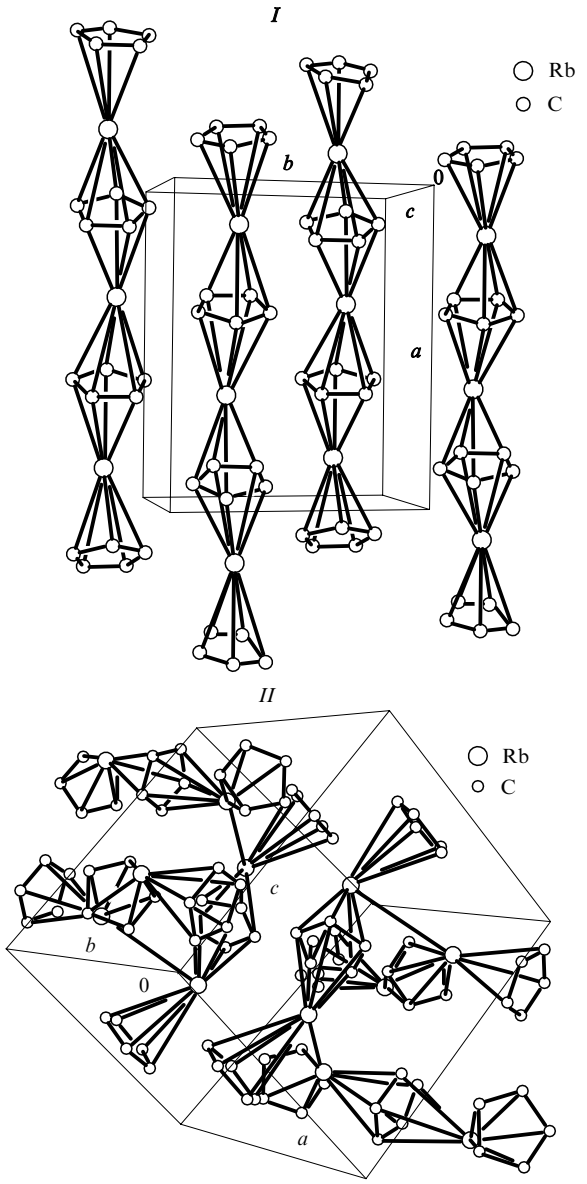

Figure 19. Crystal structures of two polymorphic modifications of $Rb(C_5H_5)$ differing from each other in spatial arrangement of infinite Cp – Rb – Cp chains. The structures have been solved *ab initio* based on the synchrotron powder diffraction pattern for their mixture.[154]
(*I*) Space group *Pnma*, a = 10.799 Å, b = 8.962 Å, c = 5.706 Å (chains are arranged along the a axis); (*II*) space group *Pbcm*, a = 9.340 Å, b = 10.967 Å, c = 10.549 Å (chains are arranged along both the b and c axes).

c. X-Ray scattering by amorphous and partially ordered samples

When X-ray radiation is scattered by a completely amorphous solid or by a liquid, the dependence of intensity on the scattering angle exhibits no sharp diffraction maxima. The Fourier transformation of smooth oscillations observed in this dependence gives rise to a radial distribution function (RDF). The maxima in this curve correspond to interatomic distances. A classical version of this method § has a limited applicability, since the interpretation of results for systems more complex than monocomponent or binary is often ambiguous. For example, noncrystalline scattering of synchrotron X-rays with the energy of 101.2 keV (HASYLAB centre) has been utilised for the analysis of RDF in normal and heavy water. In this study, small systematic differences in interatomic distances between oxygen atoms forming H-bonds with different hydrogen isotopes (the Ubbelohde effect) have been revealed.[159]

Noncrystalline scattering of hard X-rays is a promising technique for structural characterisation of glasses and other inorganic materials with disordered structures, since in this case, the amplitudes of scattering on light atoms become negligible and thus only interatomic distances related to heavy atoms are seen in RDF, which facilitates substantially their interpretation. Analysis of oscillations in the noncrystalline X-ray scattering curves up to high values of the diffraction vector

$$Q = \frac{4\pi \sin\theta}{\lambda}$$

allows determination of interatomic distances with the accuracy of *ca.* 0.01 Å.[160,161] For instance, in a study of a short-range order around barium atoms in $BaSi_2O_5$ using non-crystalline scattering

§ This method is also often referred to as the method of radial electron density (RED), wide-angle X-ray scattering (WAXS), or partial distribution functions (PDF).

of synchrotron X-rays with the energy of 150 keV over the Q range of 0.8 – 38.7 Å^{-1}, long Ba – Ba distances at 4.5 – 4.8 Å have been revealed.[162] For measurements of this kind, intense SR beams produced by insertion devices (wigglers and undulators) in third-generation storage rings are most suitable.

In substances with partially ordered structures (defect-rich, disordered and dynamic phases, liquid crystals, thin films, intercalation compounds, polymers, *etc.*) as well as in phases with non-crystallographic ordering (modulated and incommensurate phases, quasi-crystals), the types of spatial symmetry can be different for different directions and/or components of the sample. Intercalation compounds of layered matrices (such as transition metal dichalcogenides, graphite, *etc.*) may be mentioned as examples of partially ordered systems. They often exhibit a strictly parallel stacking of alternating 'guest/host' layers, long-range order within host layers combined with the possibilities of phase transitions in two-dimensional guest layers and orientational disorder of adjacent layers. Powder diffraction patterns for such systems often contain relatively narrow reflections together with wide diffuse features. Important structural information can be extracted in this case from the analysis of shapes and widths of diffraction lines [133, 135] and diffuse scattering.[163, 164]

A variety of partial ordering is particularly typical of biopolymers and other biological systems.¶ In SR-based studies of such systems, two-coordinate detectors are conveniently used. The measured patterns are usually adjusted to fit some *a priori* model, which corresponds to a structure of a segment of polymer chain, conformation of the chain, fibre orientation, *etc.*[165, 166]

d. Small-angle X-ray scattering

Small-angle X-ray scattering (SAXS) is based on the scattering of X-rays on optical inhomogeneities of the sample (atomic aggregates, cavities) with the size of the order of several tens of nm. Experimentally, scattering intensity is registered as a function of scattering angle in the region of small angles from several angular minutes up to a few degrees, *i.e.*, for diffraction vector moduli $0 < Q \leqslant 0.2$ (see Refs 167 – 169). In such small angle diffraction patterns, usual diffraction maxima corresponding to reflections from long-periodicity atomic planes with interplanar distances 10 – 50 nm (100 – 500 Å) can be observed. A periodic structure can also be formed by packing of supramolecular objects (polymer globules, nanoparticles, *etc.*). By analysing the scattering intensity decrease function for a sample with completely irregular structure, one may retrieve information on the mean particle size (or inhomogeneity regions) in the sample as well as estimate the shape and size distribution of such particles (Fig. 20).

SAXS plays a very important role in characterisation of polymer morphology (including biopolymers), conformations of macromolecules in solutions,[170, 171] colloid systems,[172] submicro- and nanoparticles as well as in studies of such processes as phase segregation in amorphous glasses, gelation, nucleation, crystal growth, amorphisation, *etc.*[173 – 175] Small divergence of synchrotron X-ray beams extends the capabilities of the technique enabling collection of scattering data at very small angles corresponding to interplanar distances up to ~1000 nm [ultra-small angle X-ray scattering (USAXS)].[176 – 178]

¶ Studies of biological objects using X-ray crystallography, non-crystalline diffraction, small angle scattering (see below) and XAFS are often merged under the common term 'structural biology'.

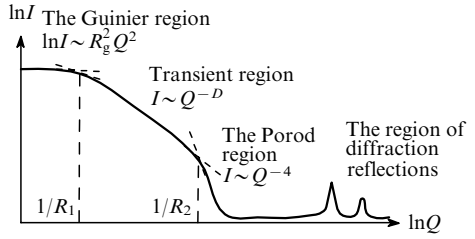

Figure 20. General view of a small angle X-ray scattering curve on an inhomogeneous sample.
R_1 is radius of aggregates; R_2 is radius of particles composing fractal aggregates; R_g is gyration radius of aggregates; D is fractal dimensionality.

3. Inelastic X-ray scattering

Analysis of energy distribution of scattered X-rays forms the basis of a number of methods.[179 – 181] As has been mentioned above (see Section III), inelastic losses accompanying X-ray scattering are due to several distinct physical processes (Fig. 21). Processing of phonon and plasmon loss spectra allows one to reconstruct dynamic structural factors (which describe the collective dynamics of a multiparticle system) for nuclei and electrons, respectively. The dynamic factor of nuclei is linked with many important characteristics of materials, such as strength, compressibility, sound velocity, *etc.*

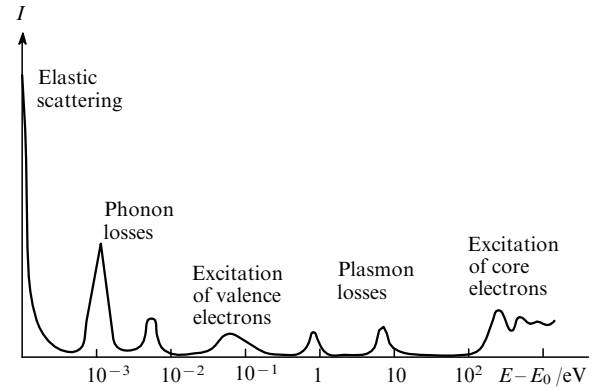

Figure 21. Characteristic energy losses in inelastic X-ray scattering spectra.

Phonon spectra of solids are close analogues of vibrational molecular IR spectra. For studies of phonon structure of crystals, inelastic neutron scattering is traditionally used. However, application of synchrotron X-rays has a number of advantages, in particular, for small crystals as well as for amorphous or liquid samples.[182, 183] In order to study atomic vibrations using inelastic X-ray scattering, a very high degree of the incident beam monochromaticity is required, so development of this method has become possible after the appearance of third-generation SR sources, systems of nested monochromators and monochromatisation techniques based on resonance nuclear diffraction (see Section IV.4).

Spectra of plasmon vibrations of electrons in the conduction zone for such solids as metals, semi- and superconductors contain important information on microscopic mechanisms of conductivity and other electrophysical properties. Spectra of energy losses corresponding to electron excitations allow determination of electron transitions, *i.e.*, studies of energy band structure of solids (similarly to the analysis of electronic states of molecules by UV spectroscopy).[184, 185] The Compton scattering profiles can be transformed into the Fermi surface maps, which reveal the distribution of electron moments in the conduction zone.[186] Many electrophysical characteristics of metals and semiconductors can be calculated based on this distribution.

X-Ray Raman scattering becomes increasingly important in chemical studies.[187, 188] Similarly to conventional Raman scattering employed in Raman spectroscopy, X-ray Raman satellites are produced by a quantified transfer of energy from photons to the sample under study. However, it is phonon loss spectra that are the closest analogues of molecular Raman spectra, whereas X-ray Raman scattering has several special features. First of all, the energy lost by an X-ray photon is consumed to induce photo-

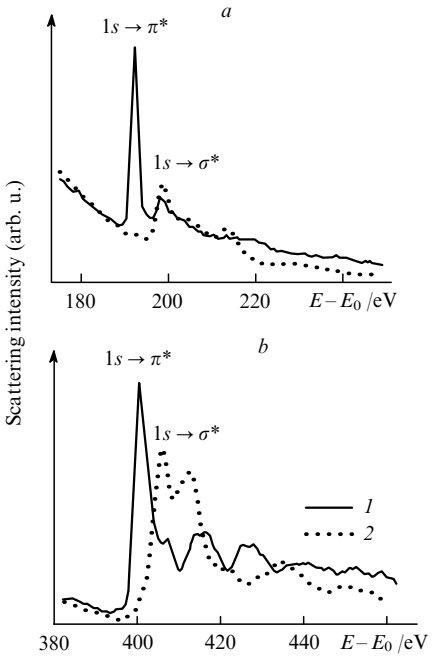

Figure 22. Boron (*a*) and nitrogen (*b*) *K*-edge X-ray absorption fine structures according to X-ray Raman scattering on a boron nitride single crystal in transmission (*1*) and reflection (*2*) modes.[180]
(*1*) The scattering vector is parallel to the *c*-axis of the crystal; (*2*) scattering vector is perpendicular to the *c*-axis of the crystal; excitation energy ~7 keV.

ionisation of light elements rather than excitation of vibrational modes and thus the respective amount of energy transfer exceeds the energy of vibrations by 5–6 orders of magnitude. Second, only low-energy satellites are observed in X-ray Raman scattering which represent triangular-shaped extended bands with an edge rather than narrow resonance maxima (Fig. 22).

Low-energy Raman satellites observed in inelastic scattering of a hard monochromatic X-ray beam (~10 keV) due to photoionisation of 1*s* shells manifest XAFS-like fine structure. Thus, X-ray Raman scattering allows one to measure XAFS spectra for the elements, the absorption edges of which lie in the soft X-ray region (50–500 eV), if one operates with ordinary hard X-ray radiation in air. This technique allows one to obtain the same information on the electronic state and local atomic environment of light elements as is given by NEXAFS or electron energy loss spectroscopy (EELS) under ultrahigh vacuum conditions. This technique is particularly promising for investigations of substances under extreme conditions, since such experiments usually require sample environment non-transparent for soft X-rays. X-Ray Raman scattering has been applied to study electronic structure of light elements, such as Li, Be, C, *e.g.*, in graphite intercalation compounds with alkaline metals (carbon 1*s*-edge) as well as in LiC_6 intercalate (lithium 1*s*-edge).[189–191]

When the energy of inelastically scattered X-ray radiation is close to resonance absorption of one of elements in the sample, the so-called resonant inelastic X-ray scattering (RIXS) is observed. The physical background of RIXS is very similar to that of resonant X-ray emission (see above). The difference in these two processes is reflected in their quantum description: the RIXS is a one-stage process; meanwhile in the resonant X-ray emission, two stages can be distinguished, *viz.*, absorption and re-emission (during lifetime of the excited state, part of the information on absorbed photon, such as its initial moment, can be lost due to internal conversion processes). The RIXS method can be efficiently used to explore fine features of electronic structures of solids: many electron transitions (excitation channels) non-detectable in absorption or non-resonant inelastic scattering spectra clearly manifest themselves in RIXS.[192, 193]

4. Synchrotron radiation Mössbauer spectroscopy

Transitions of atomic nuclei to low-lying quantum excited states for many elements lie in the hard X-ray region of the energy range 10–100 keV. When the energy of the incident X-ray radiation coincides with the energy of a nuclear transition, resonance nuclear absorption occurs, also known as nuclear γ-resonance or the Mössbauer effect. Each Mössbauer isotope (possessing low-lying excited states) is characterised with its own distinct set of nuclear transitions. Nuclear absorption bands are very narrow, their widths are usually 10^{-8}–10^{-10} eV ($\Delta E/E \approx 10^{-14}$). For comparison, the width of absorption bands associated with valence electron transitions is $\sim 10^{-7}$ eV ($\Delta E/E \approx 10^{-8}$) and that with core electron transitions is 1–10 eV ($\Delta E/E \approx 10^{-3}$). In this connection, measurements of resonance nuclear absorption are possible only with X-ray beams of the extremely high degree of monochromaticity. In the conventional laboratory modification of Mössbauer spectroscopy, excited nuclei of the isotope under study produced upon a radioactive decay are normally used as an excitation energy source; for example:

$$^{57}Co \rightarrow {}^{57}Fe^{*} \rightarrow {}^{57}Fe + \gamma. \qquad (6)$$

Other techniques of strictly monochromatic γ-rays generation, such as target activation with a neutron beam or collision of atoms with high-kinetic-energy ions (Coulomb nuclei activation) are available in nuclear research centres.†

Isotopic (or chemical) shift of the nuclear excited level energy and quadrupole splitting of the level are the parameters that are measured in Mössbauer spectra. Furthermore, hyperfine magnetic splitting of spectral lines is observed for magnetically ordered systems. These parameters represent fingerprints for each individual compound; so these allow rather straightforward and unambiguous determination of the oxidation states of an element, symmetry of coordination environment and degree of its distortion.

A major disadvantage of the conventional Mössbauer spectroscopy is a limited number of monochromatic γ-sources available. The predominant part of all Mössbauer studies is performed for a few elements which have convenient γ-active isotopes, such as ^{57}Fe, ^{119}Sn, ^{121}Sb, ^{151}Eu. In principle, utilisation of SR eliminates this restriction since X-ray radiation with continuous energy distribution up to 100 keV and higher is made available (this is particularly true for the third-generation SR sources and insertion devices). The Mössbauer effect on synchrotron radiation was first observed in the mid 80's.[194] Now, experimental stations for the experiments in this field are installed in several SR centres, such as HASYLAB, ESRF, APS, SPring-8.[195, 196]

Single crystal X-ray monochromators do not provide the degree of monochromaticity required for the convenient modification of Mössbauer absorption spectroscopy. In this relation, the so-called nuclear forward scattering (NFS) technique is under active development in the field of synchrotron Mössbauer spectroscopy. In this method, a sample is irradiated by a very fast pulse of monochromatised SR with energy close to the energy of resonance nuclear absorption and photons scattered in the direction of the primary beam (forward scattering) are registered.[197]

Under such experimental conditions, a fast-decaying background signal of X-rays elastically scattered by electrons is observed immediately after the excitation pulse followed by a coherent nuclear scattering (nuclear fluorescence) with a delay of the order of 100 ns, corresponding to the lifetime of a nuclear

† In the classical version of Mössbauer spectroscopy, the energy difference between the incident radiation emitted by nuclei of a source and resonance absorption of target nuclei is compensated by movement of a sample due to the Doppler effect; thus shifts of Mössbauer spectral lines are usually measured in velocity units (mm s^{-1}).[26]

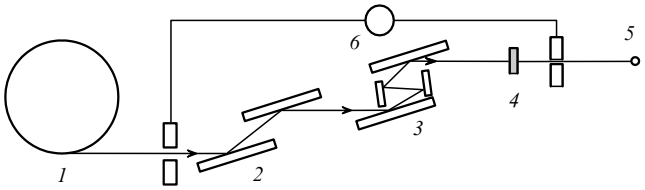

Figure 23. A scheme of a device for measurement of Mössbauer spectra in the NFS mode with utilisation of pulsed synchrotron radiation.
(*1*) Pulsed SR source, (*2*) pre-monochromator ($\Delta E/E \simeq 10^{-4}$), (*3*) high-resolution monochromator ($\Delta E/E \simeq 10^{-7}$), (*4*) sample, (*5*) APD, (*6*) delay circuit (~ 100 ns).

excited state (Fig. 23). In this signal extracted with a specialised delay circuit and measured with a fast-counting detector, such as an avalanche photodiode (APD), decaying oscillations of the scattered beam intensity (quantum beats) are observed. Quantitative parameters of these oscillations can be transformed into normal Mössbauer characteristics [197] implying that the information similar to that of conventional Mössbauer spectra can be obtained (sometimes with higher accuracy).

Up to now, first experiments have been conducted on 'exotic' Mössbauer nuclei, which however are potentially important for chemistry, such as ^{67}Zn, ^{61}Ni, ^{40}K, ^{73}Ge and a number of lanthanides and actinides. Synchrotron Mössbauer spectroscopy is a promising research tool in bioinorganic chemistry [196, 197] and structural materials science (materials under high pressures,[198–200] time-resolved studies of fast processes, magnetic properties [201, 202]).

Coherence of nuclear scattering can be violated as a result of various dynamic processes involving excited nuclei.[203] For instance, diffusion of excited nuclei leads to a faster decay of quantum beats. This phenomenon (quasi-elastic nuclear scattering [204–206]) is used in NFS studies of single crystals for determination of length and direction of elementary diffusion jumps. Energy distribution of nuclear fluorescence at non-zero scattering angles relative to the excitation beam (inelastic nuclear scattering [207]) gives information on phonon structure of a crystal lattice, *i.e.*, on collective dynamics of nuclei in the time scale comparable to the lifetime of excited states.[208]

Yet another important trend in development of synchrotron Mössbauer spectroscopy is the so-called resonance nuclear diffraction.[209] When a single crystal containing a Mössbauer isotope (for example, yttrium iron garnet enriched with ^{57}Fe isotope) is irradiated by a synchrotron X-rays with the energy close to resonance excitation of the nucleus (under Bragg's conditions), all the inelastic nuclear scattering processes are suppressed and the beam reflected becomes highly monochromatic. X-Ray monochromators based on the resonance nuclear diffraction provide the highest energy resolution available to date allowing one to extract exceptionally narrow spectral lines corresponding to energies of Mössbauer nuclei resonance absorption from incident beams of a medium degree of monochromaticity. Such high-resolution monochromators are used in Mössbauer studies and in phonon structure studies of solids by means of inelastic X-ray scattering.[210]

5. Imaging techniques

Synchrotron X-ray radiation (as well as electromagnetic radiation of other spectral regions) can be used for production of magnified images of various objects. SR-based imaging techniques include X-ray microscopy, X-ray diffraction topography, computed tomography along with methods widely adopted in medical applications, such as radiography, subtraction angiography, mammography, *etc*.

With respect to spatial resolution, X-ray microscopy occupies an intermediate position between optical and electron microscopy. Synchrotron radiation-based X-ray microscopy benefits from the possibility of varying such characteristics of the incident X-ray beam as energy and polarisation. Besides, utilisation of hard X-rays (7–30 keV) does not require an ultrahigh vacuum analytical chamber (in contrast to all modifications of electron microscopy). This enables *in vivo* studies of biological systems and strongly facilitates investigations of large objects. Standard spatial resolution of hard X-ray microscopy is ~ 0.25 μm. Utilisation of soft X-rays (0.2–1.2 keV) in combination with advanced X-ray optics, such as FZP and BFO, makes spatial resolution of 30–50 nm attainable. Penetration depth of soft X-rays into a condensed matter is higher than that of electrons, thus, the samples which are opaque for transmission electron microscope can be studied by X-ray microscopy. Furthermore, the use of electron beams induces greater radiation damage of the sample compared to synchrotron X-rays.

Yet another advantage of X-ray microscopy is the possibility to achieve element and even valence contrast by varying the incident radiation wavelength and using absorption edges. Studies of biological objects are usually performed in the energy range referred to as the 'water window', *viz*., 280–550 eV. In this range, absorption by oxygen atoms (and thus by water molecules always abundantly present in biological samples) is relatively weak. By varying the beam energy within the 'water window' it becomes possible to achieve contrast in visualisation of, for example, carbon and nitrogen atoms and thus independently estimate the spatial distribution of proteins and nucleic acids in the sample. X-Ray microscopy can be subdivided into contact, projection and scanning modifications depending on mutual orientation of SR source, sample and detector.[211–214] Recent achievements in the field of synchrotron X-ray microscopy are considered in detail in the monograph.[215]

X-Ray diffraction topography is a method of defect imaging in crystals. It is based on the analysis of intensity distribution of scattered radiation within the diffraction spot.[216] Using X-ray topography it is possible to visualise point defects and dislocations with spatial resolution of 2–3 μm, to analyse their dynamics upon application of a mechanical stress (for example, in piezoelectric crystals), as well as to study local distortions, deformations, inhomogeneities and microcracks in nearly perfect crystals.[217] Diffraction topography is sensitive to gradients of unit cell parameter deformations $\Delta a/a$ of the order of $\sim 10^{-7}$. This method can be used efficiently in studies of large single crystals which are opaque for visible light. The principal field of application of this technique is technological control of perfect crystals, for example, in manufacturing semiconductors. Utilisation of SR in this field leads to increase in the spatial resolution and decrease in exposure times (and therefore radiation damage to the sample).[216–219] X-Ray topography can be utilised as a fast preliminary test of single crystal quality. This can be particularly important in protein crystallography where diffraction experiments are very expensive and time-consuming.

X-Ray computed tomography allows visualisation of internal structure of samples in different cross-sections. The image is reconstructed by mathematical processing of transmitted intensity profiles for various mutual orientations of the sample and radiation source.[220, 221] This method is used for characterisation of such objects as technological workpieces, biological and geological samples (*e.g.*, microcavities and micropores in minerals). For image reconstruction, parallel or divergent, 'white' or monochromatic synchrotron X-ray beams can be used. The spatial resolution of X-ray tomography is a few micrometers.[222] As in the case of X-ray microscopy, the contrast of reconstructed images can be noticeably enhanced if incident radiation wavelength is chosen close to the absorption edges of certain elements in the sample. For instance, distribution of light and heavy elements throughout the sample may be independently reconstructed from X-ray tomography data collected at two strongly different wavelengths [dual photon absorptiometry–computed tomography (DPA-CT)].

In modern imaging techniques, utilisation of the coherent properties of SR acquires increasing importance. In this connection, coherent synchrotron X-ray radiation of third-generation SR sources allows one to achieve phase contrast besides standard absorption contrast in images. Absorption contrast is obtained as a result of differences in X-ray absorption coefficients of different points in the sample, whereas phase contrast is due to phase shifts of scattered coherent radiation, which gives rise to an interference pattern superimposed on the sample image. This interference pattern depends upon sample-to-detector distance and therefore very high contrast images may be obtained by adjusting this distance.[223–225]

Coherent properties are also utilised in a new SR-based visualisation technique, *viz*., X-ray photon correlation spectroscopy (XPCS) or intensity fluctuation spectroscopy. This method is an X-ray analogue of visible light dynamic scattering, which is widely used in studies of colloid systems. The X-ray photon correlation spectroscopy is based on observation of a real-time evolution of the speckle interference pattern produced by scattering of coherent X-ray radiation on disordered samples. Using this method, it is possible to study low-frequency dynamic processes (10^{-3}–10^{6} Hz) in the sample and visualise short-range density fluctuations within the distances range of the order of 1 nm.[226] This method has been successfully applied to study Brownian motion of metal nanoparticles[227] and copolymer micelles in solutions,[228] dynamics of charge density waves, critical fluctuations near the point of order–disorder phase transitions in amorphous alloys,[229] conformational dynamics of polymers upon glassification,[230] *etc*.

6. Other methods

a. Utilisation of anomalous scattering

In the theoretical description of X-ray scattering on atoms, the atomic scattering factor f_0 (sometimes also referred to as atomic form factor) is of key importance. The atomic scattering factor is a smooth function of scattering angle θ, monotonically decreasing with an increase in θ from 0° to 180°. Atomic scattering factors for adjacent elements in the D I Mendeleev Periodic Table are close. Over a wide range of wavelengths, f_0 is virtually independent of incident radiation energy.

However, if incident radiation energy approaches an X-ray absorption edge of an element in the sample, a wavelength-dependent correction to f_0 has to be introduced into the scattering formalism. This correction term is commonly referred to as anomalous dispersion (Fig. 24). In the energy range of X-ray resonance absorption, scattering is accompanied by intensity attenuation. In this case, the total atomic scattering factor $f(\theta,\lambda)$ formally acquires a complex value

$$f(\theta,\lambda) = f_0(\theta) + f'(\theta,\lambda) + if''(\theta,\lambda), \tag{7}$$

where f_0 is the wavelength-independent part of atomic scattering factor (rapidly decreasing with an increase in scattering angle);

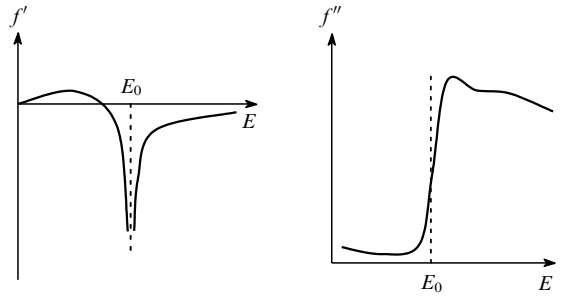

Figure 24. Real (f') and imaginary (f'') parts of anomalous dispersion correction to the atomic scattering factor as functions of the radiation energy.

f' and f'' are real and imaginary parts of the anomalous dispersion, respectively. The imaginary part of the anomalous dispersion is directly proportional to the X-ray absorption cross-section, *i.e*., to X-ray absorption coefficient μ, and its real part is linked with the imaginary part by the Kramers–Kronig dispersion relation

$$f'(\omega) = \frac{2}{\pi}\int_0^\infty \frac{\omega' f''(\omega')}{\omega^2 - (\omega')^2}\,\mathrm{d}\omega', \tag{8}$$

where ω is the radiation frequency.

An anomalous dispersion contribution may substantially distort scattering intensities compared to values calculated on the base of f_0 only. In contrast to f_0, the f' and f'' terms only weakly depend on the scattering angle, so the relative contribution of anomalous dispersion is higher for large scattering angles. As a rule, the energies of X-ray absorption edges for adjacent elements in the D I Mendeleev Periodic Table differ from each other by a few hundreds of eV, consequently, account for anomalous dispersion leads to substantial differences in atomic scattering factors (and thus to different X-ray scattering patterns) for such elements when the scattered radiation wavelength is close to an X-ray absorption edge of one of these two elements. Moreover, due to different chemical shifts of X-ray absorption edges in different compounds of one element, atomic scattering factors can become noticeably different even for atoms of one element in different chemical environment or charge state (valence contrast). Advanced techniques based on application of anomalous scattering and respective experimental diffraction results are thoroughly discussed in a number of recent publications.[231–233]

The anomalous scattering combines X-ray absorption and scattering phenomena. In order to utilise it in diffraction experiments, it is necessary to collect diffraction data with incident radiation of continuously variable wavelength (which is possible only with synchrotron sources) or to carry out a series of diffraction experiments at several wavelengths, at least one of which being close to an X-ray absorption edge of an element in the sample. In the latter case, the difference between two diffraction patterns in the proximity of the edge and apart from it will be primarily caused by scattering on the absorbing atoms.

Anomalous scattering of synchrotron radiation is widely used in powder X-ray diffraction. Using this approach, atoms of certain elements can be precisely located in the unit cell, which substantially facilitates structure solution. This technique is often referred to as resonance X-ray diffraction. In studies of amorphous samples using anomalous wide-angle X-ray scattering (AWAXS), partial radial distribution functions may be determined separately for each heavy element.[232] This makes interpretation of experimental results much more reliable and unambiguous. A similar approach is adopted in anomalous small-angle X-ray scattering (ASAXS), for example, for determination of mean size and size distribution of particles in supported metal catalysts and nanoparticles stabilised in polymer matrices or for analysis of metal distribution in bimetallic nanoclusters.[234–236]

In conventional single crystal X-ray crystallography, account for anomalous dispersion can be used in determination of the absolute configuration of a non-centrosymmetrical (chiral) crystal and its constituent molecules. When SR is used, data collection at the wavelength of resonance absorption allows unambiguous establishment of the chemical nature of anomalously scattering atoms as well as charge states for crystallographically non-equivalent atoms of one element in mixed-valence complexes, the so-called valence contrast X-ray crystallography. Capabilities of this technique has been demonstrated for a series of inorganic substances in which atoms of one element in different oxidation states occupy crystallographically non-equivalent positions, *e.g*., Fe_3O_4,[237] $GaCl_2$,[238] $NbSe_3$,[239] as well as for a number of mixed-valence polynuclear complexes.[240, 241]

Utilisation of anomalous dispersion in X-ray crystallography is most logically implemented in the multi-wavelength anomalous diffraction (MAD) method, which becomes increasingly popular in protein crystallography.[242–245] For a single crystal containing atoms of heavy elements, it is possible to estimate experimentally the phase of any reflection based on its intensity at three different wavelengths before, directly at and above the X-ray absorption edge of the corresponding element. Thus, MAD helps to overcome the key problem of single crystal X-ray crystallography, the so-called problem of initial phases: in order to transform the set of diffraction data into the target electron density distribution map, it is necessary to assign certain phases (which cannot be directly determined from standard diffraction experiment) to experimentally measured intensities of reflections. In small-molecule crystallography, reliable direct methods of statistical estimation of the initial phases have been developed, whereas in protein crystallography, the search for initial phases remains very complicated and not always solvable problem.

Determination of reflection phases using MAD is a much more laborious procedure than common diffraction measurements, however the information obtained is often worth the time spent. The MAD method gradually displaces multiple isomorphous replacement (MIR) method in protein crystallography. This formerly popular but much less versatile method is based on comparison of diffraction data sets for crystallographically isomorphous derivatives of a protein with different heavy substituents. Many biological macromolecules in their native form contain heavy elements (iron, molybdenum, zinc, copper, manganese, *etc.*) and thus the MAD-phasing procedure is directly applicable to them. Recently, first experiments have been undertaken, which demonstrated in principle the possibility of MAD application in the soft X-ray region at the absorption edges of sulfur and phosphorus. However technical problems arose related to rapid radiation-induced decomposition of the sample due to strong X-ray absorption.[246, 247]

Heavy anomalously scattering atoms can be introduced into samples under study by chemical methods. For instance, calcium or magnesium ions in biological molecules can be replaced by heavier lanthanide ions; zinc ions, by mercury, *etc.* In this case, the substituted derivative does not have to be crystallographically isomorphous to the native protein (which is a prerequisite for MIR), it is sufficient that the primary amino acid sequence and the main conformation of the protein molecule are conserved. Heavy elements can be introduced into biological molecules as labelling fragments, which are chemical analogues of their native building blocks. Among such labels, selenomethionine for proteins (MAD at the Se *K*-edge) and brominated uracil for nucleic acids (MAD at the Br *K*-edge) are most often used. Yet another route for incorporating heavy elements into crystals is to perform a diffraction experiment under pressure of Xe. In this case, Xe atoms replace water molecules in cavities of the crystal lattice without disturbing the general structure of the biopolymer, and MAD-phasing at Xe *K*-edge is then applied.[248]

Anomalous dispersion can be efficiently used to enhance research capabilities of X-ray absorption spectroscopy.[249] In this connection, the diffraction anomalous fine structure (DAFS) method, which can be considered as a diffraction modification of XAFS, is actively developing. In the DAFS method, the intensity of a selected diffraction reflection is measured while varying the incident radiation energy so as to pass across an X-ray absorption edge of a certain element. Since imaginary part of the anomalous dispersion is directly proportional to the X-ray absorption coefficient μ, the dependence of reflection intensity upon the incident radiation energy manifests XAFS-like fine structure.

The DAFS method can be applied to studies of both single crystals and polycrystalline powders. In particular, it is useful for investigations of mixtures of polycrystalline powders since it allows registration of XAFS spectra at the edge for a certain element separately for each phase. Furthermore, since crystallographically non-equivalent atoms of one element make different contributions to the intensity of different reflections, DAFS data measured for several diffraction reflections allow one to extract contributions into XAFS spectrum from each crystallographically independent group of atoms of a certain element. Capabilities of DAFS have been demonstrated on such classes of substances as spinels, complex oxides, superconductors, *etc.*[250–252]

b. X-Ray standing waves

In addition to anomalous dispersion, X-ray absorption and diffraction phenomena are manifested simultaneously in the method of X-ray standing waves (XSW).[253] Under conditions of a specular reflection or Bragg's diffraction in a nearly perfect single crystal, the intensity of the electromagnetic wave is redistributed so as to form a standing wave. Differences in local intensities of the electromagnetic field in points of nodes and antinodes of the standing wave lead to different absorption and thus to different yield of all secondary processes, such as X-ray florescence, photo- and Auger electron emission, *etc.* in the corresponding atomic layers.[254, 255] Experimentally, it is manifested in a strong dependence of intensity of respective secondary processes on the incidence angle of the X-rays on the crystal or on the wavelength of the X-rays at constant incidence angle. In the latter case, the geometry of normal incidence of radiation to the surface of the crystal is often selected; this technique is referred to as normal incidence X-ray standing waves (NIXSW).[256]

The XSW method, among very few other instrumental techniques, allows structural investigations of amorphous near-surface layers of crystals with thicknesses from several nm to several μm. It is also used for precise measurement of layer thickness in multilayer periodic structures as well as for localisation of impurity atoms in crystal lattices, *e.g.*, dopant atoms in semiconducting single crystals, implanted ions, guest metal ions in biomembranes, *etc.*[257–259] For example, XSW has been applied to study gallium arsenide single crystals with a surface doped with silicon using various techniques. As has been shown in the case of molecular beam epitaxy, all silicon atoms occupy the gallium positions of the crystal lattice. In contrast, in the case of ion implantation followed by annealing (or thermally activated diffusion), only 30% of Si atoms regularly occupy the gallium positions, the rest of Si atoms occupy random positions and of them $\sim$6% occupy the As positions.[260] Modern theoretical concepts underlying the XSW method, its instrumentation and applications are discussed in recent reviews.[256, 261]

c. Surface study methods in the geometry of grazing incidence

X-Ray reflectometry method is based on the analysis of X-ray reflectivity coefficient as a function of the X-ray incidence angle. In a number of cases, this method gives important information on the atomic structure of near-surface layers.[262] As has been mentioned above (see Section III), under conditions of total external reflection, the ratio of reflected radiation approaches unity and the incident radiation does not penetrate deep into the sample interacting only with the thin near-surface layer ($\sim$10 nm). This effect can be used in order to increase surface sensitivity of 'classical' bulk X-ray methods (such as X-ray spectroscopy and diffraction). In particular, total reflection X-ray fluorescence (TRXRF) is used for quantitative analysis of trace atoms (including light elements starting from boron) in near-surface regions of semiconductors, materials modified by ion implantation, *etc.*[263–265] Due to small penetration depth of X-rays into the sample under total reflection conditions, the method is extremely sensitive: the lowest detection limit expressed as absolute mass of an admixture is of the order of femtograms (10^{-15} g).[266] This method is used for admixture level control in such very pure objects as semiconducting single crystals.[267]

Grazing-incidence X-ray diffraction (GI-XRD) is used in studies of single crystal surfaces and other materials with atomically ordered surfaces, in particular, those with specific two-dimensional ordering. Recently, this method has been applied to such objects as self-assembled monomolecular layers, Langmuir–

Blodgett, epitaxial, atomic deposition and CVD films, as well as two-dimensional crystals of lipophilic systems (fatty acids and their salts, ω-amino acids, phospholipids) at the water–air interface.[268–275]

Grazing incidence small-angle X-ray scattering is used for characterisation of thin films and supported catalysts.[276] Measurement of X-ray reflectivity coefficient as a function of incident radiation energy at the incidence angle close to the angle of total external reflection allows registration of XAFS spectra for near-surface layers: X-ray reflectivity coefficient is correlated with complex refraction coefficient, imaginary part of which is directly proportional to the absorption coefficient $\mu(E)$ [see Eqn (7)]. This technique is commonly referred to as Refl-EXAFS. The term SEXAFS (surface EXAFS) is also sometimes used but it combines an entire set of surface-sensitive techniques for EXAFS registration including, in addition Refl-EXAFS, total electron yield, yield of photon stimulated ion desorption and so on.[277–279]

d. The use of polarisation of synchrotron radiation

The use of polarisation of electromagnetic radiation in physicochemical analysis of substances with anisotropic atomic structures is based on dichroism, *i.e.*, the dependence of optical properties of substances on the direction of the electric vector in the electromagnetic wave propagating through the substance. For instance, plane-of-polarisation rotation angle per optical path unit is a key characteristic of substances with asymmetric (chiral) atomic structures; meanwhile, circular dichroism (CD) spectra give important information on mutual orientation of chromophore groups in molecules.

In contrast to X-ray radiation produced by traditional sources, *viz.*, X-ray tubes, synchrotron radiation is always completely polarised. Similarly to visible light optics, two types of dichroism, *viz.*, linear and circular, can be distinguished in the X-ray region. Polarisation of SR is most widely used in X-ray spectroscopy, since it primarily affects the probability of electron transitions. In the case of molecule excitation by a linearly polarised SR, the probability of an electronic transition of a certain symmetry depends on the mutual orientation of the electronic transition dipole moment (difference between dipole moments of the molecule in the ground and excited states) and polarisation direction of the excitation radiation. Upon resonant photoionisation of an atom by linearly polarised X-rays, the photoelectron wave generated does not possess spherical symmetry: the probability of the photoelectron propagation is the maximum in the plane of polarisation and is equal to zero in the perpendicular plane. In EXAFS, in particular, this results in the situation where atoms from the local environment lying exactly in this plane dominate in the Fourier transforms.[280]

A prerequisite for manifestation of linear X-ray dichroism is ordering and strict orientation of the sample under study relative to the incident SR beam. For example, adsorbed monolayers, which exhibit strong anisotropy of properties in the directions parallel to the layer (interaction within the layer) and perpendicular to the layer (adsorbate–support interactions), can be efficiently studied using polarisation-dependent NEXAFS spectroscopy. This anisotropy causes a distinct dependence of X-ray absorption spectra on the incidence angle of the polarised SR beam or on the polarisation direction at the constant incidence angle. In particular, in the case of grazing-incidence, σ and π polarisations of the incident beam are often used, which probe interactions parallel and perpendicular to the sample surface, respectively.[281] Utilisation of linear polarisation of SR in X-ray microscopy with element contrast allows one to determine real-space orientation of atomic fragments in polymeric fibres, since the shape of the absorption edge (NEXAFS spectrum) becomes sensitive to the orientation of certain chemical bonds, such as C=C and C=O, which have a pronounced π*-resonance.[54, 212, 282]

Intercalation compounds into layered matrices (such as graphite and its chemical derivatives, transition metal dichalcogenides, phosphates, *etc.*) constitute another group of objects for which the application of X-ray spectroscopy with linearly polarised SR is particularly informative. These systems in many cases manifest virtually ideal texture with the layers of matrix strictly parallel to the surface of the sample. Thus, using polarisation-dependent XAFS it is possible to determine, for instance, orientation of molecules within the intercalated layers.[283, 284]

Analysis of polarisation-dependent EXAFS spectra for potassium niobate (perovskite type) made it possible to determine crystallographic directions of niobium atom shifts out of centres of octahedra formed by oxygen atoms in the phase transition.[285] Studies of distortions in planar square CuO_4 fragments in single crystals of high-temperature superconducting phases gave additional information on the mechanism of superconductivity.[286, 287]

In quantum mechanical description of polarised light properties, the term photon spin is often used. A photon, being a boson, possesses spin quantum number $S = 1$ and two allowed spin moment projections $m_S = \pm 1$ (the projection $m_S = 0$ is prohibited for a photon due to its zero rest mass). A beam of photons with $m_S = 1$ corresponds to the right and with $m_S = -1$ to the left circular polarisation. The electrons with a defined spin direction (coinciding with the photon spin) are excited upon absorption of circularly polarised photons (spin polarisation). If in the substance under study, all atomic magnetic moments are co-aligned (this is the case for a one-domain ferromagnetic or for a paramagnetic placed in a magnetic field), a distinct dependence of X-ray absorption coefficient on mutual orientation of the sample macroscopic magnetic moment and circular polarisation direction of the synchrotron radiation is manifested in XANES spectra (Fig. 25). This phenomenon first observed in 1987[288] was called X-ray magnetic circular dichroism (XMCD). Over recent years, the field of XMCD experienced rapid development since using this technique it is possible to analyse magnetic properties of materials at the atomic level, *viz.*, with element specificity determine magnetic moments of atoms and identify spin and orbital contributions.[289, 290]

XMCD (its realisation is possible only in synchrotron radiation centres) has already become an established technique for characterisation of magnetic materials: thin films of 3*d*-metals

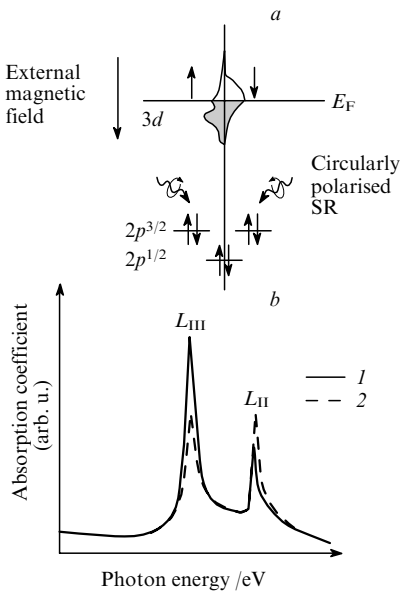

Figure 25. Scheme of the origin of circular dichroism in X-ray absorption spectra (*a*) and typical XMCD spectrum at $L_{II,III}$-edges of 3*d*- and 4*d*-metals (*b*).
Circular polarisation of the incident beam is chosen so as to excite electrons with spins parallel (*1*) and antiparallel (*2*) to the external magnetic field.

(Fe, Co, Ni), lanthanide and actinide derivatives, materials with giant magnetoresistance (strong dependence of conductivity on the applied magnetic field), *etc*. Giant magnetoresistance is typical, for instance, of multilayers with alternating ferro- and diamagnetic layers. Such materials are promising in information storage technology.[291–294]

In 1995, X-ray natural circular dichroism XNCD (*i.e*., X-ray circular dichroism, which is manifested without application of external magnetic field) was observed in some chemical systems, *e.g*., in chiral paramagnetic crystals.[295–297] Soft X-ray circular dichroism spectroscopy is widely used for characterisation of helical protein structures.[298]

The EXAFS spectra measured with circularly polarised SR produce RDF curves where atoms with non-zero magnetic moments dominate (spin-polarised or 'magnetic' EXAFS) (Fig. 26).[299, 300] The X-ray circular dichroism is actively employed in modern versions of spin-resolved photoelectron spectroscopy.[301, 302]

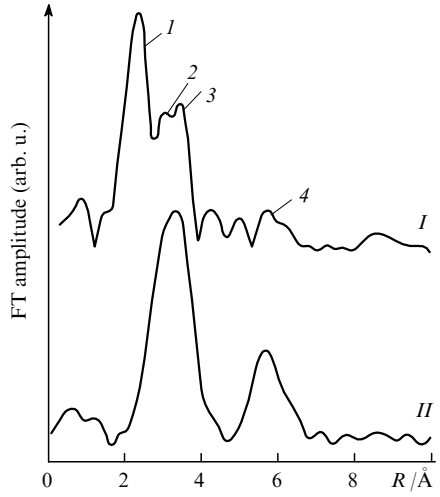

Figure 26. Normal (*1*) and magnetic (*2*) EXAFS spectra taken at Ho L_{II}-edge for $Ho_3Fe_5O_{12}$.
(*1*) Ho–O 2.3–2.4 Å; (*2*) Ho–Fe 3.0–3.7 Å; (*3*) Ho–Ho 3.7 Å; (*4*) Ho–Ho 5.6 Å.[299]

In contrast to X-ray spectroscopy, polarisation properties of SR have not found broad applications in X-ray diffraction techniques, though many phenomena accompanying diffraction exhibit polarisation dependence, which can be used for extraction of additional information. Besides, polarisation has to be taken into consideration in development and optimisation of X-ray optical elements designed for experiments with SR. Thus when linearly polarised X-rays with energy close to an X-ray absorption edge of an element in the sample is scattered by a low-symmetry single crystal, the dependence of atomic scattering factor on the scattering angle becomes anisotropic. This anisotropy is due to the fact that the absorption coefficient for the crystal (and thus corrections to the atomic scattering factor owing to the anomalous dispersion) will be different for non-equivalent crystallographic directions. In particular, this leads to the appearance of diffraction reflections forbidden by extinction conditions. This phenomenon is called anisotropic anomalous scattering (AAS) or forbidden reflection near-edge diffraction (FRNED). It can be used for determination of positions of anomalously scattering atoms within the unit cell.[303–305] For such forbidden reflections, the polarisation type and direction of the scattered wave can be different from those of the incident SR, this change being dependent on the specific crystal structure.[306] Utilisation of circularly polarised SR in X-ray crystallography makes determination of absolute configurations of chiral molecules in single crystals more reliable. X-Ray topography with circularly polarised SR is used for visualisation of magnetic domains.[307] Polarisation dependence of reflection intensities in magnetic scattering allows separation of total magnetic moment density into spin and orbital contributions.[308]

V. The main trends of applied studies using synchrotron radiation

1. Combined X-ray techniques

In majority of cases, application of only one, even quite powerful instrumental method, appears insufficient to get insight into the atomic and electronic structure of real objects (a probable exception is X-ray crystallography of small molecules). Therefore, complex SR-based studies with involvement of a number of complementary X-ray techniques are more desirable. The organisational structure of synchrotron centres itself (concentration of highly skilled staff and advanced instrumentation in one building) promotes such a convergence stimulating interchange of ideas between different experimental techniques. Moreover, a limited number of experimental stations installed at modern international synchrotron radiation centres is used by numerous research groups with diverse scientific interests. Under such operational conditions, each experimental station has to be sufficiently flexible and versatile and allow solution of a wide range of research problems with minimum hardware modifications.[309–312]

Among many advanced combined techniques routinely applied in SR centres to the studies of short- and long-range atomic order in various materials, the following combinations are most popular: XRD/XAFS (simultaneous registration of powder diffraction pattern and EXAFS spectrum) and XRD/DAFS (simultaneous registration of powder diffraction pattern and diffraction anomalous fine structure spectrum).[313–315] Specialised software has been developed for simultaneous refinement of crystal structure parameters from the experimental data of both methods.[316] For structural characterisation of semi-crystalline and amorphous polymers, SAXS/XRD or SAXS/WAXS combinations are used.[317] Protein crystallography is often supplemented with EXAFS data in order to determine exact geometry of metal centres.[318] Besides, in experiments based on the MAD method, measurement of X-ray absorption spectrum from the very same crystal as used in the diffraction experiment is required for the calculation of f' and f'' anomalous dispersion terms [see Eqn (8)] used in the phasing procedure. An ultrahigh vacuum chamber is the most expensive part of any device designed for surface studies. In order to use it with maximum efficiency, the respective device should be equipped with a broad range of functionality, for example, for utilisation of angular resolved photoelectron spectroscopy, X-ray standing waves, SEXAFS, *etc*.[319] A similar consideration is applicable to techniques based on utilisation of circularly polarised SR, where combination of magnetic scattering, XMCD, spin-polarised EXAFS, spin-resolved X-ray photoelectron spectroscopy, *etc*., in one device could be required.

Synchrotron radiation-based methods are often combined with traditional laboratory analytical methods, for example, XRD can be combined with differential scanning calorimetry for studies of phase transitions,[317, 320] the combination 'Quick-EXAFS/IR' can be used for the characterisation of matrix synthesis products.[321] Laboratories for chemical, biological and materials science studies in modern SR centres are equipped with the modern instruments for realisation of traditional analytical techniques. The availability of traditional facilities (chromatographs, lasers, presses, scanning tunnelling and transmission electron microscopes, *etc*.) is particularly important for investigations of such complex objects as surfaces, advanced materials, biological systems, *etc*.

The trend to combine several different techniques in one device is realised in a new SR-based method, *viz*., event correlation or coincidence spectroscopy. In this method, several types of secondary emissions (fluorescent photons, photoelectrons, Auger

electrons, secondary ions) initiated by resonance absorption of X-ray photons are simultaneously detected using specialised electronic circuits. As an example of this approach, mention can be made of photoelectron-photoion coincidence (PEPICO) spectroscopy, which implies simultaneous registration of photoelectrons and ions (with a time-of-flight mass spectrometer) produced by photoionisation of a free molecule by an X-ray photon. Other event correlation methods, such as Auger-photoelectron coincidence, photoelectron-fluorescent photon coincidence, *etc*., are also developing. These methods are used in investigations of photochemical reactions, determination of electronic structure and lifetime of excited states, studies of dynamics of photoionisation and photodissociation of chemical bonds in free molecules or ions in the gas phase.[322–327]

2. Studies of substances under extreme conditions

Studies of matter under extreme conditions are of great importance for many fields of modern materials science, condensed state physics, geochemistry, mineralogy and geology. A key component of devices for high-pressure researches is a diamond anvil cell (DAC), which allows production of pressures up to a few hundreds GPa at areas of several square micrometers (Fig. 27). The choice of diamond as the material for such a high-pressure cell is dictated by its unique properties, such as extremely high mechanical strength combined with transparency for hard X-rays. A disadvantage in this case is unavoidable presence of glitches due to Bragg's reflections from walls of the cell. For local heating of the sample, a laser beam can be used and for cooling, a flow of liquid helium. The temperature and pressure inside the DAC can be monitored using structural (unit cell parameters, bond lengths) or spectral characteristics of an internal standard. A ruby crystal is often used as an internal standard with the shift of optical luminescence line as a parameter enabling monitoring. Experimental stations capable to achieve conditions ($T \approx 6000$ K, $P \approx 200$ GPa) close to that in the Earth's core ($T \approx 5000$ K, $P \approx 300$ GPa) are in routine operation for several years in a number of synchrotron radiation centres.[328–333]

Along with static studies, dynamic investigations of substances and materials under microsecond impacts or in propagating blast waves are of significant practical importance. The usefulness of synchrotron radiation in studies of this kind relates primarily to its high intensity (which allows beam penetration through the sample environment) and to the temporal beam modulation in the single-bunch mode of the storage ring operation.

XRD (especially its energy-dispersive modification), X-ray crystallography, EXAFS and X-ray topography are most commonly applied for characterisation of substances under high pressures. High-pressure studies using synchrotron Mössbauer spectroscopy are also under rapid development over recent years.[199, 200] It has to be stressed that on most of specialised devices for high-pressure studies, several physical techniques are

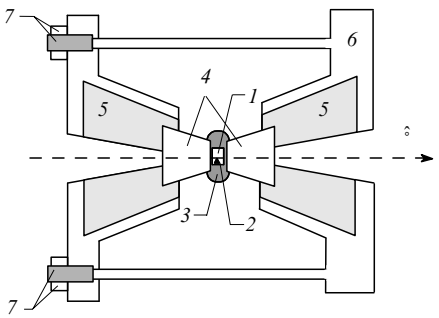

Figure 27. General view of a high-pressure cell.
(*1*) A sample under study, (*2*) a ruby crystal (internal standard used for pressure monitoring), (*3*) gasket, (*4*) tapered diamond anvils, (*5*) diamond anvil holder made of hard alloy, (*6*) steel housing, (*7*) pressure regulation mechanism (mechanic, pneumatic, hydraulic, *etc*.).

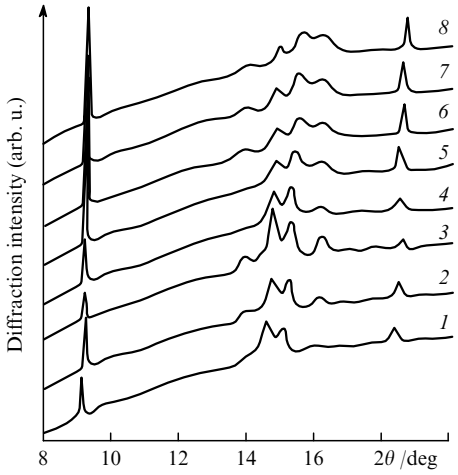

Figure 28. X-Ray powder diffraction patterns of solid oxygen at room temperature in the pressure range of 77–116 GPa (ESRF, Grenoble, France).[341]
P /GPa: (*1*) 77, (*2*) 85, (*3*) 88, (*4*) 96, (*5*) 101, (*6*) 105, (*7*) 110, (*8*) 116. At $P \sim 96$ GPa, a structural phase transition associated with oxygen metallisation occurs.

realised.[333, 334] Recently, equations of state for such substances as molecular hydrogen, helium, oxygen, carbon and water have been determined up to pressures > 100 GPa (Fig. 28) based on results obtained using SR. Phase diagrams of compounds which form the Earth's mantle and thus are very important in order to achieve understanding of geochemical processes (metallic iron, silicon, quartz, silicates and aluminosilicates) have been studied in a broad range of temperatures and pressures.[335–337] Results on structural monitoring of catalytic graphite–diamond transformation in the presence of magnesium carbonates and metallic nickel[338] and structural transition of carbon dioxide into polymeric quartz-like structure and further to metallic state have been reported.[339] In the last years, metallic states of substances and their mixtures which are gaseous under normal conditions (H_2, NH_3, CH_4, *etc*.), have become attainable, which allows simulation of the state of the matter in cores of distant planets of the Solar system: Saturn, Uranus and Neptune.[340–342]

A large part of all experiments with substances under extreme conditions is devoted to detection of unusual chemical properties and to studies of structure and properties of compounds not existing under normal temperatures and pressures. In particular, single crystals of molecular complexes formed in the hydrogen–methane system under high pressures, *viz*., $(CH_4)_2H_2$ and $(CH_4)(H_2)_2$, have been studied by synchrotron X-ray crystallography.[342] In another study, structural behaviour of potassium under high pressures has been investigated.[343] It has been shown that K forms intermetallides with 3*d*-metals, which implies that its chemical properties approach those of transition metals. Pressure-induced phase transitions in semiconducting, superconducting and magnetic materials often become subjects of SR-based studies.[344–347] Such transitions are sometimes accompanied by a change of coordination type or charge state of one of elements in the sample with preservation of overall stoichiometry.[348, 349] Structures and transformations of substances in supercritical media are widely studied. In particular, in a series of studies,[350–352] structural changes of hydration shells of such ions as Rb^+, Sr^{2+} and Br^- upon transition of water into a supercritical state have been monitored and a decrease of mean coordination number in the first coordination sphere has been revealed as a common effect.

3. Studies with high spatial resolution

Modern X-ray optics is capable of producing soft X-ray beams with linear size of several tens nm and hard X-ray beams of

submicron size. Technical progress in this field stimulates development of X-ray microprobe techniques: spatial resolution of such techniques has approached that of classical microprobe techniques utilising beams of charged particles, *viz*., electrons, protons or ions.[353–355] At the same time, synchrotron radiation gives access to a broader range of experimental techniques due to the possibility of detecting secondary radiation of various types, varying excitation energy, using polarisation and so on.‡

Microdiffraction (especially in the Laue modification) is used in studies of single grains and intergrain regions in compact polycrystalline materials (metals, composites, ceramics, semi- and superconductors),[362, 363] in analysis of local ordering areas in liquids or systems with a heavy disorder, in X-ray crystallographic investigations of submicron single crystals (clays, micas, zeolites)[364] and in structural characterisation of microscopic mineral inclusions in biological tissues.[365] Single fibre molecules are studied with synchrotron X-ray microdiffraction.[366] Spatially resolved X-ray fluorescence spectroscopy allows one to map the distribution of elements in a sample with resolution of the order of micrometers. Microprobe modifications of X-ray absorption spectroscopy (EXAFS, XANES, NEXAFS) give additional information on the chemical state and local environment of atoms in the sample under study (Fig. 29).[212, 367] Microprobe modification of XPS (sometimes referred to as 'Super-ESCA') is actively used for characterisation of minute amounts of hardly accessible or hazardous substances. For instance, an XPS study of curium oxide available in the amount of ~ 1 μg has been performed at the ALS synchrotron radiation centre (Berkley, USA).[368] The average beam size in this experiment was ~ 50 μm and the mass of the sample actually irradiated and contributing to the spectrum is estimated by the authors as only 4 ng. Spatially resolved information on supramolecular organisation of various objects can be obtained using microprobe modification of SAXS.[369, 370]

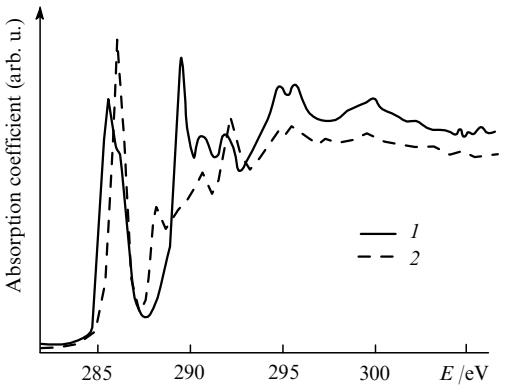

Figure 29. Micro-NEXAFS spectra (carbon *K*-edge) for thin polymeric films with area of 0.1 μm^2 on a scanning X-ray microscope (NSLS, Stony Brook, USA).[212]
(*1*) Polyethylene terephthalate; (*2*) polycarbonate.

Synchrotron X-ray microprobe techniques are routinely used for characterisation of spatially inhomogeneous objects including biological systems (cells, living tissues, bones), natural samples (microinclusions in minerals, coals, soils), advanced materials (ceramics, nanocomposites) as well as for environmental control of industrial wastes. Recently, the use of X-ray microdiffraction has been suggested as an express diagnostic tool for multilayer optoelectronics devices.[371] A set of synchrotron microprobe techniques (X-ray fluorescence, diffraction, XANES) with spatial resolution of 3×20 μm^2 has been used for determination of chemical composition, crystal structure and charge states of atoms in thin phosphor films of $MAlO_3$ (M is a rare-earth metal) grown by combinatorial synthesis.[372] Convergence of SR-based microprobe spectroscopic techniques and X-ray microscopy (see Section IV) during the last decade has lead to emergence of a new research area, *viz*., spectromicroscopy.[356]

‡ Instrumental realisation of X-ray microprobe techniques in modern synchrotron radiation centres and results of recent applications of these techniques are thoroughly discussed in a special issue of *Journal of Electron Spectroscopy and Related Phenomena*,[356] as well as in a number of books and reviews (see, for example, Refs 215, 357–361).

4. Time-resolved studies of processes

Evolution of SR sources and instrumentation, *viz*., gain in brightness, focusing optics optimisation, design of fast and sensitive detectors, development of specialised techniques for data collection and processing, has lead to a substantial decrease in the time required for conduction of an X-ray experiment with SR. Collection of XRF, EXAFS or SAXS data on facilities of modern SR centres may take only a few milliseconds. This approach is of great interest for chemistry, since it makes real-time studies of reaction dynamics possible. SR intensity is sufficiently high to obtain reliable results when the beam passes through walls of a chemical reactor (reaction chamber) or sample environment of another type. That is why most of synchrotron radiation-based methods can be realised *in situ* (see, for example, a special issue of *MRS Bulletin* dedicated to *in situ* studies of materials using synchrotron techniques[373]).

Real-time diffraction (the term 'diffraction cinema' is sometimes used) allows one to investigate dynamics of solid-state reactions, to detect formation of crystalline intermediates and, in the case of heterogeneous reactions, to follow the movement of the reaction front (interface).[20] Hydrothermal synthesis is one of the most promising fields in modern inorganic chemistry. This allows simulation of geochemical processes of natural mineral synthesis and preparation of new micro- and mesoporous materials, which can be applied as molecular sieves, ion-exchange resins, adsorbents, *etc*. The applicability of synchrotron real-time X-ray powder diffraction to studies of hydrothermal synthesis reactions is discussed in Refs 374, 375.

Changes in local environment of a reacting centre in the course of a chemical reaction can be analysed by means of Quick-EXAFS. In particular, such an approach has been utilised for detection of changes in local atomic order in active centres of catalysts.[376, 377] Time-resolved EXAFS can be used as well for structural monitoring of chemical transformations in solutions.[378, 379] Under the term Quick-EXAFS, the techniques with a rapid rotation of a standard crystal monochromator or so-called energy-dispersive EXAFS with a fixed crystal polychromator and a linear detector, are usually meant.[380–382]

Recently,[383] a new method aimed at a decrease in the XAFS data acquisition time has been proposed. It is based on a variation of the electron beam trajectory within insertion devices by adjusting operational parameters of the electromagnetic focusing system (Fig. 30) In this case, the crystal monochromator remains immobile and the beam intensity can be measured with a 'point' detector, *i.e*., ionisation chamber, which has better characteristics (such as counting rate, accuracy and sensitivity) compared to modern linear detectors. As an alternative of the aforementioned instrumental techniques of Quick-EXAFS, a stop-flow method can be used. This implies withdrawal of samples from a reaction mixture at required time intervals followed by their instant freezing and investigation using standard techniques.[384]

Time-resolved X-ray photoelectron spectroscopy enables investigations of chemical reactions at surfaces. For instance, this technique has been applied in studies of kinetics of NO reduction by molecular hydrogen on a single crystal face (553) of rhodium.[385] Data collected at the Super-ESCA station of the ELETTRA synchrotron centre allowed authors to detect intermediate unstable species (atomic nitrogen, atomic hydrogen, NH_x) and suggest a mechanism explaining the oscillatory dynamics of this reaction.

Time-resolved studies of biological processes give insights into mechanisms of key biochemical processes. For example, over the

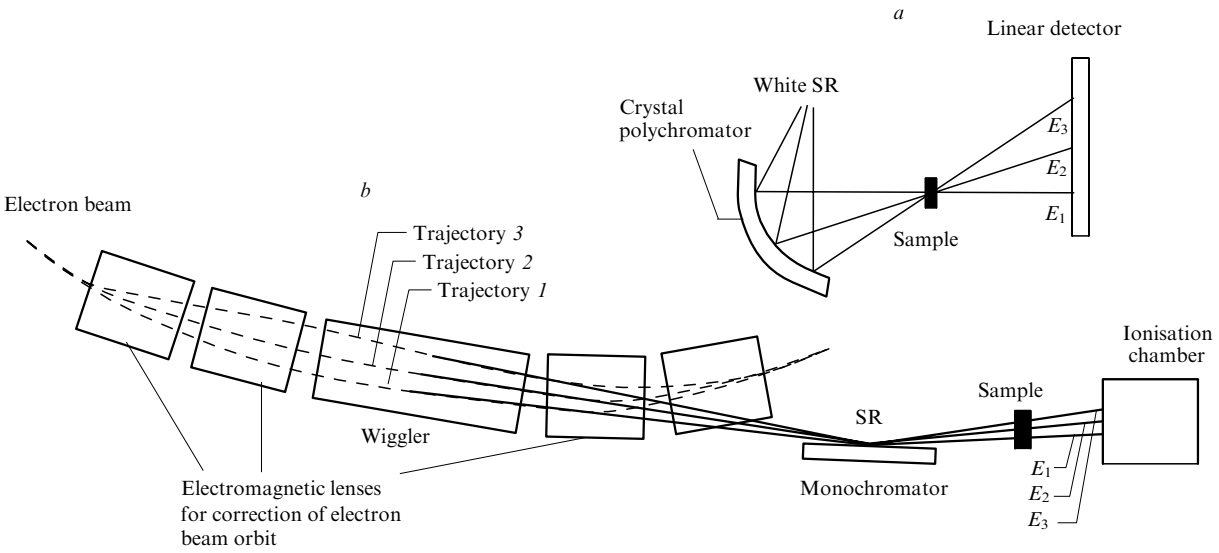

Figure 30. Experimental schemes for Quick-XAFS registration.[383]
(*a*) Energy-dispersive XAFS, (*b*) fast registration of XAFS by varying the electron trajectory within the channel of a storage ring.

last years, a substantial progress has been reached in understanding molecular mechanisms of muscle functioning thanks to SR-based studies of conformational transitions and supramolecular organisation changes of muscles under contraction and relaxation. Systematic real-time diffraction and SAXS studies of muscles are carried out in several international SR centres.[386, 387]

A combination of powerful third-generation SR sources and fast-counting 2*D* position-sensitive detectors opens new avenues in dynamic structural studies by means of Laue diffraction. Within this approach, a method of single crystal X-ray crystallography with time resolution down to tens of picoseconds is realised for biological macromolecules.[388, 389] In this modification of the 'diffraction cinema', a series of Laue patterns is registered during successive pulses of SR with a storage ring operating in the single-bunch mode. This approach is of great potential importance for investigations of enzymatic reactions. As one of the first applications of this technique, structural changes occurring in a single crystal of carboxy-myoglobin upon visible light-induced decarbonylation (Fig. 31) have been investigated.[390–392]

Capabilities offered by storage rings operating in the single-bunch mode are far from full realisation. A traditional method in this field is optical luminescence excited by X-ray pulse: its spectrum and decay dynamics are the key parameters in characterisation of new semiconducting and scintillating materials.[393] With a high level of confidence, we may suggest that in the immediate future, the interest of researchers in temporally modulated SR will increase, since this can supplement research capabilities of many of the aforementioned techniques with time resolution.

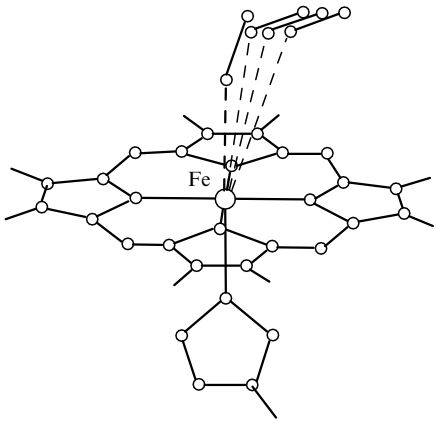

Figure 31. Migration of CO (dashed lines) in the initial stages of carboxy-myoglobin decarbonylation initiated by a visible light flash (ESRF). Atomic positions are determined by refinement of a common initial structural model *versus* a series of successive Laue-diffractograms measured for a single crystal of the substance with time resolution of ~ 10 ps.[392]

VI. Conclusion

Research capabilities of SR in chemistry and related sciences are wide and yet not fully realised. Over the last 30 years, introduction of synchrotron radiation into physicochemical analysis has resulted in substantial improvement of the accuracy and sensitivity of a few tens of physical methods. New synchrotron radiation centres are being constructed and the user community of the existing ones expands rapidly. The number of research papers reporting results obtained with the use of SR is thousands per year.

Starting from 1994, the International Union of Crystallography publishes a dedicated *Journal of Synchrotron Radiation*, in which over 1000 papers on various synchrotron radiation-related topics have already been published.

Key international and Russian national conferences with a dominant or major portion of synchrotron studies in their scope that took place over the period of 1994–2000, are listed in Table 2.

In certain fields of modern science (such as protein crystallography or XAFS), the synchrotron techniques has taken a leading position. And in such directions as development of MAD applications in crystallographic studies of biological polymers or time-resolved structural studies using Laue-diffraction, the last few years can be considered as a real breakthrough. Investigations of magnetic properties of materials using circularly polarised X-ray SR play an important role in modern technology.

Instrumentation of SR studies is under constant upgrade and sophistication. SR sources are evolving leading to even higher brilliance and stability and lower divergence of SR beams. According to predictions of machine R&D groups from several synchrotron centres [SSRL (Stanford, USA), ESRF, NSLS], fourth-generation SR sources may come into reality in the immediate future. In parallel, new ideas in the field of X-ray optics are emerging, which allows production of highly intense narrow-focus beams. Progress in this field is based to a great

Table 2. Large conferences held in 1994 – 2000 with a substantial portion of synchrotron topics in their scopes.

Year	Conference name	City	Country	Ref.[a]
1994	The Fifth International Conference on Synchrotron Radiation Instrumentation (SRI'94)	New York	USA	394
1994	The Tenth All-Russian Conference on Synchrotron Radiation (SR-94)	Novosibirsk	Russia	395
1994	The Eighth International Conference on X-ray Absorption Fine Structure (XAFS-8)	Berlin	Germany	396
1995	The 16th European Crystallography Meeting (ECM-16)	Lund	Sweden	–
1996	The First International Conference on Application of SR in Materials Science (SRMS-1)	Chicago	USA	–
1996	XAFS-9	Grenoble	France	397
1996	SR-96	Novosibirsk	Russia	398
1996	The 17th Symposium of the International Union of Crystallography (IUCr-17)	Seattle	USA	
1997	SRI'97	Himeji	Japan	399
1997	European Conference 'SR and Surface'	Castelvecco Pascoli	Italy	
1997	International Conference Frontiers in Synchrotron Radiation Spectroscopy' (FSRS'97)	Tokyo	Japan	400
1997	The First All-Russian Conference on the Application of X-rays, Synchrotron Radiation, Neutrons and Electrons to Studies of Materials (XRSNE-97)	Dubna	Russia	–
1997	ECM-17	Lisbon	Portugal	–
1998	SRMS-2	Kobe	Japan	–
1998	The Sixth International Conference on Applications of SR in Biophysics	Chicago	USA	–
1998	The Fourth European Conference on High-Resolution X-ray Diffraction and Topography (XTOP98)	Durham	England	–
1998	International School-Symposium 'SR in Natural Sciences'	Ustron-Jazovec	Poland	401
1998	XAFS-10	Chicago	USA	402
1998	ECM-18	Prague	Chech Republic	
1998	SR-98	Novosibirsk	Russia	403
1999	IUCr-18	Glasgow	Scotland	–
1999	XRSNE-99	Moscow	Russia	–
2000	SRI'2000	Berlin	Germany	–
2000	XAFS-11	Ako City	Japan	404
2000	ECM-19	Nancy	France	–
2000	SR-2000	Novosibirsk	Russia	–

[a] References to conference proceedings published in refereed journals.

extent on the latest achievements of X-ray lithography applications, which is also under active development in synchrotron centres. New fast, precise and sensitive X-ray detectors as well as X-ray monochromators with higher energy resolution appear. With improvement of coherent properties of SR, essentially new directions, such as X-ray holography, become possible. A breakthrough in imaging techniques can be expected with development of X-ray free-electron lasers.

Therefore, we may conclude that synchrotron radiation is one of the most promising points of growth for modern science. Starting from the 90's, the main SR centres turned into a new type of economic enterprises aimed at production of complex physical data. The overwhelming part of studies in modern centres have applied character and are tightly linked to technology. Despite the essentially profitless nature of 'photon factories' (for instance, costs of 1 h of beamtime on an EXAFS station, which is one of the 'cheapest' synchrotron techniques, is US \$200 – 400), contribution of synchrotron studies into modern competitive production is substantial. It explains, why the bulk of synchrotron studies in developed countries steadily increases and why many commercial companies tend to construct own stations at third-generation SR sources (for example, see review [405] on the use of synchrotron methods for characterisation of microelectronics materials prepared by the IBM R&D division on the basis of experimental results obtained at the NSLS).

Up to the 80's, the Soviet Union has been one of the world leaders in the field of synchrotron radiation theory and instrumentation. Many important steps in maturation of synchrotron radiation as a research tool have been made in the USSR. One of the first synchrotrons was constructed in 1964, experimental observation of synchrotron radiation dates back to 1971, undulators were designed in 1977, superconducting multipole wigglers in 1979 and helical undulators — sources of circularly polarised quasi-monochromatic radiation in 1983. Presently, G I Budker Institute of Nuclear Physics, where Siberian Synchrotron Radiation Centre (SSRC) operates, maintains a leading position in this field. Insertion devices, position-sensitive detectors and other high-tech devices designed and produced in BINP are used in many SR centres over the world: CAMD (Baton Rouge, USA), HASYLAB (Hamburg, Germany), Photon Factory (Tsukuba, Japan), PLS (Pohang, South Korea).

Meanwhile, the level and the volume of the applied synchrotron studies in Russia is noticeably lower than those in the largest world centres in USA, Japan and Western Europe. To the date of publication of this review, there is only one routinely operating national SR centre, Siberian synchrotron radiation centre (SSRC) in Novosibirsk, with a first-generation storage ring VEPP-3. Kurchatov synchrotron radiation source with the dedicated 'Sibir'-2' storage ring is on the stage of startup already for several years. Neither of the advanced complex techniques discussed above is involved in routine studies, which directly determine the level of modern science instrumentation. The authors hope that this review will draw attention of Russian researchers to this hot area of modern science.

This review has been written with the financial support of the Russian Foundation for Basic Research (Project No. 99-03-

32810), International Center for Diffraction Data (ICDD) and INTAS (Y V Z Grant YSF00-4095). We would like to thank our colleagues A A Ulyanov (Department of Geology, Moscow State University) and V A Strel'tsov (University of West Australia), who have kindly provided the results of their studies used as illustrations in this review, and O A Belyakova who provided us with materials of School on Synchrotron Radiation (Trieste, Italy, December 1997). The authors also express deep gratitude to D I Kochubey, B P Tolochko and specialists of SSRC for help in collaboration for many years.

References

1. E-E Koch (Ed.) *Handbook of Synchrotron Radiation* Vol. 1 (Amsterdam: North-Holland, 1983)
2. G V Marr (Ed.) *Handbook of Synchrotron Radiation* Vol. 2 (Amsterdam: North-Holland, 1987)
3. G B Brown, D E Moncton (Eds) *Handbook of Synchrotron Radiation* Vol. 3 (Amsterdam: North-Holland, 1991)
4. S Ebashi, M Koch, E Rubenstein (Eds) *Handbook of Synchrotron Radiation* Vol. 4 (Amsterdam: North-Holland, 1991)
5. I M Ternov, V V Mikhailin *Sinkhrotronnoe Izluchenie. Teoriya i Eksperiment* (Synchrotron Radiation. Theory and Experimnt) (Moscow: Energoatomizdat, 1986)
6. G N Kulipanov, A N Skrinskii, in *Rentgenospektral'nyi Metod Izucheniya Struktury Amorfnykh Tel. EXAFS-Spektroskopiya* (X-Ray Spectral Method for Investigation of the Structure of Amorphous Solids. EXAFS Spectroscopy) (Ed. G M Zhidomirov) (Novosibirsk: Nauka, 1988) p. 94
7. I M Ternov *Usp. Fiz. Nauk* **165** 429 (1995) [a]
8. H Winick *J. Synchr. Radiat.* **5** 168 (1998)
9. M Madou *Fundamentals of Microfabrication* (Boca Raton, FL; New York: CRC Press, 1997)
10. M Ando, C Uyano (Eds) *Medical Application of Synchrotron Radiation* (Berlin: Springer, 1998)
11. D G Schulze, P M Bertch *Adv. Agronomy* **55** 1 (1995)
12. *Otchet Sibirskogo Tsentra Sinkhrotronnogo Izlucheniya za 1998 g.* (Report of the Siberian Centre of Synchrotron Radiation for 1998) (Novosibirsk: Institute of Nuclear Physics, Siberian Branch of Russian Academy of Sciences, 2000)
13. *Kurchatov Synchrotron Radiation Source, 1993-1994. Activity Report, Moscow, 1995*
14. Y Utsumi, J Takahashi *Jpn. J. Appl. Phys. 2, Lett,* **37** L1268 (1998)
15. R K Kupka, F Bouamrane, C Cremers, S Megtert *Appl. Surf. Sci.* **164** 97 (2000)
16. P Dumas, G L Carr, G P Williams *Analysis* **28** 68 (2000)
17. R A Palmer, G D Smith, P Chen *Vib. Spectrosc.* **19** 131 (1999)
18. B Diviacco, R P Walker *Nucl. Instrum. Methods Phys. Res. A* **368** 522 (1996)
19. J L Laclare *J. Phys. IV, Colloq. (France)* **7** C2-39 (1997)
20. G N Kulipanov (Ed.) *Difraktometriya s Ispol'zovaniem Sinkhrotronnogo Izlucheniya* (Difractometry with the Use of Synchrotron Radiation) (Novosibirsk: Nauka, 1989)
21. V V Aristov, A I Erko, B Vidal *Diffraction X-Ray Optics* (London: IOP Publ., 1995)
22. A G Michette *Optical Systems for Soft X-Rays* (New York: Plenum, 1986)
23. B K Vainshtein *Sovremennaya Kristallografiya* (Modern Crystallography) (Moscow: Nauka, 1979) Vol. 1
24. L A Aslanov *Instrumental'nye Metody Rentgenostrukturnogo Analiza* (Instrumental Methods of X-Ray Diffraction Analysis) (Moscow: Moscow State University, 1982)
25. D Briggs, M P Seach (Eds) *Practical Surface Analysis by Auger and X-ray Photoelectron Spectroscopy* (New York: Wiley, 1983)
26. F F Fujita *Contemp. Phys.* **40** 323 (1999)
27. D C Koningsberger, R Prins (Eds) *Principles, Applications, Technique of EXAFS, SEXAFS and XANES* (New York: Wiley, 1988)
28. S S Husnain (Ed.) *X-Ray Absorption Fine Structure* (New York: Ellis Horwood, 1991)
29. G M Zhidomirov (Ed.) *Rentgenospektral'nyi Metod Izucheniya Struktury Amorfnykh Tel. EXAFS-Spektroskopiya* (X-Ray Spectral Method for Investigation of the Structure of Amorphous Solids. EXAFS Spectroscopy) (Novosibirsk: Nauka, 1988)
30. B K Teo *EXAFS: Basic Principles and Data Analysis* (Berlin: Springer, 1986)
31. G A Waychunas, G E Brown Jr *Adv. X-Ray Anal.* **37** 607 (1994)
32. H Ebel, R Svagera, M F Ebel *Microchim. Acta* **125** 165 (1997)
33. A Rogalev, J Goulon *J. Phys. IV, Colloq. (France)* **7** C2-565 (1997)
34. G Thornton, D R Warburton, I W Owen, C H Richardson, R Mcgrath, I T Mcgovern, D Norman *J. Phys. (France)* **47** NC-8-179 (1987)
35. B A Bunker, Z Wang, Q Islam *Ferroelectrics* **120** 23 (1991)
36. A Di Cicco, M Berrettoni *Phys. Lett. A* **176** 375 (1993)
37. A Di Cicco, M Minicucci *J. Synchr. Radiat.* **6** 255 (1999)
38. R G Linford *Chem. Soc. Rev.* **24** 267 (1995)
39. M Gautier-Soyer *J. Eur. Ceram. Soc.* **18** 2253 (1998)
40. C D Garner *Adv. Inorg. Chem.* **36** 303 (1991)
41. V K Yachandra *Methods Enzymol.* **246** 638 (1995)
42. P J Riggs-Gelasco, T L Stemmler, J E Penner-Hahn *Coord. Chem. Rev.* **144** 245 (1995)
43. P Johnston, P B Wells *Radiat. Phys. Chem.* **45** 393 (1995)
44. Y Iwasawa (Ed.) *X-Ray Absorption Fine Structure for Catalyst and Surfaces* (Singapore: World Sci., 1996)
45. J Evans *Chem. Soc. Rev.* **26** 11 (1997)
46. K Asakura, W-J Chun, M Shirai, K Tomishige, Y Iwasawa *J. Phys. Chem. B* **101** 5549 (1997)
47. N Toshima, T Yonezawa *New J. Chem.* **22** 1179 (1998)
48. I I Moiseev, M N Vargaftik, in *Catalysis by Di- and Polynuclear Metal Cluster Complexes* (Eds R D Adams, F A Cotton) (New York: Wiley-VCH, 1998) p. 395
49. H Huang, C H Liang, J E Penner-Hahn *Angew. Chem., Int. Ed. Engl.* **37** 1564 (1998)
50. H Tanida, H Sakane, I Watanabe *J. Chem. Soc., Dalton Trans.* **15** 2321 (1994)
51. Y Inada, K Sugimoto, K Ozutsumi, S Funahashi *Inorg. Chem.* **33** 1875 (1994)
52. L R Sharpe, W R Heineman, R C Elder *Chem. Rev.* **90** 705 (1990)
53. A Di Cicco, M Minicucci, A Filipponi *Phys. Rev. Lett.* **78** 460 (1997)
54. J Stöhr *NEXAFS Spectroscopy* (Berlin: Springer, 1992)
55. J Kukuma, B P Tommer *J. Electron Spectrosc. Relat. Phenom.* **82** 53 (1996)
56. J Taborski, P Vaterlein, H Dietz, U Zimmermann, E Umbach *J. Electron Spectrosc. Relat. Phenom.* **75** 129 (1995)
57. G Hühner, M Kinzler, Ch Wlll, M Grunze *Phys. Rev. Lett.* **67** 851 (1991)
58. R Mitsumoto, H Oji, I Mori, Y Yamamoto, K Osato, Y Ouchi, H Shinohara, K Seki, K Umishita, S Hino, S Nagase, K Kikushi, Y Achiba *J. Phys. IV, Colloq. (France)* **7** C2-525 (1997)
59. J Wong, Z U Rek, M Rowen, T Tanaka, F Schafers, B Muller, G N George, I J Pickering, G Via, B Devries, G E Brown, M Froba *Physica B* **208**–**209** 220 (1995)
60. P Ildefonse, G Cals, A M Flank, P Lagarde *Nucl. Instrum. Methods Phys. Res. B* **97** 172 (1995)
61. D C Koningsberger, J T Miller *Catal. Lett.* **29** 77 (1994)
62. M Kamijo, N Umesaki, K Fukui, C Guy, K Tadanada, M Tasumisago, T Minami *J. Non-Cryst. Solids* **177** 187 (1994)
63. S Paste, V Gotte, C Goulon-Ginet, A Rogalev, J Goulon, P Georget, J Marcilloux *J. Phys. IV, Colloq. (France)* **7** C2-665 (1997)
64. P J Potts, A T Ellis, P Kregsamer, C Streli, M West, P Wobrauschek *Annu. Rep. Anal. At. Spectrom.* **14** 1773 (1999)
65. V A Trounova, K Z Zolotarev, V B Baryshev, M A Phedorin *Nucl. Instrum. Methods Phys. Res. A* **405** 532 (1998)
66. L N Tarasov, A F Kudryashova, A A Ulyanov, V B Baryshev, K V Zolotarev *Nucl. Instrum. Methods Phys. Res. A* **405** 590 (1998)
67. E J Nordgren *J. Electron Spectrosc. Relat. Phenom.* **78** 25 (1996)
68. A N Artemiev, M M Vsevolodov, D P Grechukhin, A V Zabelin, V N Kosyakov, S V Romanov, A A Soldatov *Nucl. Instrum. Methods Phys. Res., A* **359** 266 (1995)
69. J Nordgren, J Guo *J. Electron Spectrosc. Relat. Phenom.* **110**–**111** 1 (2000)
70. E J Nordgren *J. Phys. IV, Colloq. (France)* **7** C2-9 (1997)
71. J Guo, J Nordgren *J. Electron Spectrocs. Relat. Phenom.* **110**–**111** 105 (2000)

72. F M F De Groot *J. Electron Spectrosc. Relat. Phenom.* **92** 207 (1998)
73. G M Bancroft, Y-F Hu *Inorg. Electron Struct. Spectrosc.* **1** 443 (1999)
74. M Taniguchi *J. Alloys Compd.* **286** 114 (1999)
75. A Nillson, in *Application of Synchrotron Radiation* (Berlin: Springer, 1995) p. 65
76. C Laubschat *J. Electron Spectrosc. Relat. Phenom.* **96** 127 (1998)
77. J C Green, N Kaltsoyanis, K H Sze, M MacDonald *J. Am. Chem. Soc.* 116 (1994)
78. X Li, G M Bancroft, R J Puddephatt, Y-F Hu, K H Tan *Organometallics* **15** 2890 (1996)
79. A M Bradshaw, C S Fadley, N Mertensson (Eds) *Future Perspectives of X-Ray Photoelectron Spectroscopy with Synchrotron Radiation. J. Electron Spectrosc. Relat. Phenom.* **75** (0) (Special Issue) (1995)
80. A M Bradshaw, D P Woodruff, in *Application of Synchrotron Radiation. Springer Ser. Surface Science* Vol. 35 (Ed. W Ebernardt) (Berlin, Heidelberg: Springer, 1995) p. 127
81. C S Fadley, A P Kaduwela, M A Vannove, Z Hussain *J. Electron Spectrosc. Relat. Phenom.* **75** 273 (1995)
82. C S Fadley *Prog. Surf. Sci.* **54** 341 (1997)
83. L J Terminello, B L Petersen, J J Barton *J. Electron Spectrosc. Relat. Phenom.* **75** 299 (1995)
84. C S Fadley, in *Synchrotron Radiation Research: Advances in Surface and Interface Science. Techniques* Vol. 1 (Ed. R Z Bachrach) (New York: Plenum, 1992) p. 421
85. M M Harding *Acta Crystallogr., Sect. B* **51** 432 (1995)
86. J R Helliwell *Acta Crystallogr., Sect. A* **54** 738 (1998)
87. P Coppens *Synchrotron Radiation Crystallography* (London: Academic Press, 1992)
88. P Coppens *J. Appl. Crystallogr.* **26** 499 (1993)
89. M M Harding *Mater. Sci. Forum* **228** 3 (1996)
90. P Coppens, R Bolotovsky, V Kezerashvili, A Darovsky, Y Gao *Trans. Am. Crystallogr. Assoc.* **31** 11 (1997)
91. P Coppens, G Wu, A Volkov, Y Abramov, Y Zhang, W K Fullagar, L Ribaud *Trans. Am. Crystallogr. Assoc.* **34** 51 (2000)
92. W Rieck, H Euler, H Schulz *Acta Crystallogr., Sect. A* **44** 1099 (1988)
93. R W Broach, R L Bedard, S G Song, J J Pluth, A Bram, C Riekel, H-P Weber *Chem. Mater.* **11** 2076 (1999)
94. E F Skelton, J D Ayers, S B Qudri, N E Moulton, K P Cooper, L W Finger, H K Mao, Z Hu *Science* **253** 1123 (1991)
95. K D Eichnorn *Eur. J. Mineral.* **9** 673 (1997)
96. R B Neder, M Bourghammer, Th Grasl, H Schulz *Z. Kristallogr.* **211** 763 (1996)
97. K Oshumi, K Hagiya, M Okhmasa *J. Appl. Crystallogr.* **24** 340 (1991)
98. R B Neder, M Burghammer, T Crasl, H Schulz *Z. Kristallogr.* **211** 365 (1996)
99. R Flaig, T Koritzansky, J Janczak, H-G Krane, W Morgenroth, P Luger *Angew. Chem., Int. Ed. Engl.* **38** 1397 (1999)
100. E N Maslen, V A Streltsov, N R Streltsova, N Ishizawa *Acta Crystallogr., Sect. B* **51** 929 (1995)
101. K Eichhorn, A Kirfel *Acta Crystallogr., Sect. B* **47** 843 (1991)
102. B B Iversen, F K Larsen, A A Pinkerton, A Martin, A Darovsky, P A Reynolds *Inorg. Chem.* **37** 4559 (1998)
103. H Graafsma, M Souhassou, A Puig-Molina, S Harkema, E Kvick, C Lecomte *Acta Crystallogr., Sect. B* **54** 193 (1998)
104. F Frolow, L Chernyak, D Cahen *Tern. Mult. Compd.* **152** 67 (1998)
105. F S Nielsen, P Lee, P Coppens *Acta Crystallogr., Sect. B* **42** 359 (1986)
106. T Koritsanszky, R Flaig, D Zobel, H G Krane, W Morgenroth, P Luger *Science* **279** 356 (1998)
107. T Koritzanszky, in *International Union Crystallography XVIIIth Congress and General Assembly (Collected Abstracts), Glasgow, 1999* M09.OD.002
108. B B Iversen, in *International Union Crystallography XVIIIth Congress and General Assembly (Collected Abstracts), Glasgow, 1999* M09.OD.003
109. B K Vainshtein, V M Fridkin, V L Indenbom *Sovremennaya Kristallografiya* (Modern Crystallography) (Moscow: Nauka, 1979) Vol. 2, p. 193
110. P F Lindley *Radiat. Phys. Chem.* **45** 367 (1995)
111. K Moffat, Z Ren *Curr. Opin. Struct. Biol.* **7** 689 (1997)
112. J R Helliwell, S Ealick, P Doing, T Irring, M Szemenyi, *Acta Crystallogr., Sect. D* **49** 120 (1993)
113. W Minor, D R Tomchick, Z Otwinowski *Structure* (*London*) **8** R105 (2000)
114. *Structural Biology and Synchrotron Radiation: Evaluation of Resources and Needs* http://www.ornl.gov/hgmis/biosync
115. A Deacon, T Gleichmann, A J Kalb, H Price, J Raftery, G Bradbrook, J Yariv, J R Helliwell *J. Chem. Soc., Dalton Trans.* **93** 4305 (1997)
116. C Jelsch, M M Teeter, V Pickon-Pesme, R H Blessing, C Lecomte, in *International Union Crystallography XVIIIth Congress and General Assembly (Collected Abstracts), Glasgow, 1999* M11.BB.004
117. J P Abrahams, A G W Leslie, R Lutter, J E Walker *Nature (London)* **370** 621 (1994)
118. D H Bilderback, S A Hoffmann, D J Thiel *Science* **263** 201 (1994)
119. B M Kariuki, M M Harding *J. Synchr. Radiat.* **2** 185 (1995)
120. X J Yang, Z Ren, K Moffat *Acta Crystallogr., Sect. D* **54** 367 (1998)
121. R B G Ravelli, M L Raves, S H W Scheves, A Schouten, J Kroon, *J. Synchr. Radiat.* **6** 19 (1999)
122. T Bruckel, M Lippert, B Bouchard, T Schmidt, J R Schneider, W Jauch *Acta Crystallogr., Sect. A* **49** 679 (1993)
123. M J Cooper, W G Stirling *Radiat. Phys. Chem.* **56** 85 (1999)
124. T Bruckel *Acta Phys. Pol. A* **91** 669 (1997)
125. D Mannix, S Langridge, G H Lander, J Rebizant, M J Longfield, W G Stirling, W J Nutall, S Coburn, S Wasserman, L Soderholm *Physica B* **262** 125 (1999)
126. D Gibbs, D E Moncton, K L D'Amico, J Bohr, B H Grier *Phys. Rev. Lett.* **55** 234 (1985)
127. H Graafsma, G W J C Heunen, C Schulze *J. Appl. Crystallogr.* **31** 414 (1998)
128. H Graafsma, A Paturle, L Wu, H-S Sheu, J Majewski, G Poorthuis, P Coppens *Acta. Crystallogr., Sect. A* **48** 113 (1992)
129. S J van Reeuwijk, H Graafsma, in *International Union Crystallography XVIIIth Congress and General Assembly (Collected Abstracts), Glasgow, 1999* P05.10.005
130. A Puig-Molina, H Mueller, H Graafsma, A Kvick, in *International Union Crystallography XVIIIth Congress and General Assembly (Collected Abstracts), Glasgow, 1999* P11.19.025
131. L X Chen, M K Bowman, Zh Wang, P A Montano, J R Norris *J. Phys. Chem. B* **98** 9457 (1994)
132. H Fuess *An. Quim. Int. Ed.* **94** 388 (1998)
133. A N Fitch, in *Proceedings of the 6th Summer School on Neutron Scattering: Complementary between Neutron and Synchrotron X-Ray Scattering* (Ed. A Furrer) (New York: World Sci., 1998) p. 41
134. B A Latella, B H O'Connor *J. Am. Ceram. Soc.* **80** 2941 (1997)
135. P Norby *J. Appl. Crystallogr.* **30** 21 (1997)
136. P G Fagan, R B Hammond, K J Roberts, R Docherty, A P Chorlton, W Jones, G D Potts *Chem. Mater.* **7** 2322 (1995)
137. W I F David, K Shankland, N Shankland *Chem. Commun.* 931 (1998)
138. K D Knudsen, P Pattison, A N Fitch, R J Kernik *Angew. Chem., Int. Ed. Engl.* **37** 2340 (1997)
139. A Kern, A Coelho, in *International Union Crystallography XVIIIth Congress and General Assembly (Collected Abstracts), Glasgow, 1999* P05.OD.001
140. R J Chernik, A K Cheetham, C K Prout, D J Watkin, A P Wilkinson, B T M Willis *J. Appl. Crystallogr.* **24** 222 (1991)
141. A N Fitch, H Jobic *J. Chem. Soc., Chem. Commun.* 1516 (1993)
142. R E Dennibier, M Pink, J Sieler, P W Stephens *Inorg. Chem.* **36** 3398 (1997)
143. R E Morris, J J Owen, A K Cheetham *J. Phys. Chem. Solids* **56** 1297 (1995)
144. M A Roberts, A N Fitch, A V Chadvick *J. Phys. Chem. Solids* **56** 1353 (1995)
145. R W Broach, R M Kirchner, N K McGuire, C C Chao *J. Phys. Chem. Solids* **56** 1363 (1995)
146. T R Jensen, P Norby, A N Christensen, J C Hanson *Microp. Mesop. Mater.* **26** 77 (1998)
147. D M Poojary, A Clearfield *J. Organomet. Chem.* **512** 237 (1995)
148. R E Dennibier, U Behrens, F Olbrich *J. Am. Chem. Soc.* **120** 1430 (1998)

149. J E Fischer, G Bendele, R Dinnebier, P W Stephens, C L Lin, N Bykovets, Q Zhu *J. Phys. Chem. Solids* **56** 1445 (1995)
150. E Nishibori, M Takata, M Sakata, M Inakuma, H Shinohara *Chem. Phys. Lett.* **298** 79 (1998)
151. E Nishibori, M Takata, M Sakata, H Shinohara *J. Synchr. Radiat.* **5** 977 (1998)
152. C M Brown, L Cristofilini, K Kordatos, K Prassides, C Bellavia, R Gonzales, K M Keshavorz, F Wude, A K Cheetham, J P Zhang, W Andreoni, A Currion, A N Fitch, P Pattison *Chem. Mater.* **8** 2548 (1996)
153. R E Dinnebier, P W Stephens, J K Carter, A N Lommen, P A Heiney, A R McGhie, L Branrd, A B Smith *J. Appl. Crystallogr.* **28** 327 (1995)
154. R E Dennibier, F Olbrich, S van Smaalen, P W Stephens *Acta Crystallogr., Sect. B* **53** 153 (1997)
155. Y Kubota, M Takata, M Sakata *J. Phys., Condens. Matter* **5** 8245 (1993)
156. M Takata, Y Kubota, M Sakata *Z. Naturforsch., A Phys. Sci.* **48** 75 (1993)
157. S Yamamura, M Takata, M Sakata *J. Phys. Chem. Solids* **58** 117 (1997)
158. T Wessels, C Baerlochev, L B McCusker *Science* **284** 477 (1999)
159. C J Benmore, B L Tomberli, P A Egelstaff, in *International Union Crystallography XVIIIth Congress and General Assembly (Collected Abstracts), Glasgow, 1999* P06.OF.001
160. J Poulsen, J Neuefeind, H B Neumann, J R Schneider, M D Zeider *J. Non-Cryst. Solids* **188** 63 (1995)
161. S Mobilio, C Meneghini *J. Non-Cryst. Solids* **232**–**234** 25 (1998)
162. H Schlenz, R Grabinski, A Kirfel, in *International Union Crystallography XVIIIth Congress and General Assembly (Collected Abstracts), Glasgow, 1999* P07.10.001
163. T R Welberry, Th Proffen *Acta Crystallogr., Sect. A* **54** 661 (1998)
164. T R Welberry, in *International Union Crystallography XVIIIth Congress and General Assembly (Collected Abstracts), Glasgow, 1999* K07.03.001
165. A Mahendrasingam, V T Forsyth, R Hussain, R J Greenall, W J Pigram, W Fuller *Science* **233** 195 (1986)
166. G Büldt, K Konno, K Nakanishi, H-J Plöhn, B N Rao, N A Dencher *Photochem. Photobiol.* **54** 873 (1991)
167. W Bras, A J Ryan *Adv. Colloid Interface Sci.* **75** 1 (1998)
168. J C Dore, A N North, J C Rigden *Radiat. Phys. Chem.* **45** 413 (1995)
169. C Riekel, P Bosecke, O Diat, P Engstrom *J. Mol. Struct.* **383** 291 (1996)
170. G Panick, R Malessa, R Winter, R Gert, K J Frye, C A Royer *J. Mol. Biol.* **275** 90 (1998)
171. G Barone, Z Sayers, D Svergun, M H J Koch *J. Synchr. Radiat.* **6** 1031 (1999)
172. M Megens, C M Van Kats, P Bosecke, V L Vos *J. Appl. Crystallogr.* **30** 637 (1997)
173. A F Craevich, O L Alves, L C Barbosa *Rev. Sci. Instrum.* **66** 1338 (1995)
174. A Craevich *J. Phys. I, Gen Phys. Stat. Phys Condens. Matter Cross.-Discipl. Phys.* **2** 801 (1992)
175. M F Butler, A M Donald, A J Ryan *Polymer* **38** 5521 (1997)
176. P P E A de Moor, T P M Beelen, B U Komanchek, O Dlat, R A Santen *J. Phys. Chem. B* **101** 11077 (1997)
177. J S Rigden, A N North, A R Mackie *Prog. Colloid Polym. Sci.* **93** 63 (1993)
178. A N North, J S Rigden, A R Mackie *Rev. Sci. Instrum.* **63** 1741 (1992)
179. E D Isaacs, P M Platzman *Phys. Today* **49** 40 (1996)
180. H Hayashi, N Watanabe, Y Udagawa *J. Synchr. Radiat.* **5** 1052 (1998)
181. F Sette, G Ruocco *Eur. News* **26** 78 (1995)
182. G Ruocco, F Sette *Bull. Soc. Fr. Phys.* **115** 25 (1998)
183. E Burkel *Rep. Prog. Phys.* **63** 171 (2000)
184. N G Alexandropoulos *Nucl. Instrum. Methods Phys. Res. A* **308** 267 (1991)
185. W Schülke, U Bonse, H Nagasawa, A Kaprolat, A Berthold *Phys. Rev. B* **38** 2112 (1988)
186. C Blaas, J Redinger, S Manninen, V Honkimäki, K Hämäläinen, P Suortti *Phys. Rev. Lett.* **75** 1984 (1995)
187. K Tohji, Y Udagawa *Phys. Rev. B* **39** 7590 (1989)
188. F Gelmukhanov, H Agren *Physica B* **208**–**209** 100 (1995)
189. H Nagasawa *J. Phys., Pt 2 (Paris)* **48** (C-9) 863 (1987)
190. W Schülke, A Berthold, A Kaprolat, H-J Güntherodt *Phys. Rev. Lett.* **60** 2217 (1988)
191. W Schülke, K-J Gabriel, A Berthold, H Shulte-Schrepping *Solid State Commun.* **79** 657 (1991)
192. Y Ma, *J. Electron Spectrosc. Relat. Phenom.* **79** 131 (1996)
193. G Dräger *Surf. Invest.* **13** 447 (1998)
194. U van Bärck, R L Mössbauer, E Gerdau, R Rüffer, R Holletz, G Smirnov, P Hanson *Phys. Rev. Lett.* **59** 355 (1987)
195. H Grünsteudel, W Meyer-Klaucke, A X Trautwein, H Winkler, O Leupold, J Metge, E Gerdau, H D Rüter, A Q R Baron, A I Chumakov, H F Grünsteudel, R Rüffer, M Haas, E Realo, D Mandon, R Weiss, H Toftlund, in *Bioinorganic Chemistry: Transition Metals in Biology and Their Coordination Chemistry* (Ed. A X Trautwein) (New York: Wiley-VCH, 1997) p. 760
196. A X Trautwein, H Paulsen, E Realo, H D Rüter, H Grünsteudel, R Weiss, M Haas, H Winkler, O Leupold, D Mandon, B F Matzanke, W Meyer-Klaucke *Inorg. Chim. Acta* **275** 334 (1998)
197. V Schünemann, H Winkler *Rep. Prog. Phys.* **63** 263 (2000)
198. W Sturhahn, E E Alp, T S Toellner, P Hession, M Hu, J Sutter *Hyperfine Interact. (Netherlands)* **113** 47 (1998)
199. S Nasu *Hyperfine Interact. (Netherlands)* **113** 97 (1998)
200. M Pleines, R Lübbers, M Strecker, G Wortmann, O Leupold, Yu Shvyd'ko, E Gerdau, J Metge *Hyperfine Interact. (Netherlands)* **120** 181 (1999)
201. R Lübbers, M Pleines, H-J Hesse, G Wortmann, H F Grünsteudel, R Rüffer, O Leupold, J Zukrowski *Hyperfine Interact. (Netherlands)* **120** 49 (1999)
202. L Nielsen, A Mugarza, M F Rozu, R Coehoorn, R M Junglblut, F Rozeboom, A Q R Baron, A I Chumakov, R Rüffer *Phys. Rev. B* **58** 8590 (1998)
203. V G Kohn, G V Smirnov *Hyperfine Interact. (Netherlands)* **123**–**124** 327 (2000)
204. B Sepiol, C Czihak, A Meyer, G Vogl, J Metge, R Rüffer *Hyperfine Interact. (Netherlands)* **113** 449 (1998)
205. B Sepiol, A Meyer, G Vogl, R Rüffer, A I Chumakov, A Q R Baron *Phys. Rev. Lett.* **76** 3220 (1996)
206. B Sepiol, A Meyer, G Vogl, H Franz, R Rüffer *Phys. Rev. B* **57** 10433 (1998)
207. A Chumakov, R Rüffer *Hyperfine Interact. (Netherlands)* **113** 59 (1998)
208. A I Chumakov, A Barla, R Rüffer, J Metge, H F Grünsteudel, H Grünsteudel, J Plessel, H Winklemann, M M Abd-Elmeguid *Phys. Rev. B* **58** 254 (1998)
209. E Gerdau, U van Bürck, in *Resonant Anomalous X-Ray Scattering* (Eds G Materlik, C J Sparks, K Fischer) (Amsterdam: Elsevier, 1994) p. 589
210. R Rohlsberger *Hyperfine Interact. (Netherlands)* **123**–**124** 455 (2000)
211. J Kirz, M Howells *Q. Rev. Biophys.* **28** 33 (1995)
212. H Ade, X Zhang, S Cameron, C Costello, J Kirz, S Williams *Science* **258** 972 (1992)
213. H Ade, B Hsiao, G Mitchell, E Rightor, A P Smith, R Cieslinski *Mater. Res. Soc. Proc.* **375** 293 (1995)
214. H Ade *Trends Polym. Sci.* **5** 58 (1997)
215. J Thieme, G Schmahl, E Umbach, D Rudolf (Eds) *X-Ray Microscopy and Spectromicroscopy* (Berlin: Springer, 1998)
216. M Moore *Radiat. Phys. Chem.* **45** 427 (1995)
217. F Zontone, L Moncini, R Barrett, J Baruchel, J Hartwig, Y Epelboin *J. Synchr. Radiat.* **3** 173 (1996)
218. B K Tonner *Acta Phys. Pol.* **86** 537 (1994)
219. J Baruchel, in *X-Rays and Neutrons Dynamical Diffraction. Theory and Applications* (Ed. A Authier) (New York: Plenum, 1996) p. 199
220. P Jacobs, E Sevens, M Kunnen *Sci. Total Environ.* **167** 161 (1995)
221. U Bonse, F Busch *Prog. Biophys. Mol. Biol.* **65** 133 (1996)
222. W S Haddad, I McNulty, J E Trebes, E H Anderson *Proc. SPIE — Int. Soc. Opt. Eng.* **2516** 102 (1995)
223. A Snigirev, I Snigireva, V Kohn, S Kuznetsov, I Schelokov *Rev. Sci. Instrum.* **66** 5486 (1995)
224. A Snigirev, I Snigireva, A Suvorov, M Kocsis, V Kohn *ESRF Newslett.* **24** 23 (1995)
225. A A Snigirev, C Raven *Bull. Soc. Fr. Phys.* **110** 10 (1997)

226. G Grmbel, D Abernathy, T Thurn-Albrecht, W Steffen, A Patkowski, G Meier, E W Fischer *ESRF Newslett*. **26** 10 (1996)
227. S B Dieker, R Pindak, R M Fleming, I K Robinson, L Berman *Phys. Rev. Lett*. **75** 449 (1995)
228. S G J Mochrie, A M Mayes, A R Sandy, M Sutton, S Brauer, G B Stephenson, D L Albernathy, G Grmbel *Phys. Rev. Lett*. **78** 1275 (1997)
229. S Brauer, G B Stephenson, M Sutton, R Brmning, E Dufresne, S G J Mochrie, G Grübel, J Als-Nielsen, D Abernathy *Phys. Rev. Lett*. **74** 2010 (1995)
230. Z H Kai, B Lai, W B Yun, I McNulty, K G Huang, T P Russel *Phys. Rev. Lett*. **73** 82 (1994)
231. K Burger, D Cox, R Papoular, W Prandl *J. Appl. Crystallogr*. **31** 789 (1998)
232. K Burger, W Prandl, S Doyle *Z. Kristallogr*. **212** 493 (1997)
233. D M Proserpio, G Artioli, S Mulley, G Chacon, C Zheng *Chem. Mater*. **9** 1463 (1997)
234. A Noudon *NATO Adv. Stady Inst. Ser. C, Math. Phys. Sci*. **452** 203 (1995)
235. H G Haubold, X H Wang, H Jungbluth, G Goerigk, W Schilling *J. Mol. Struct*. **383** 283 (1996)
236. B Bouchetfabre, P Dangelo, N V Pvel *Nucl. Instrum. Methods Phys. Res. B* **97** 539 (1995)
237. S Sasaki, T Toyoda, K Yamanaki, K Okhubo *J. Synchr. Radiat*. **5** 920 (1998)
238. A P Wilkinson, A K Cheetham, D E Cox *Acta Crystallogr., Sect. B* **47** 155 (1991)
239. Y Gao, M R Pressprich, P Coppens *Acta Crystallogr., Sect. A* **49** 21 (1993)
240. Y Gao, A Frast-Jensen, M R Pressprich, P Coppens *J. Am. Chem. Soc*. **114** 9214 (1992)
241. G Wu, Y Zhang, L Ribaud, P Coppens, C Wilson, B B Iversen, F K Larsen *Inorg. Chem*. **37** 6078 (1998)
242. W A Hendrickson *Science* **254** 54 (1991)
243. W A Hendrickson, C M Ogata *Methods Enzymol*. **276** 494 (1997)
244. W A Hendrickson *J. Synchr. Radiat*. **6** 845 (1999)
245. A Cassetta, A M Deacon, S E Ealick, J R Helliwell, A W Thompson *J. Synchr. Radiat*. **6** 822 (1999)
246. S Stuhrmann, K S Bartels, W Brannwarth, R Doose, F Dauvergne, A Gabriel, A Knochel, M Marmotti, H B Stuhrmann *J. Synchr. Rad*iat. **4** 298 (1997)
247. S Sturmann, K Bartels, M Hütch, M Marmottti, Z Zaiers, J Tomas, K Trams, H B Sturmann, in *Problemy Sovremennoi Kristallografii. Strukturnye Issledovaniya Kristallov* (Problems in Modern Crystallography. Structural Investigation of Crystals) (Moscow: Nauka, 1996) p. 276
248. M Schiltz, A Kvick, O S Svensson, W Shepard, E dela Fortelle, T Pranfe, R Kahn, G Brigogne, R Fourme *J. Synchr. Radiat*. **4** 287 (1997)
249. I J Pickering, M Sansone, J Marsch, G N George *J. Am. Chem. Soc*. **115** 6302 (1993)
250. J Vacinova, J L Hadeau, P Wolfers, J P Lauriat, E Elkain *J. Synchr. Radiat*. **2** 236 (1995)
251. J P Attfield *Mater. Sci. Forum* **228** 201 (1996)
252. G Materlik, C J Sparks, K Fischer (Eds) *Resonant Anomalous X-Ray Scattering. Theory and Applications* (Amsterdam: Elsevier, North-Holland, 1994)
253. R M Imamov, E Kh Mukhamedzhanov, in *Problemy Sovremennoi Kristallografii. Strukturnye Issledovaniya Kristallov* (Problems in Modern Crystallography. Structural Investigation of Crystals) (Moscow: Nauka, 1996) p. 132
254. J B Peclka, A Cedola, S Lagomarsino, S di Fonzo, W Jark, G Soullie *J. Alloys Compd*. **286** 313 (1999)
255. S-H Yang, B S Mun, A W Kay, S-H Kim, J B Kortright, J H Underwood, Z Hussain, C S Fadley *Surf. Sci*. **461** L557 (2000)
256. D P Woodruff *Prog. Surf. Sci*. **57** 1 (1998)
257. A Lessmann, S Brennan, B Materlik, M Schuster, H Riechert *Rev. Sci. Instrum*. **66** 1428 (1995)
258. Y Qian, N C Sturchio, R P Chiarello, P F Lyman, T-L Lee, M J Bedzyk *Science* **265** 1555 (1994)
259. M Sugiyama, S Maeyama, M Oshima *Rev. Sci. Instrum*. **67** 3182 (1996)
260. A Shi, P L Cowan, S Southworth, L Fotiadis, C Hor, B Harlin, F Moore, E Dobisz, H Dietrich *J. Appl. Phys*. **73** 8161 (1993)
261. M V Kovalchuk, A Y Kazimirov, S I Zheludeva *Nucl. Instrum. Methods Phys. Res. B* **101** 435 (1995)
262. J Als-Nielsen, in *Handbook of Synchrotron Radiation* (Eds G B Brown, D E Moncton) (Amsterdam: North-Holland, 1991) Vol. 3, p. 471
263. H Aiginger, P Wobrauschek, C Streli *Anal. Sci*. **11** 471 (1995)
264. R S Hockett *Mater. Res. Soc. Symp. Proc*. **354** 377 (1995)
265. C Streli *J. Trace Microprobe Techn*. **13** 109 (1995)
266. P Wobrauschek *J. Anal. At. Spectrom*. **5** 333 (1998)
267. R S Hockett *Adv. X-Ray Anal*. **37** 565 (1994)
268. Z H Ming, Y L Soo, S W Huang, Y H Kao, K Stair, G Devane, C Choi-Feng, T Chang, L P Fu, G D Gilliland, J Klem, M Hafich *Mater. Res. Soc. Symp. Proc*. **417** 325 (1996)
269. F D'Acapito, F Zontone *J. Appl. Crystallogr*. **32** 234 (1999)
270. G Capiccio, M Leoni, P Scardi, V Sessa, M L Terranova *Adv. Cryst. Growth* **203** 285 (1996)
271. J Reiche, D Janietz, T Baberka, D Hofmann, L Brehmer *Nucl. Instrum. Methods Phys. Res. B* **97** 416 (1995)
272. D Jacqemain, S G Wolf, F Leveiller, M Deutsch, K Kjaer, J Als-Nielsen, M Lanav, L Leiserowitz *Angew. Chem., Int. Ed. Engl*. **31** 130 (1992)
273. J F Legrand, A Renault, O Konovalov, E Chevigny, J Als-Nielsen, G Grübel, B Berge *Thin Solid Films* **248** 95 (1994)
274. C Bohm, F Leveiller, D Jacquemain, H Mohwald, K Kjaer, J Als-Nielsen, I Weissbuch, L Leiserowitz *Langmuir* **10** 830 (1994)
275. I Weissbuch, I Kuzmenko, M Berfeld, L Leiserowitz, M Lahav *J. Phys. Org. Chem*. **13** 426 (2000)
276. A Naudon, D Thiaudiere *J. Appl. Crystallogr*. **30** 822 (1997)
277. P Borthen, H H Strehblow *J. Phys. IV, Colloq. (France)* **7** C2-187 (1997)
278. K Tani, T Nanjyo, S Masui, H Saisho *J. Synchr. Radiat*. **5** 1141 (1998)
279. J Kowai, S Hayakawa, Y Kitajima, Y Gohshi *Anal. Sci*. **11** 519 (1995)
280. E Dartyge, A Fontaine, F Baudelet, C Giorgetti, S Pizzini, H Tolentiono *J. Phys. I (France)* **2** 1233 (1992)
281. G P Hastie, J Johnstone, K J Roberts, D Fisches *J. Cryst. Growth* **166** 67 (1996)
282. H Ade, B Hsiao *Science* **262** 1427 (1993)
283. N V Bausk, S B Erenburg, N F Yudanov, L N Mazalov *J. Phys. IV, Colloq. (France)* **7** C2-1167 (1997)
284. N V Bausk, S B Erenburg, N F Yudanov, L N Mazalov *Zh. Strukt. Khim*. **36** 932 (1995) [b]
285. V A Shuvaeva, K Yanagi, K Sakaue, H Terauchi *J. Synchr. Radiat*. **6** 367 (1999)
286. N V Bausk, L N Mazalov, A I Rykov, V F Vratskikh, V P Predtechenskii, Yu S Varlamov *Bull. Mater. Sci*. **14** 865 (1991)
287. N V Bausk, L N Mazalov, A I Rykov, V F Vratskikh, M R Predtechenskii, Yu D Varlamov *Zh. Strukt. Khim*. **33** 88 (1992) [b]
288. G Schütz, W Wagner, W Wilhelm, P Kienele, R Zeller, R Frahm, G Materlik *Phys. Rev. Lett*. **58** 737 (1987)
289. S G Ovchinnikov *Usp. Fiz. Nauk* **42** 869 (1999) [a]
290. J B Kortright, D D Awschalom, J Stohr, S D Bader, Y U Idzerda, S S Parkin, I K Schuller, H-C Siegmann *J. Magn. Magn. Mater*. **207** 7 (1999)
291. J Stöhr *J. Electron Spectrosc. Relat. Phenom*. **75** 253 (1995)
292. J Stlhr, R Nakajima *J. Phys. IV, Colloq. (France)* **7** C2-47 (1997)
293. E Dartyge, F Baudelet, C Giorgetti, S Odin *J. Alloys Compd*. **277** 526 (1998)
294. G A Sawatzky, F M F De Groot, S Altieri, N B Brookes, S L Hulbert, J B Goedkoop, B Sinkovic, E Shekel, L H Tjeng, R Hesper, E Pellegrin *J. Electron Spectrosc. Relat. Phenom*. **92** 11 (1998)
295. L Alagna, T Prosperi, S Turchini, J Goulon, A Rogalev, C Goulon-Ginet, C R Natoli, R D Peacock, B Stewart *Phys. Rev. Lett*. **80** 4799 (1998)
296. J Goulon, C Goulon-Ginet, A Rogalev, V Gotte, C Malgrange, C Brouder, C R Natoli *J. Chem. Phys*. **108** 6394 (1998)
297. B Stewart *J. Phys. IV, Colloq. (France)* **4** C9-179 (1994)
298. J C Sutherland, in *Circular Dichroism: Conformational Analysis of Biomolecules* (Ed. G D Fasman) (New York: Plenum, 1996) p. 599
299. G Schütz, D Ahlers *J. Phys. IV, Colloq. (France)* **7** C2-59 (1997)

300. G Schümtz, P Fischer, K Attenkofer, M Knulle, D Ahlers, S Stahler, C Detlefs, H Ebert, F M F De Groot *J. Appl. Phys.* **76** 6453 (1994)
301. S Imada, S Suda *J. Electron Spectrosc. Relat. Phenom.* **92** 1 (1998)
302. G Schonhense *J. Phys., Condens. Matter* **11** 9517 (1999)
303. V A Belyakov, V E Dmitrienko *Usp. Fiz. Nauk* **158** 679 (1989) [a]
304. V E Dmitrienko, in *Problemy Sovremennoi Kristallografii. Strukturnye Issledovaniya Kristallov* (Problems in Modern Crystallography. Structural Investigation of Crystals) (Moscow: Nauka, 1996) p. 84
305. A Kirfel, A Petcov *Acta Crystallogr., Sect. A* **48** 247 (1992)
306. A Kirfel, W Morgenroth *Acta Crystallogr., Sect. A* **49** 35 (1993)
307. J Baruchel, M Shlenker, in *X-Rays and Neutrons Dynamical Diffraction. Theory and Applications* (Ed. A Authier) (New York: Plenum, 1996) p. 187
308. M Sacchi *Surf. Rev. Lett.* **7** 175 (2000)
309. J Als-Nielsen, G Materlik *Phys. Today* **48** 34 (1995)
310. J V Smith *Analyst* **120** 1231 (1995)
311. A R Gerson, P J Halfpenny, S Pizzini, R Ristic, K J Roberts, D B Sheen, J N Sherwood *X-Ray Charact. Mater.* 105 (1999)
312. S K Sinha *Jpn. J. Appl. Phys., Part 1* **38** 1 (1999)
313. B S Clausen *Catal. Today* **39** 293 (1998)
314. J M Thomas, G N Greaves *Catal. Lett.* **20** 337 (1993)
315. B S Clausen, H Topsoe, R Frahm *Adv. Catal.* **42** 315 (1998)
316. N Binsted, M J Pack, M G Weller, J Evans *J. Am. Chem. Soc.* **118** 10200 (1996)
317. W Bras, G R Mant, G E Derbyshire, D Bouch, J Sheldon, J Dingis, J Ryan *Rev. Sci. Instrum.* **66** 1314 (1995)
318. S Husnain, K O Hodgson *J. Synchr. Radiat.* **6** 852 (1999)
319. H Oyanagi, I Owen, M Grimshaw, P Head, M Martini, M Saito *Rev. Sci. Instrum.* **66** 5477 (1995)
320. I Haita, H Takahashi, S Matuoka, Y Amemiya *Thermochim. Acta* **253** 149 (1995)
321. O M Wilkin, N A Young *J. Synchr. Radiat.* **6** 204 (1999)
322. M Richter *J. Electron Spectrosc. Relat. Phenom.* **76** 21 (1995)
323. J-E Rubensson, J Lüning, M Neeb, B Kuepper, S Eisebitt, W Eberhardt *Phys. Rev. Lett.* **76** 3919 (1996)
324. R A Bartynski, E Jensen, S L Hulbert, C-C Kao *Prog. Surf. Sci.* **53** 155 (1996)
325. S Vinton, S P Harte, G Charlton, V R Dhanak, G Thornton, W B Westerveld, J van Eck, J van de Weg, H G M Heideman, J B West *Chem. Phys. Lett.* **252** 107 (1996)
326. H Biehl, K J Boyle, D M Smith, R P Tuckett *Chem. Phys.* **214** 357 (1997)
327. U Becker *J. Electron Spectrosc. Relat. Phenom.* **112** 47 (2000)
328. A R Ravishankara, S Solomon, A A Turnipseed, R F Warren *Science* **259** 194 (1993)
329. R J Nelmes, M I McMahon *J. Synchr. Radiat.* **1** 69 (1994)
330. H K Mao, R J Hemley *High Press. Res.* **14** 257 (1996)
331. M I McMahon *Mater. Sci. Forum* **278** 1 (1998)
332. K Brister *Rev. Sci. Instrum.* **68** 1629 (1997)
333. J P Itié, A Polian, D Martinez, V Briois, A Di Cicco, A Filipponi, A San Miguel *J. Phys. IV, Colloq. (France)* **7** C2-31 (1997)
334. A San Miguel, J P Itié, A Polian *Physica B* **208 – 209** 506 (1995)
335. S K Saxena, L S Dubovinsky, P Haggvist, Y Cerenius, G Shen, H K Mao *Science* **269** 1703 (1995)
336. M Hanfland, U Schwarz, K Syassen, K Takemura *Phys. Rev. Lett.* **82** 1197 (1999)
337. K J Kingma, H K Mao, R J Hemley *High Press. Res.* **14** 363 (1996)
338. W Utsumi, T Muzutani, O Shimomura, T Taniguchi, S Nakano, N Nishiyama, K Funakoshi, in *International Union Crystallography XVIIIth Congress and General Assembly (Collected Abstracts), Glasgow, 1999* P08.CC.007
339. Ch-S Yoo, in *International Union Crystallography XVIII Congress and General Assembly. (Collected Abstracts)* Glasgow 1999. M08.OC.004
340. P Loubeyre, R Le Toullec, D Häusermann, M Hanfland, R J Hemley, H K Mao, L W Finger *Nature (London)* **383** 702 (1996)
341. D Hüusermann *Phys. Scr.* **66** 102 (1996)
342. Somoyazulu, L W Finger, R J Hemley, H K Mao *Science* **271** 1400 (1996)
343. L J Parker, T Aton, J B Badding *Science,* **273** 95 (1996)
344. S H Tolbert, A P Alivisatos *Ann. Rev. Phys. Chem.* **46** 595 (1995)
345. R J Nelmes, M I McMahon, in *Semiconductors and Semimetals* (Eds T Suski, W Paul) (New York: Academic Press, 1998) . 34
346. H Wilhelm, C Cros, E Reny, G Demazlau, M Hanfland *J. Mater. Chem.* **8** 2729 (1998)
347. Y Soldo, J L Hazemann, D Aberdam, M Inui, K Tamura, D Raoux, E Pernot, J F Jal, J Dupuy-Philon *Phys. Rev. B* **57** 258 (1998)
348. D Andrault, J Peryronnean, F Farges, J P Itié *Physica B* **208 – 209** 327 (1995)
349. C Roux, D M Adams, J P Itié, A Polian, D N Hendrickson, M Verdaguer *Inorg. Chem.* **35** 2846 (1996)
350. D M Pfund, J C Darab, J L Fulton, Y Ma *J. Phys. Chem. B* **98** 13 102 (1994)
351. J L Fulton, D M Pfund, S L Wallen, M Newville, E A Stern, Y J Ma *J. Chem. Phys.* **105** 2161 (1996)
352. S L Wallen, B J Palmer, D M Pfund, J L Fulton, M Newville, Y J Ma, E A Stern *J. Phys. Chem. A* **101** 9632 (1997)
353. K Jannsen, F C Adams, M L Rivers, K W Jones *Scanning Microsc. Suppl.* **7** 191 (1997)
354. G E Ice *X-Ray Spectrom.* **26** 315 (1997)
355. A Iida *X-Ray Spectrom.* **26** 359 (1997)
356. *J. Electron Spectrosc. Relat. Phenom.* **84** (1 – 3) (Special Issue) (1997)
357. C Riekel *Rep. Prog. Phys.* **63** 233 (2000)
358. P Chevallier, P Populus, A Firsov *X-Ray Spectrom.* **28** 348 (1999)
359. G Margaritondo *Jpn. J. Appl. Phys., Part 1* **38** 8 (1999)
360. M Kiskinova, M Marsi, E Di Fabrizio, M Gentili *Surf. Rev. Lett.* **6** 265 (1999)
361. N Fukumoto, Y Kobayashi, M Kurahashi, I Kojima *Spectrochim. Acta, B* **54** 91 (1999)
362. T Ungar, J I Langford, R J Cernik, G Voros, R Pflaumer, G Oszlanyi, I Kovacs *Mater. Sci. Eng., A* **247** 81 (1998)
363. A A MacDowell, C H Chang, H Padmore, J R Patel, A C Thompson *Mater. Res. Soc.* **524** 55 (1998)
364. A Snigirev, I Snigireva, C Riekel, A Miller, L Wess *J. Phys. IV, Colloq. (France)* **3** 443 (1993)
365. A Rindby, P Voglis, P Engström *Biomaterials* **19** 2083 (1998)
366. C Riekel, A Cedola, F Heidelbach, K Wagner *Macromolecules* **30** 1033 (1997)
367. S M Kuznetsov, I I Snigireva, A A Snigirev, P Engström, C Riekel *Appl. Phys. Lett.* **65** 1 (1994)
368. J D Denlinger, E Rotenberg, T Warwick, G Visser, J Nordgren, J-H Guo, P Skytt, S D Kevan, K S McCutcheon, D Shuh, J Bucher, N Edelstein, J G Tobin, B P Tonner *Rev. Sci. Instrum.* **66** 1342 (1995)
369. C Riekel, P Engström, C Martin *J. Macromol. Sci. Phys.* **37** 587 (1998)
370. M Müller, C Czihak, G Vogl, P Fratzl, H Schober, C Riekel *Macromolecules* **31** 3953 (1998)
371. Z H Cai, W Rodrigues, P Ilinsky, D Legnini, B Lai, W Yun, E D Isaacs, K E Lutterford, J Grenko, R Glew, S Stutz, J Vandenberg, R People, M A Alam, M Hybertsen, L J P Ketelsen *Appl. Phys. Lett.* **75** 100 (1999)
372. E D Isaacs, M Marcus, G Aeppli, X D Xiang, X D Sun, P Schultz, H K Kao, G S Kargile, R Haushalter *Appl. Phys. Lett.* **73** 1820 (1998)
373. P A Montano, H Oyanagi (Eds) *In Situ Synchrotron Radiation Research in Material Science*; *MRS Bull.* **24** (1) (Special Issue) (1999)
374. P Norby *Mater. Sci. Forum* **228** 147 (1996)
375. D O'Hare, J S O Evans, R J Francis, P S Halasyamoni, P Norby, J Hanson *Microp. Mesopor. Mater.* **21** 253 (1998)
376. T Shido, R Prins *Curr. Opin. Solid State Mater. Sci.* **3** 330 (1998)
377. J M Corker, F Levebrre, C Lecuyer, V Dufaud, F Quignard, A Choplin, J Evans, J-M Bisset *Science* **271** 966 (1996)
378. G Sankar, J M Thomas, D Waller *J. Phys. Chem.* **96** 7485 (1992)
379. N Yoshida, T Matsushita, S Soigo, H Oyanagi, H Hashimoto, M Fujimoto *J. Chem. Soc., Chem. Commun.* 354 (1990)
380. L M Murphy, B R Dobson, M Neu, C A Ramsdale, R W Strange, S S Hasnain *J. Synchr. Radiat.* **2** 64 (1995)
381. A Dent, J Evans, M Newton, J Corke, J A Russell, M B Abdul-Rahman, S Fiddy, R Mathew, R Farrow, G Salvini, P Atkinson *J. Synchr. Radiat.* **6** 381 (1999)
382. M Hagelstein, A Fontaine, J Goulon *Jpn. J. Appl. Phys., Part 1* **32** 240 (1993)

383. S G Nikitenko, B P Tolochko, A N Aleshaev, G N Kulipanov, S I Mishnev *J. Phys. IV, Colloq. (France)* **7** C2-549 (1997)
384. Y Inada, H Hayashi, S Funahashi, M Nomura *Rev. Sci. Instrum.* **68** 2973 (1997)
385. P D Cobden, B E Nieuwenhuys, F Esch, A Baraldi, G Vomelli, S Lizzit, M Kiskinova *Surf. Sci.* **416** 264 (1998)
386. J Harford, J Squire *Rep. Prog. Phys.* **60** 1723 (1997)
387. A A Vazina, P M Sergienko, A M Gadzhiyev, V M Aulchenko, Yu V Usov, M V Yasenev *Nucl. Instrum. Methods Phys. Res. A* **359** 220 (1995)
388. K Moffat *Acta Crystallogr., Sect. A* **54** 833 (1998)
389. K Moffat *Trans. Am. Crystallogr. Assoc.* **34** 39 (2000)
390. V Srajer, T-Y Teng, T Ursby, C Pradervand, Z Ren, S Adachi, W Schieldkamp, D Bourgeois, M Wulff, K Moffat *Science* **274** 1726 (1996)
391. M Wulff, F Schotte, G Naylor, D Bourgeois, K Moffat, G A Mourou *Nucl. Instrum. Methods Phys. Res. A* **398** 69 (1997)
392. T-Y Teng, V Črajer, K Moffat *Biochemistry* **36** 12087 (1997)
393. V V Mikhailin *Nucl. Instrum. Methods Phys. Res. A* **448** 461 (2000)
394. J B Hasting, S L Hulbert, G P Williams (Eds) *Proceedings of the 5th International Conference on Synchrotron Radiation Instrumentation*; *Rev. Sci. Instrum.* **66** (2) (1995)
395. G N Kulipanov, V F Pindyurin (Eds) *Proceedings of the 10th National Synchrotron Radiation Conference* (*SR-94*); *Nucl. Instrum. Methods Phys. Res. A* **359** (1 – 2) (1995)
396. K Baberschke, D Arvanitis (Eds) *Proceedings of the 8th International Conference on X-Ray Absorption Fine Structure*; *Physica B* **208** – **209** (1995)
397. *Proceedings of the 9th International Conference on X-Ray Absorption Fine Structure*. (Eds. J.Goulon C.Goulon-Ginet N.B.Brookes). *J. Phys. IV Colloq. (France)* **7** (C2) 1997
398. *Proceedings of the 11th National Synchrotron Radiation Conference (SR-96). (Ed. G.N.Kulipanov). Nucl. Instrum. Methods Phys. Res., A* **405** (23) 1998
399. S S Hasnain, R Helliwell, H Kamitsubo (Eds) *Proceedings of the 6th International Conference on Synchrotron Radiation Instrumentation*; *J. Synchr. Radiat.* **5** (3) (1998)
400. A Kakizaki, A Kotani (Eds) *Proceedings of the 6th International Symposium 'Frontiers in Synchrotron Radiation Spectroscopy'*; *J. Electron. Spectrosc. Relat. Phenom.* **92** (1 – 3) (1998)
401. W Pazkowicz, E Sobczak (Eds) *Proceeding of the 4th Inthernational School and Symposium on Synchrotron Radiation in Natural Science; J. Alloys Compd.* **286** (1998)
402. S S Hasnain, R Helliwell, H Kamitsubo (Eds) *Proceedings of the 10th International Conference on X-ray Absorption Fine Structure*; *J. Synchr. Radiat.* **6** (3) (1999)
403. G N Kulipanov (Ed.) *Proceedings of the 12th National Synchrotron Radiation Conference* (*SR-98*); *Nucl. Instrum. Methods Phys. Res. A* **448** (1 – 2) (2000)
404. S S Hasnain, H Kamitsubo, D M Mills (Eds) *Proceedings of the 11th International Conference on X-Ray Absorption Fine Structure*; *J. Synchr. Radiat.* **8** (2) (2001)
405. J L Jordan-Sweet *IBM J. Res. Dev.* **44** 457 (2000)

[a] — *Physics-Uspekhi (Engl. Transl.)*
[b] —*J. Struct. Chem. (Engl. Transl.)*